Development of Biological Interfaces for Photonic Biosensors

Shrishty Bakshi

Doctor of Philosophy

University of York

School of Physics, Engineering and Technology

October 2024

ABSTRACT

Biosensors can play a crucial role in biomedical diagnosis, benefiting point-of-care monitoring and the guided treatment of diseases. In addition to biomedical diagnosis, biosensing devices can contribute to environmental monitoring, drug discovery, and food quality monitoring. A wide range of biosensors, such as optical, electrochemical, etc., are being developed. Photonic biosensors appear to be a good candidate for wide-scale commercialisation and deployment because of their high sensitivity, the possibility of cost-effective large-scale fabrication, and easy miniaturisation. One of the significant obstacles in the wide-scale deployment of silicon nitride photonic biosensors is the lack of a robust surface functionalisation method to immobilise receptors on the sensor's surface to capture the target analyte. In this thesis, I have studied the analytical performance of bioinspired polydopamine-based surface chemistry for the immobilisation of bioreceptors on the surface of guided-mode resonance-based silicon nitride photonic biosensors and observed that this protocol provides high bioreceptor immobilisation density that, in turn, enhances the signal observed for antigen binding. A detection limit of 10 pg/mL and a wide dynamic range (10 pg/mL-10 μg/mL) was achieved for Immunoglobulins (IgG), C-Reactive Protein (CRP,) and Matrix Metalloproteinase-9 (MMP-9) antigens detection, using polydopamine functionalised guided mode resonance based photonic sensors. Moving forward, I studied polydopamine surface chemistry optimised guided mode resonance-based sensing platform for detecting inflammatory wound biomarkers Tumor Necrosis Factor-α (TNF-α) and Interleukin-6 (IL-6) in hydrogel-based wound dressings absorbed with human matrix and clinical wound exudate. Additionally, I further studied the suitability of the photonic biosensing device for trypsin enzyme detection in human urine, an essential biomarker for pancreatic diseases, by developing the biological interface using beta-casein as the substrate for trypsin. Our platform can detect trypsin with high sensitivity and wide dynamic range in human urine. In brief, this thesis describes an optimisation of biological interfaces for guided mode resonances-based silicon nitride photonic sensors using a polydopamine layer. The sensor achieves sensitive detection of protein-based biomarkers in complex human fluids such as 10 % human serum, wound fluid-absorbed hydrogel, and human urine in label-free manner.

Author's Declaration

I declare that this thesis is a presentation of original work and I am the sole author. This work has not previously been presented for a degree or other qualification at this University or elsewhere. All sources are acknowledged as references.

Shrishty Bakshi

List of Publications, Conferences, and Summer Schools

Publications arising from the work reported in this thesis:

1. **Shrishty Bakshi**, Kezheng Li, Pin Dong, Isabel Barth, Casper Kunstmann-Olsen, Steven Johnson, Thomas F Krauss, Bio-inspired polydopamine layer as a versatile functionalisation protocol for silicon-based photonic biosensors. Talanta (ELSEVIER), Volume 268, February 2024, 125300.

2. **Shrishty Bakshi**, Pankaj K. Sahoo, Kezheng Li, Steven Johnson, Michael J. Raxworthy, Thomas F Krauss, Nanophotonic and hydrogel-based diagnostic system for the monitoring of chronic wounds. Biosensors and Bioelectronics (ELSEVIER), Volume 242, December 2023, 115743.

3. **Shrishty Bakshi**, Kezheng Li, Pankaj K. Sahoo, Thomas F Krauss, Nanophotonic platform for highly sensitive detection of trypsin enzyme in human urine. Chemical Communications (Royal Society of Chemistry) 2025, 61 (28), 5321-5324

Conference Proceedings

1. **Shrishty Bakshi**, Kezheng Li, Pin Dong, Steven Johnson, Thomas Krauss, Mussel inspired polydopamine surface chemistry as a one-step method for bioreceptor immobilisation on silicon photonic biosensors, 2023 IEEE BioSensors Conference (BioSensors).

Publications arising from working on other projects:

6. **Shrishty Bakshi**, Preeti Pandey, Yousuf Mohammed, Joanna Wang, Michael J. Sailor, Amirali Popat, Harendra S Parekh, Tushar Kumeria, Porous silicon embedded in a thermoresponsive hydrogel for intranasal delivery of lipophilic drugs to treat rhinosinusitis. Journal of Controlled Release (ELSEVIER), Volume 363, November 2023, 452-463. **Equal First Author**

5. **Shrishty Bakshi**, Aaron J. Snoswell, Kei Yeung Kwok, Lung Hei Cheng, Tariq A. Altalhi, Abel Santos, Amirali Popat, Tushar Kumeria, Spray-n-Sense: Sprayable Nanofibers for On-Site Chemical Sensing. Advanced Functional Materials (WILEY), Volume 32, April 2022, 2103496.

4. Gunjan Singh, **Shrishty Bakshi**, K.K. Bandyopadhyay, Sudeep Bose, Ranu Nayak, Debarati Paul, Enhanced biodegradation of melanoidin pigment from spent wash using PDMS immobilized microbes via 'repeated addition' strategy. Biocatalysis and Agricultural Biotechnology (ELSEVIER), Volume 33, May 2021, 101990. **Equal first author**.

3. Samriddhi Mehta, **Shrishty Bakshi**, Sangeeta Choudhury, Sudeep Bose, Ranu Nayak, Hierarchical gold nanostructures based sensor for sensitive and fast detection of cancer biomarker. Indian Journal of Biochemistry and Biophysics, Volume 58, April 2021, 135-140.

2. **Shrishty Bakshi**, Samriddhi Mehta, Tushar Kumeria, Muhammad. J.A. Shiddiky, Amirali Popat, Sangeeta Choudhury, Sudeep Bose, and Ranu Nayak, Rapid fabrication of homogeneously distributed hyper-branched gold nanostructured electrode based electrochemical immunosensor for detection of protein biomarkers. Sensors and Actuators B: Chemical (ELSEVIER), Volume 326, January 2021, 128803.

1. **Shrishty Bakshi**, Kritika Pandey, Sudeep Bose, Gunjan, Debarati Paul, Ranu Nayak, Permanent superhydrophilic surface modification in microporous polydimethylsiloxane sponge for multi-functional applications. Journal of Colloid and Interface Science (ELSEVIER), Volume 552, September 2019, 34–42.

Summer Schools:

1. **Shrishty Bakshi**, Kezheng Li, Ping Dong, Isabel Barth, Casper Olsen Kunstmann, Steven Johnson, Thomas F Krauss. Mussel-inspired one-step biofunctionalisation protocol for photonic biosensors. SUSSP 79 Summer School in Photonic Sensing and Spectroscopy (2023), University of St. Andrews, Scotland, United Kingdom. Poster Presentation

2. **Shrishty Bakshi**, Kezheng Li, Thomas F. Krauss. Optical biosensors to monitor Ageing related Biomarkers in human blood serum. Cognitive Frailty Interdisciplinary Network ECR summer school (2023), Lancaster University, United Kingdom (Remote). Oral Presentation

Conferences:

1. **Shrishty Bakshi**, Kezheng Li, Pin Dong, Steven Johnson, Thomas F. Krauss. IEEE Biosensors (2023) Conference, London, United Kingdom. Poster Presentation

2. **Shrishty Bakshi**. Guided Mode Resonance based sensors for biosensing applications. Physics Postgraduate Conference 2023, School of Physics Engineering and Technology, University of York, United Kingdom. Oral Presentation

3. **Shrishty Bakshi**, Kezheng Li, Pankaj K. Sahoo, Thomas F. Krauss, Guided mode resonance based sensing platform for highly sensitive detection of trypsin enzyme in human urine, Europtrode 2024, University of Birmingham, Birmingham. Poster Presentation

CONTENTS. Page Number

List of Figures

List of tables

Acknowledgements

I would like to thank my advisors, Prof. Thomas Krauss and Prof. Steven Johnson, for giving me the opportunity to work on the exciting topic of Photonic Biosensors, which helped me gain knowledge about a lot of new concepts and techniques.

I am very thankful to Dr. Kezheng Li for always being so kind and helpful and helping me in learning the concepts of nanofabrication and photonics. I am also very grateful to him for fabricating sensors for this work. I want to thank Dr. Donato Conteduca for all the help and interesting and fruitful discussions regarding biosensing experiments and for always giving the best advice. I am grateful to Dr. Pankaj K. Sahoo for fabricating the sensors used in the work. I want to thank Dr. Christopher Reardon for all his help with ordering stuff and making the process very convenient. I am very thankful to Dr. Pin Dong for the valuable discussions on the biochemistry part of the experiments. I want to thank Dr. Isabel Barth, Dr. Alexander Drayton, and Dr. Giampaolo Pitruzzello for their help in clearing the doubts regarding the theory of guided-mode resonance-based sensing. I am very grateful to Dr Nyasha Suliali for his help with the experiments and for the interesting discussions.

I sincerely acknowledge Prof. Michael J. Raxworthy for providing hydrogel and helping us acquire clinical wound exudate. I also acknowledge Professor Matthew J. Hardman, Wound Group Lead, Hull-York Medical School, for providing clinical wound exudate.

I am very thankful to Prof. Alison Laird, for all the encouragement and constructive feedback she gave in the Thesis advisory meetings.

I wish to express my sincere gratitude to my master's thesis advisor, Dr. Tushar Kumeria, for giving me the opportunity to pursue my master's thesis research work in his lab in Australia and enabling me to work on different projects in the field of drug delivery and biosensing and supporting my learning of so many new methods and techniques. I am very grateful to my undergraduate thesis advisor, Prof. Ranu Nayak, for allowing me to pursue my undergraduate research in her lab and giving me the chance to work on exciting projects very early, and always being there for any guidance.

I am very thankful to all my amazing friends in Australia, Singapore, Canada, India, and the UK for always being there and keeping in touch, even in different time zones.

Last and most importantly, I am very thankful to my family, Maa, Papa, Divay, and Nani Maa, for all their love, help, support, and encouragement over the years. Thank you so much for everything.

Chapter 1. Introduction to Biosensors

1.1. Biosensors:

Biosensors are emerging as an important tool for identifying and managing diseases [1]. Currently, most tests are conducted in centralised clinical laboratories with delicate instruments that require skilled personnel and are time-consuming. In recent years, the urgent need for healthcare checkups in various scenarios has given rise to an immense interest in developing point-of-care tests. Every year, millions of deaths are caused by infectious diseases, more prominently in developing countries [2, 3]. Enzyme-linked immunosorbent assay-based tests and polymerase chain reaction-based tests are used to detect diseases. These methods suffer from disadvantages such as time delays and high costs [4]. Developing efficient biosensors can make an essential contribution to the healthcare system by providing platforms for decentralised near-patient testing, thus improving patient healthcare.

Looking back, the first commercial biosensor for glucose detection was developed by Yellow Springs Instruments analyzer in 1975 [5]. I-STAT came up with the first handheld blood biosensor in 1992 [6]. Since the development of the I-STAT sensing system, significant progress has been made in developing different biosensing devices.

Figure 1 depicts the point-of-care diagnostic system enabling rapid results.

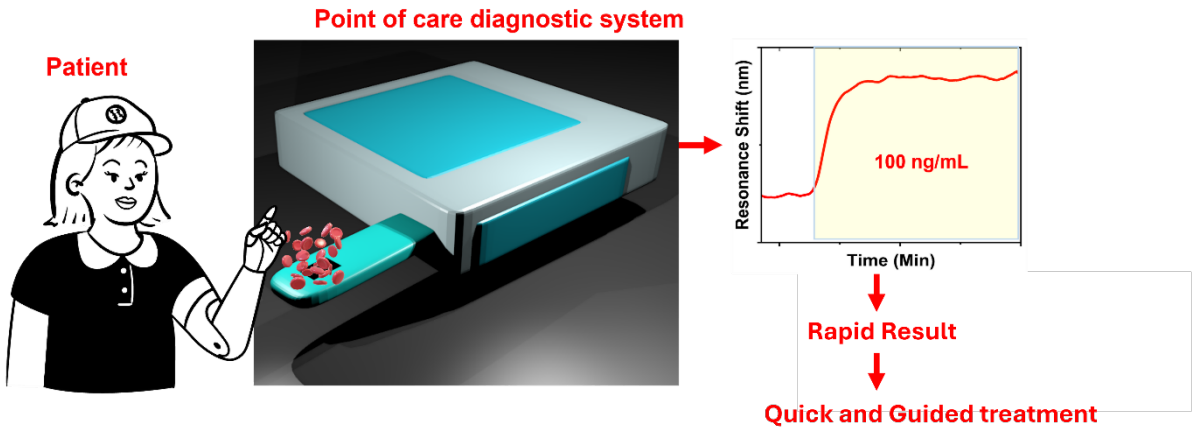

FIGURE 1: Picture depicting point-of-care diagnostics enabling rapid results and guided treatment of diseases.

1.2. Applications of biosensors:

Biosensors can play an important role in the early detection of diseases such as cancer, neurological disorders, and infectious diseases [7-9]. Wearable biosensing technologies can be used for continuous monitoring of biological analytes [10]. In addition, biosensing devices can be used to perform remote patient surveillance in real-time [11]. Developing nanosized biosensors can be utilised to gain insights into intracellular processes [12]. Other than the healthcare industry, developing efficient biosensing systems can also play an important role in the food industry for testing the quality of food [13]. Environmental conditions tracking and monitoring can be another important area where biosensors can play a significant role [14]. Biosensing devices can be very beneficial in the defence and security sectors to protect against biological warfare agents [15]. Biosensing devices can be used for studying genetic patterns, detecting mutating genes, and improving and designing treatments according to observations [1, 16]. In developing efficient and intelligent drug delivery systems and performing therapeutic drug monitoring, biosensors can play a critical role [17, 18]. Fluorescence-based biosensing devices can be used for applications in the field of drug discovery [19].

1.3. Elements and characteristics of a typical biosensor:

1.3.1. Elements of a typical biosensor:

(a) Analyte: An analyte can be defined as a molecule of interest that needs to be identified, sensed or quantified [6].
(b) Bioreceptor: Bioreceptors are biological molecules that a biosensing device uses to capture the analyte on the sensor surface. Some examples of bioreceptors are antibodies and aptamers [20, 21].
(c) Transducer: The transducer converts biomolecular interactions on the sensor's surface into a measurable output signal. Different types of transducers used for biosensing applications are optical, electrochemical, thermal, and gravimetric [22].
(d) Signal processing and Display: A biosensor’s signal processing and display unit converts the transduced signal into a readable, user-friendly format. The signal processing unit is designed using intricate electronics and displays consisting of computers, printers, etc. The output produced is generally in the form of a graph, image, or number [6].

(e) Biological Matrix: A biological matrix, in reference to a biosensor can be defined as a medium or biofluid containing the analyte of interest that needs to be measured or quantified together with other biomolecules [23]. Examples of the matrix are blood, urine and saliva [24].

Figure 2 shows the different elements of a typical biosensing system.

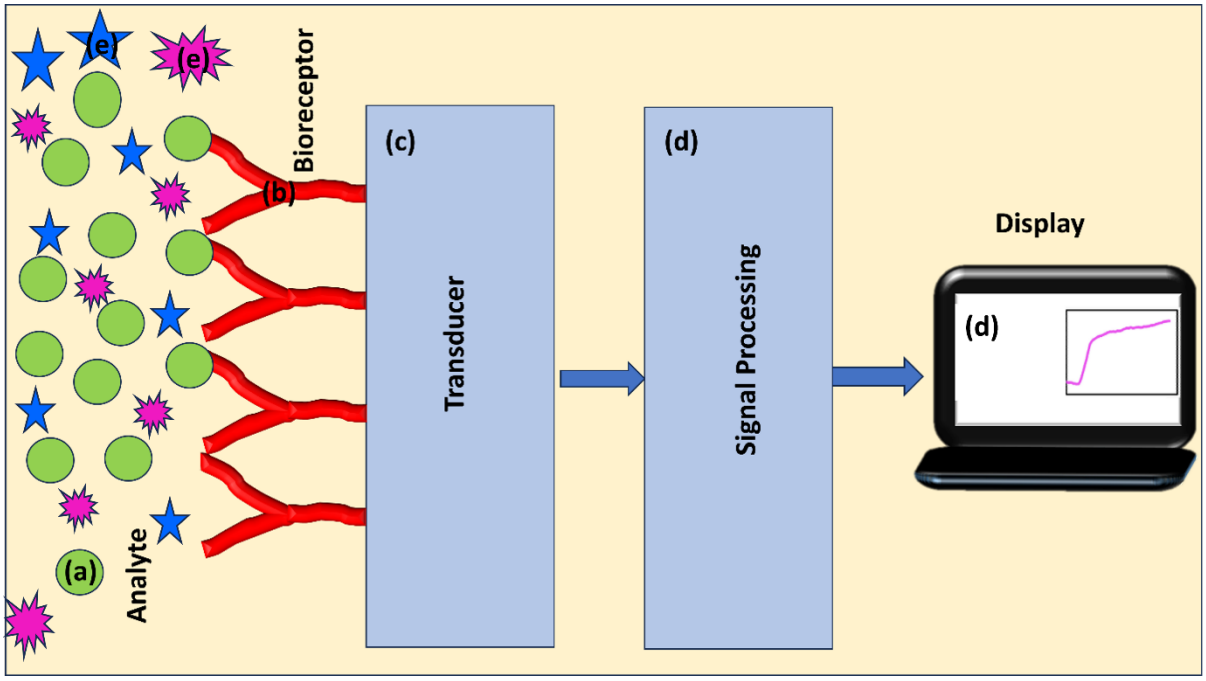

FIGURE 2: General components of a typical biosensor; (a) Analyte-the molecule of interest or target (b) Bioreceptor-to capture the analyte; (c) Transducer to convert biological interaction into a measurable signal; (d) Signal processing and display unit; (e) Biological matrix.

1.3.2. Characteristics of biosensors:

An ideal biosensor has the following characteristics:

1. Sensitivity: The sensitivity of the biosensor is its ability to produce measurable signals per unit change in the concentration of the analyte molecule. The biosensor's sensitivity can be calculated by calculating the slope of the calibration curve [25-27]. The lowest analyte concentration that a biosensor device can detect with reliability is defined as the limit of detection of the biosensing device, and factors such as the sensitivity of the sensing device and the noise of the sensing system play an important role in determining the limit of detection of the biosensor [28].

2. Selectivity: The biosensor's selectivity is its ability to precisely and accurately detect the desired analytes of interest from the pool of biomolecules [6, 20]. The selectivity of the biosensor plays a key role when performing measurements in complex biofluids. The specificity of a biosensor can be defined as the biosensing interface's and bioreceptor's ability to detect only one analyte specifically [29, 30].

3. Response time: Another important characteristic that describes a biosensor's robustness is the response time, which is the time the developed biosensing device takes to give results after a biorecognition event has taken place [31].

   Different factors that affect the selectivity and response time of biosensors are the biochemistry used to functionalise the sensor surface, the composition of the analyte media, flow rate, and bioreceptors [30, 32, 33].

4. Stability: When performing continuous measurements for a longer duration of time, the stability of biosensors is an important factor to consider. Several factors play an important role in determining the stability of biosensors, such as disturbances caused by the external environment and the stability of the biological interface designed [20, 34].

5. Reproducibility: A biosensor's reproducibility is the ability to generate similar signals for repeated measurements [20].

1.4. Classification of biosensors based on transducer:

Based on different transducers, biosensors can be classified as:

1. Optical biosensors:

An optical biosensor operates by employing optical transduction methods to detect the analyte molecules. It uses light-based techniques such as evanescent waves to measure the interaction between the target analyte and bioreceptor element immobilised on the surface of the optical transducer, converting this interaction into a measurable optical signal. Optical biosensors employ various receptors for analyte capture, such as antibodies or aptamers, etc, on the transducer surface to capture the target analyte. The transduction mechanism or sensing mechanism utilised in optical biosensors produces a change in the transmission or reflection of light when biomolecules interact on the sensor's functional surface [20, 35]. Some examples of optical biosensors are surface plasmon resonance-based biosensors

[36], nanoporous anodic alumina-based biosensors [37], porous silicon-based optical biosensors [38], and the guided mode resonance-based biosensors that we have studied here.

2. Electrochemical biosensors:

Electrochemical biosensing technology are one of the most studied, characterised and developed biosensing technologies. One of the most successful examples is glucose biosensors, which are commercially available [39]. The working principle of electrochemical biosensors involves the conversion of the bio-interactions taking place on the surface of the working electrode into electrical signals, such as changes in impedance, current, or voltage [31, 40]. Electrochemical techniques employed by electrochemical biosensors for monitoring bimolecular interactions are cyclic voltammetry, chronoamperometry, linear sweep voltammetry, etc. [20].

3. Gravimetric biosensors:

Gravimetric biosensors are based on mass of the analyte based sensing and produce a signal corresponding to the mass adsorbed on the surface of sensor [41]. Quartz crystal microbalance-based sensors fall under the category of gravimetric biosensors. The quartz crystal sensors start to oscillate on the application of alternating voltage. Immobilisation or attachment of mass on the sensing surface of the quartz crystal sensor results in a shift in the resonance frequency of the sensor, and the magnitude of the shift observed is directly proportional to the mass immobilised on the sensor surface. A bioreceptor is immobilised on the surface of the quartz crystal microbalance sensors to detect the analyte molecule [42, 43].

4. Electronic Biosensors:

Biosensors utilising the field effect transistor (FET) for analyte detection fall under the category of electronic biosensors. FET-based sensing devices, in general, consist of electrodes, i.e. gate, source, and drain. It also has a dielectric insulating layer and a semiconducting layer. The interaction of the analyte with bioreceptors immobilised on the sensing layer (semiconducting or dielectric) causes the changes in electrical characteristics of the layer and as a consequence of that change in the dispersion of charge carriers within the sensing layer takes place that in turn, results in the alteration of output current values. These fluctuations in electrical signals are employed to detect the analyte molecules [44]. Ion-sensitive field-effect transistors and metal-oxide-semiconductor field-effect transistors are the mostly studied FET sensors for biological side-related applications. Different types of one-dimensional and two-dimensional materials can be used to design and develop FETs for biosensing applications [45, 46].

5. Thermal Biosensors:

Thermal biosensors utilise heat consumed or released during the biochemical reaction for sensing applications [20]. One example of thermal transducers is thermistors, which are used for various applications because of advantages such as high sensitivity and cost-effectiveness. Enzymes as biorecognition elements and thermistors together are called enzyme thermistors and are employed for applications such as the analysis of food and bioprocess monitoring. Enzyme thermistors monitor enzymatic reactions by measuring the heat change during the enzymatic reaction [47]. Additionally, thermal biosensors are used for applications such as pesticide quantification [48].

Each type of transducer discussed above has its advantages and shortcomings. For example, optical biosensors have very high sensitivity and offer non-destructive and non-interferential analysis, as well as real-time monitoring of biomolecular reactions [49-51], but often require complex setups for operation [26, 52]. In contrast, electrochemical biosensors have advantages such as simplicity, portability, and cost-effectiveness [39] but can suffer from interference from electroactive species [53] and observation of drifts with time [54]. Gravimetric biosensors offer good sensitivity and real-time analysis but suffer from some limitations, such as in the case of quartz crystal microbalance-based sensors, to enhance the sensitivity of sensors, the thickness of the quartz crystal has to be decreased, which makes sensors easily breakable and mechanically unstable, and thus makes them unsuitable candidates for practical use as point-of-care devices [55]. Thermal biosensors are sensitive and cost-effective but suffer from limitations such as lack of specificity [47]. FET-based biosensors have advantages such as fast response time and high sensitivity [56] but face challenges like charge screening in biological fluids [57].

When choosing between different transducing systems, the application's specific needs must be considered carefully. Ultimately, the best sensor choice will depend on various factors, including cost, accuracy, ease of use, and target of interest.

In this work, I have worked on silicon nitride-based photonic biosensors based on guided-mode resonances, with a primary focus on developing highly efficient bio-interfaces for silicon nitride based photonic sensors to enhance their utility as biosensing devices.

1.5. Biomarkers and Bioreceptors:

1.5.1. Biomarkers:

A biomarker can be defined as a biomolecule that is present in fluids in the body, such as urine or blood, that gives an indication of normal or uncommon processes taking place inside the body or gives an indication of the presence or absence of disease [58]. Examples of biomarkers are different types of biomolecules such as proteins, deoxyribonucleic acid, ribonucleic acids, etc [59]. Biomarker detection and quantification in biological fluids such as tears, saliva, blood, urine, breath, etc., can play a significant role in disease identification and detection and management [60, 61]. Point-of-care devices that can sensitively and efficiently detect these biomarkers in clinical fluids can help in the early diagnosis and better management of diseases [62, 63]. Various biosensors are being developed for biomarker detection and quantification using optical and electrochemical transduction technologies [64]. Additionally, studying biomarkers is gaining importance in the field of the pharmaceutical industry to optimise drug development, for example, biomarkers are employed to identify any toxicity caused by new drugs developed and understand the mechanism of drug action, etc. [65].

Based on clinical applications, the biomarkers can be further classified into different types: -

(a) Diagnostic Biomarkers: A diagnostic biomarker is a biomarker studied to confirm the presence or absence of a disease or other health condition [66]. For example, prostate-specific antigen is used to diagnose prostate cancer [67].

(b) Susceptibility Biomarkers: Susceptibility biomarkers are used or observe or to study the possibility of disease development in an individual. Increment in the levels of low-density lipoprotein cholesterol in the blood hint at the possibility of atherosclerosis development and are examples of susceptibility biomarkers [66].

(c) Safety Biomarkers: A safety biomarker is used to study any toxicity in response to a particular medical treatment or therapy. These biomarkers are helpful in identifying if patients are experiencing any harmful effects from the treatment [68]. An example of a safety biomarker is serum creatinine, which is used to monitor patients who are given drugs that can affect kidneys negatively and to look for any signs of nephrotoxicity [69].

(d) Prognostic Biomarkers: Prognostic biomarkers are used to study disease status by monitoring and screening diseases [70]. These biomarkers are used to study recurring diseases [71]. The Kiel-67 (Ki-67) biomarker is an example of a prognostic biomarker and is monitored to study breast cancer development and proliferation [72].

(e) Therapeutic Biomarkers: Therapeutic biomarkers are measured, observed or quantified to study the effect of therapy or a treatment on a patient given treatment. For example, the Cancer antigen 15-3 (CA15-3) biomarker is monitored or tracked to examine patients' responses to breast cancer therapy [70].

Figure 3 shows an example of biomarker detection using a bioreceptor immobilised on a biosensing interface from biofluid.

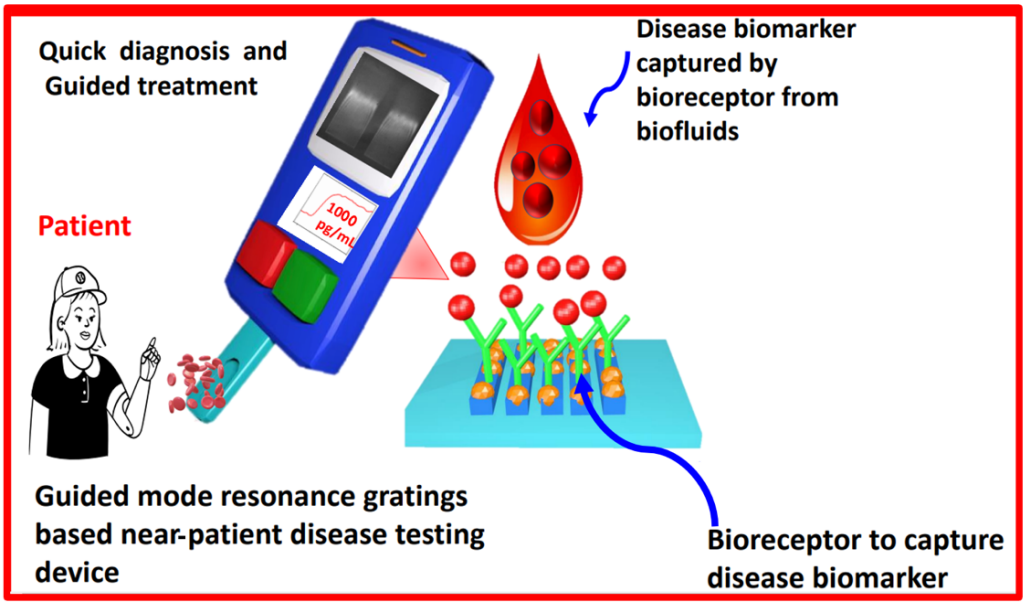

FIGURE 3: Near-patient testing device to detect disease biomarkers using immobilised bioreceptors on the sensing surface.

1.5.2. Bioreceptors:

(a) Antibody bioreceptors:

Antibodies come under the category of affinity-based bioreceptors that are used to detect the analyte when immobilised on the transducer of a biosensor. The biosensing devices that employ or use antibodies as biorecognition elements are known as immunosensors [73]. The biological interaction between the antibodies immobilised on the transducer surface and the antigen in the biofluids results in the transducer's conversion of biorecognition into measurable signals or quantifiable signals. An antibody is a Y-shaped structure that is made up of two heavy and two light polypeptide chains that are connected together by a disulfide bond [74]. Antibodies can be classified into five groups based on variations observed in their heavy chain region, such as IgG, IgM, IgA, IgD, and IgE [75]. The advantages of using antibodies as bioreceptors are their small size and high selectivity for the target molecule. The surface chemistry used to immobilise the antibodies on the biosensing surface plays an important role in determining the antibody's performance [76].

(b) Aptamer as bioreceptors:

Aptamers are artificial strands of nucleic acid sequences, such as deoxyribonucleic acids and ribonucleic acids, that are used for analyte detection [20]. Aptamers show high specificity, selectivity and sensitivity for their target or analyte of interest and also possess high stability in wide range of conditions [77]. These aptamer sequences bind or interact with their target molecule or analyte of interest and forms two-dimensional and three-dimensional conformations or structures [20]. Aptamers do not require animals for their production and can be produced by in vitro methods [78]. In addition to that, aptamers can be specifically modified to give improved performance, high specificity, and binding affinity for their target analyte [79].

Generally, affinity-based assays, are characterised by calculating the dissociation constant values, also called K_d values. K_d is an equilibrium constant that varies inversely to the binding affinity. K_d values are studied to characterise affinity-based assays and calculate the strength of binding between two molecules [80].

(c) Cells as bioreceptors:

Cell-based biosensors utilise live cells as bioreceptors in combination with transducing devices for analyte detection and monitoring. The immobilised cells, together with the transducer, sense the environmental conditions and detect the analyte. The immobilised cells on the transducer surface produce a signal when external stimuli, for example, drugs or other chemicals, are brought into the vicinity or in contact with cultured cells. With the help of a transducer, these signals can be further converted into readable output, thus giving an indication of the analyte status [81]. Cells when utilised as bioreceptors can be used to detect a wide range of analytes [20]. Cell-based biosensors can be employed and bring in use for various applications such as testing food safety, environmental monitoring, health care, and pharmaceutical research [82]. One of the interesting properties of cells as bioreceptors is the distinctive combinations of enzymes and other biological receptors and biomolecules present in cells that can be utilised for biosensing applications. Different types of transducing systems employed for cell-based biosensors are FETs, quartz crystal microbalance, surface plasmon resonance, etc [81].

(d) Enzymes as bioreceptors:

Enzymes are defined as biological catalysts that increase the rate of biological reactions [83]. In enzyme-based biosensors, the enzyme is used as a biorecognition element. It is immobilised on the transducer surface and generates a signal that is proportional to the target analyte concentration [84]. The enzymes, as biorecognition elements, have high specificity for their substrates. The process of analyte detection in enzyme-based biosensors involves monitoring and quantifying changes in the parameters such as alteration in proton concentration, the release of gases or consumption of gases, or changes in optical spectra such as emission or absorption of light, etc., in response to the interaction of the enzyme with the analyte or biochemical interactions taking place on sensor surface, followed by converting the reaction into a measurable output signal, such as an optical or electrical signal [85]. Various possible methods or mechanisms that are employed by enzyme-based biosensors are either the metabolism of the analyte by the enzyme molecule, so the concentration of the analyte can be measured by measuring or quantifying the catalysis of the analyte molecule or target by the enzyme molecule or by calculating enzyme activity inhibited by the analyte molecule [86].

In my work, the enzymes are not the bioreceptors but are the analyte of interest. The work reported in Chapter 5 demonstrates the biosensing of trypsin enzyme, where trypsin enzyme is the analyte of interest.

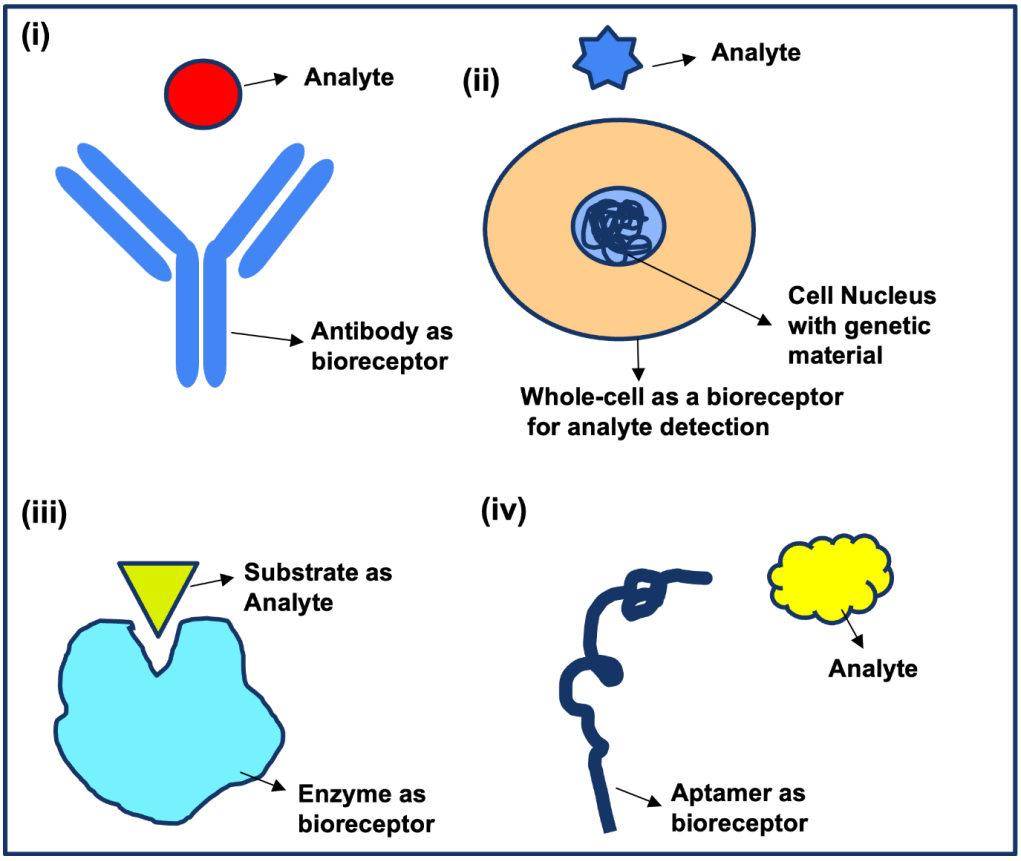

FIGURE 4: Different types of bioreceptors used in biosensing devices (i) Antibody as bioreceptor; (ii) Whole-cell as bioreceptor; (iii) enzyme as bioreceptor; (iv) Aptamer as bioreceptor.

Figure 4 shows the different types of receptors employed by biosensors. Table 1 compares all the different types of biorecognition elements.

TABLE 1: Comparison of commonly employed bioreceptors in biosensors.

Antibodies	Aptamers	Enzyme	Cells
Advantage 1. High affinity [77]. 2. High sensitivity [77]. 3. High specificity [77]. 4. High biocompatibility [77]. 5. Broad variety of targets [32]. 6. Well-settled production facilities [32].	Advantages 1. High affinity [77]. 2. High specificity [77]. 3. High sensitivity [77]. 4. High structural flexibility [77]. 5. Less batch-to-batch fluctuation [77]. 6. Animals are not required for the production [87]. 7. High stability [77].	Advantages 1. High specificity [88]. 2. Animals are not required for production [89]. 3. Commercially available at good quality [88]. 4. Compatible with a wide variety of transducers [88]. 5. A wide range of analyte detection is possible using enzymes[88].	Advantages 1. More tolerant of a wide range of conditions such as changes in pH and temperature [81]. 2. As live cells do not require isolation it makes sensor fabrication cost-effective [81]. 3. Longer life of sensors as compared to enzyme-based sensors [81]. 4. Can interact with a broad range of analytes molecules [20]
Limitations 1. Expensive to produce [77]. 2. Batch to Batch fluctuations [77]. 3. Limited thermal stability [77]. 4. Loss of activity when stored for longer times [32].	Limitations 1. The range of targets is not very wide [32]. 2. Complicated and lengthy selection process [77]. 3. Structural arrangement decides the specificity and sensitivity [77]. 4. Ribonucleic acid-based aptamers are susceptible to degradation in biological fluids [90].	Limitations 1. Poor Stability [86]. 2. Optimum pH and temperature needed for efficient working [86]. 3. Expensive production [91].	Limitations 1. The duration for which cells stay functional and alive decides the life of the sensors [81]. 2. Strict conditions need to be maintained to keep cells alive and functional [81]. 3. Immobilisation of cells has to be done efficiently to maintain their biological functions [81].

While designing a biosensing system, it is important to consider the advantages and shortcomings of each type of bioreceptor. It is challenging to develop a biosensing device with all the ideal characteristics [92]. The bioreceptor for a particular biosensor should be chosen according to the analyte that needs to be detected, and the dynamic range required for the particular application. Additionally, other factors need to be taken into consideration while choosing a particular type of bioreceptor, such as the biological matrix in which detection needs to be performed, the storage requirements of the developed biosensing device, and the stability requirements.

For most of the work reported in this thesis, I chose to work with antibodies as bioreceptors because of the properties of antibodies, such as high specificity, sensitivity, and high affinity towards the target analyte [77]. In addition to that, the acquisition of antibodies is smooth because of the availability of many suppliers. Hence, this work is limited to using antibodies as bioreceptors for nanophotonic-guided mode resonance-based biosensors. However, exploring other bioreceptors, such as aptamers and other artificial bioreceptors for detecting biomarkers in the future, will be of interest.

1.6. Labelled and Label-Free Biosensing:

In the labelled-based approach, labels or tags are utilised to detect the analyte, and features of the label play an important role in the detection process [93]. Labelled approaches can detect target molecules with high sensitivity due to the amplification in the signal provided by the label and the reduction of background noise [94, 95]. Examples of labels used for this purpose are enzymes, nanoparticles, quantum dots, etc. [96]. The labelling-based approach for biosensing suffers from several shortcomings, such as the labelling of the analyte molecule can cause the alteration of inherent properties of the analyte when conjugated with a label or a tag [97]. Also, the process of labelling the analyte or target increases the complexity of detection because of the multiple steps required to perform the process and makes the method more costly [95]. Another major shortcoming of the labelling approach is misleading results because of the possibility of the label's blockage of the binding site [98].

Label-free biosensing works by converting bimolecular interactions taking place on the surface of the transducer directly into optical or electrical output signals that can be measured. It leverages properties such as the mass of biomolecules in the case of quartz crystal microbalance sensors and the refractive index in the case of optical biosensors. Label-free methods also offer the opportunity to monitor biomolecular interactions in real time. This approach gives more straightforward information, and biomolecules are utilised in their native form without any modifications [99, 100]. The label-free

method is more suitable when developing biosensing devices, which are required on a large scale because of advantages such as cost-effectiveness and ease of use [101]. Figure 5 depicts the mechanism of biosensing using label-free method.

In this work, I have focused on developing label-free nanophotonic biosensors based on guided mode resonances. One of the major problems with label-free approaches for biomolecular detection is the difficulty of measuring analytes in complex biological fluids. I have focused on designing biological interfaces for nanophotonic biosensors to perform measurements in complex biological fluids in a label-free manner.

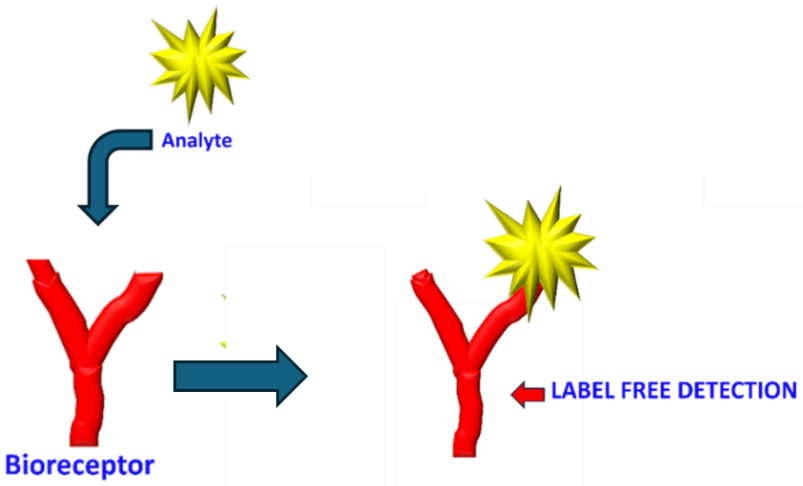

FIGURE 5: Figure depicting antibody-based label-free biosensing approach for analyte detection using antibodies as bioreceptors.

1.7. Major challenges in the wide-scale commercialisation of biosensors:

Though much research is being done on developing biosensors, there are significant hurdles in their mainstream deployment. Some of the major issues are as follows:

1. Achieving high Sensitivity: Developing biosensors with high sensitivity is a significant challenge [102]. For example, sensing or detecting biological markers of interest in biological fluids is challenging because of the high background noise in biological fluids [103]. High sensitivity is an important factor considered when developing biosensors for early disease detection, as most of the disease biomarkers at early stages of the disease are present at very low concentrations, and highly sensitive biosensors are needed to capture those biomarkers [104].

2. Designing an efficient biosensing interface: A robust and stable bio-interface is important for fabricating effective biosensors [34]. Developing a stable biological interface is challenging because of several factors, such as biorecognition elements, such as an enzyme or antibodies, which are prone to degradation over time [1, 105]. Also, the biochemistries developed so far for designing bio-interfaces for biosensors suffer from disadvantages such as high cost, multi-step process, time-consumption, and being sensitive to water and air [106, 107]. Additionally, the lack of standardised protocols for bioreceptor immobilisation is also one of the major hurdles in the wide-scale implementation of label-free biosensors because of inconsistency in sensor performances, as shown here in Table 2, the similar biosensing modalities giving different limits of detection for the same biomolecule.

TABLE 2: Performance Comparison of different photonic biosensors.

Sensing Modality	Protein	LOD	Surface functionalisation	Reference
Mach–Zehnder interferometer	CRP	184 pg/mL	3-aminopropyl) trimethoxysilane +bis(sulfosuccinimidyl)suberate	[108]
Mach–Zehnder interferometer	CRP	19.478 ng/mL	Physical adsorption of antibodies on sensor surface	[109]
Microring resonator	Avidin	6.8 ng/mL	3-aminopropyltriethoxysilane+ EZ-Link Sulfo-NHS-SS biotin	[110]
Microring resonator	Avidin	10 ng/ml.	Aminopropyl triethoxy silane+ Succinimidyl-6(biotinamido)hexanoate	[111]
Long period grating	Anti-IgG	7 ng/mL	Graphene oxide + EDC/NHS chemistry	[112]
Long period grating	Anti-IgG	0.025 mg/L	Silica titania sol-gel film coating+ Eudragit L100 +EDC/NHS	[113]
Etched Fibre gratings	CRP	0.82 pg/L	3-glycidyloxypropyl trimethoxysilane	[114]
Etched Fibre gratings	CRP	0.01 mg/L	anti-CRP and graphene oxide complex	[115]

3. Regulatory compliance: Biosensors designed for diagnostics applications are required to pass strict regulatory compliance requirements established by bodies such as the U.S. Food and Drug Administration and other regulatory bodies before they can reach the marketplace and customers. Achieving regulatory compliance for biosensors designed for the diagnosis of medical conditions involves a thorough process with multiple steps to ensure safety and effectiveness [103, 116].

4. Efficient Miniaturisation: Efficient miniaturisation is very important for realising portable and easy-to-use point-of-care biosensors. Reducing the dimensions of the active sensing surface to the nanoscale offers the advantages of an enhanced signal-to-noise ratio but can result in issues such as increasing the biosensor's response time [117]. Additionally, in the case of silicon photonic-based biosensing systems, it is difficult to couple light efficiently when reduced in size, and this is a major challenge in their deployment as point-of-care devices [26].

5. Biofouling of the sensing surfaces: Fouling of the transducer surface by clinical samples, such as blood, decreases the efficiency of biosensors. Developing efficient antifouling strategies is a challenge [118]. Figure 6 depicts an example of the sensor surface biofouling from the biomolecules present in the blood.

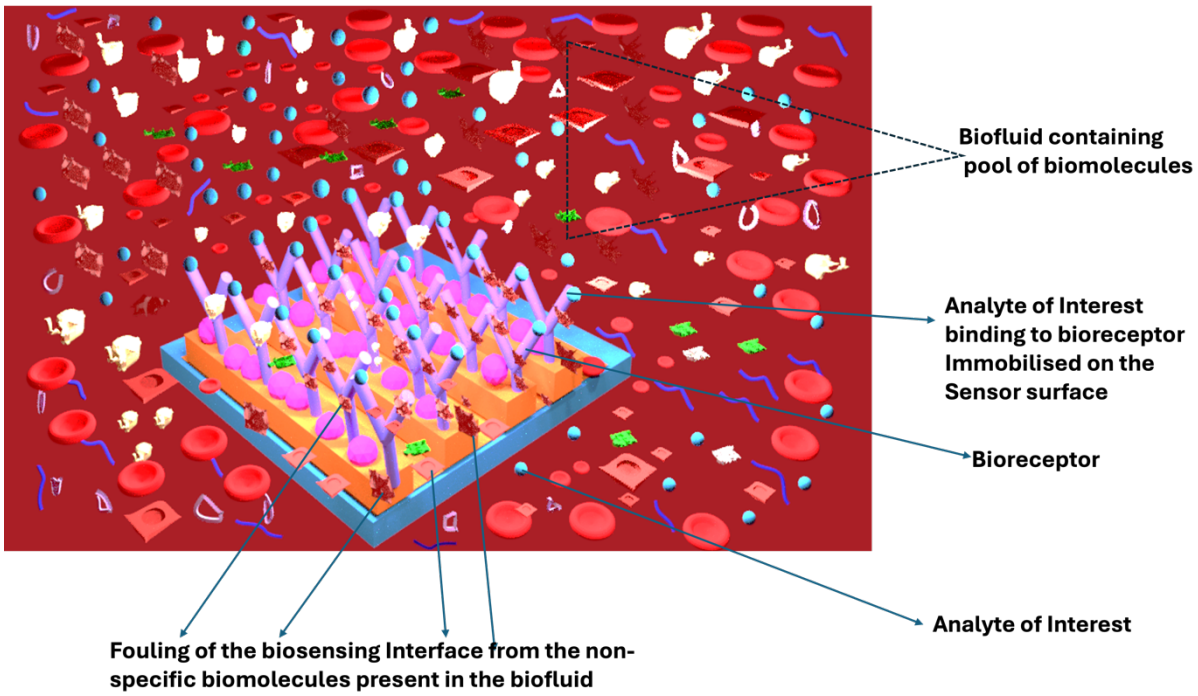

FIGURE 6: Fouling of the biosensing surface caused by blood containing a pool of biomolecules.

1.8. Scope, objectives and summary of thesis:

1.8.1. Scope of the thesis:

The guided mode resonance (GMR) based silicon nitride photonic sensing modalities being developed in our group solve some of the above-discussed problems. This sensing setup can be developed as a miniaturised lab-on-chip-based system because of advantages such as easy light coupling and eliminating the need for a spectrometer for data readout, due to the sensor's chirping, as we demonstrated here [119]. The focus of my work is on the development of a stable biological interface for chirped guided mode resonance-based photonic sensors, which can efficiently immobilise bioreceptors and perform detection in complex biological fluids in a label-free manner. I have studied bioinspired polydopamine (PDA) surface chemistry for bioreceptor immobilisation. PDA is a material-independent surface chemistry that enables simple and easy, one-step bioreceptor immobilisation on chirped silicon nitride biosensors, eliminating the need for multiple steps required in generally used surface chemistries to perform bioreceptor immobilisation on biosensors [32, 120]. The combination of chirped silicon nitride-based guided mode resonance (GMR)-based sensors with polydopamine (PDA) presents a compelling approach for enhancing optical biosensing platforms, by simplifying the functionalisation workflow and offering a promising pathway toward developing highly sensitive, robust, and easily functionalisable optical biosensors for next-generation diagnostics and environmental monitoring.

1.8.2. Objectives of the thesis:

The primary aim of the work is to study and validate bioinspired polydopamine-based chemistry for immobilising bioreceptors on chirped silicon nitride guided-mode resonance photonic sensing chips. The key objectives outlined are:

1. To evaluate the performance of polydopamine-based surface chemistry for the immobilisation of various bioreceptors, on chirped guided mode resonance biosensors and stability of polydopamine surface chemistry in different environmental conditions.
2. To investigate the analytical performance of the functionalised chirped guided mode resonance-based biosensors in detecting a range of clinically relevant protein biomarkers (IgG, CRP, MMP-9, TNF-α, IL-6) and study the suitability of the polydopamine-based interface to perform measurements in complex human biofluids.
3. To develop a bio interface for the detection of wound biomarkers and perform detection of wound biomarkers in phosphate buffer, hydrogel-based wound dressings and wound

biomarkers in clinical wound fluid absorbed hydrogel dressings using chirped guided mode resonance-based sensing chips.

4. To develop a bio interface for the detection of enzymes as an analyte in phosphate buffer saline and clinical urine using chirped guided mode resonance-based biosensors.

1.8.2. Summary of the thesis:

The results reported in this thesis indicate that the PDA surface functionalisation protocol for bioreceptor immobilisation seems to be a good choice when wide-scale fabrication of biosensors is required as it is cost-effective, gives high bioreceptor immobilisation density, is easy to implement, stable in aqueous environments and thus addresses some of the limitations associated with the so far used surface functionalisation protocols for bioreceptor immobilisation. The analytical performance of PDA-based surface chemistry to perform measurements in complex biofluids, such as 10 % human serum, was also studied. Furthermore, the optimised biosensing system was utilised to make progress towards the development of a near-patient testing system for monitoring of chronic wounds in a non-invasive manner by measuring the inflammatory biomarkers IL-6 and TNF-α in the hydrogel dressings containing human matrix and clinical wound exudate. In addition to that, the bio interface was developed for trypsin enzyme detection in human urine by monitoring the hydrolysis of the substrate (beta (β)-casein here) by the enzyme.

Overall, the thesis reports the design of PDA surface chemistry-based biological interfaces for silicon nitride based guided mode resonance photonic biosensors for the detection of protein-based disease biomarkers such as antigens and enzymes, in complex biological fluids such as human urine, 10 % human serum, human wound exudate, and human matrix absorbed hydrogel dressings in a label-free manner.

Chapter 2. Nanophotonic Biosensors

2.1. Label-free nanophotonic biosensors:

The label-free detection of analytes is gaining interest because of advantages such as rapid and cost-effective detection [100]. Label-free sensors use biological receptors immobilised on the transducer surface to detect analyte molecules [32]. Using label-free biosensors, detailed information such as affinity and kinetics of biomolecular interaction can be extracted [121].

Nanophotonic sensors can be employed to detect analytes with high sensitivity in a label-free manner [122]. Nanophotonic structures can control light in below-wavelength scale volumes and magnify light-matter interactions. These sensors perform the biosensing function by utilising the properties of the evanescent wave. The evanescent wave exponentially decays along the vertical axis of the biosensing surface. The evanescent wave decay length is hundreds of nanometres, and it is possible to detect various analyte molecules by choosing a suitable bioreceptor and employing evanescent wave-based nanophotonic biosensors [123, 124].

The most popular and widely used evanescent wave-based biosensing technology is surface plasmon resonance-based sensing technology since its introduction in 1990 [125]. Plasmonic biosensing technologies utilise metal-based structures such as metal films or other metal-based nanomaterials. When a light photon touches the surface of the metal at a certain angle of incidence, the coupling of light energy with the free electrons present in the metal layer takes place, which causes oscillation of the electrons and this movement of electrons on the surface is called surface plasmon resonance [126, 127]. The resonance can be classified or identified in two types as propagating surface plasmon resonance, that is, the resonance that is propagating along the surface, or localised or confined surface plasmon resonance. Both these types of resonances result in the formation of an evanescent field that permeates the surroundings. This generated evanescent field can be used to monitor the bimolecular reactions taking place on the surface [128, 129]. Thus, plasmonic biosensors can be used to monitor real-time biomolecular interactions taking place on the surface of these sensors and to obtain information such as affinity and kinetics of biomolecular interactions [127]. The bulk detection limits that plasmonic sensors have been able to achieve are in the range of 10^{-5} and 10^{-7} refractive index units [128]. The limitations of biosensors based on plasmonic materials are high-temperature instability, incompatibility with the complementary metal oxide semiconductor technology (CMOS) fabrication processes, and high optical losses [123, 130].

2.2. Silicon nitride-based photonic biosensor:

Silicon nitride is a widely used material to develop optical biosensors. Some of the important features of silicon nitride are its compatibility with CMOS fabrication, making it a cost-effective material for wide-scale biosensor production, low scattering losses, its ability to operate in the visible and infrared regions, strong light interaction, and thus making silicon nitride a robust platform for developing biosensors [131]. Moreover, silicon nitride offers better chemical resistance, making it a good choice of material to operate in different types of biofluids [132, 133], and it is possible to clamp silicon nitride-based optical sensors and microfluidics compactly for fluid transfer onto the sensor surfaces to develop biosensor surfaces [134]. Furthermore, silicon nitride-based surfaces can be easily functionalised for bioreceptor immobilisation [135]. Different types of biosensing architectures developed using silicon nitride as biosensing material are Mach-Zehnder interferometers and ring resonator-based biosensors [136, 137].

Like silicon nitride, silicon material is also widely employed and utilised for the development of biosensing devices. Biosensing devices with high sensitivity, cost-effectiveness, and easy multiplexing properties can be fabricated using silicon as a material for biosensor fabrication. It is possible to easily miniaturise because of compatibility with CMOS fabrication technology [138]. Silicon microring resonators and interferometric waveguide-based sensors, such as Young interferometers and Mach-Zehnder interferometers, are some examples of silicon photonic biosensors [26, 139]. Some of the limitations of silicon material are lower chemical resistance and limited operational wavelength [132, 133].

2.3. Guided mode resonance (GMR) based phenomenon:

Guided mode resonance gratings consist of a dielectric slab structure periodically modulated. The periodicity of the modulation is comparable to the wavelength of light, so the periodicity results in the slab exhibiting the properties of both diffraction gratings and waveguides. The waveguide can support guided modes that can couple to external incident light to excite guided mode resonances. Because these modes leak energy into the far field, they are called “leaky” or “quasi-guided” modes. For a specific choice of parameters (such as period, polarisation, incidence angle, and wavelength), the light coupled out of the structure can interfere destructively with the transmitted light. This results in constructive interference with the reflected light, producing an efficient resonant reflection for a specific wavelength (Figure 7) [26].

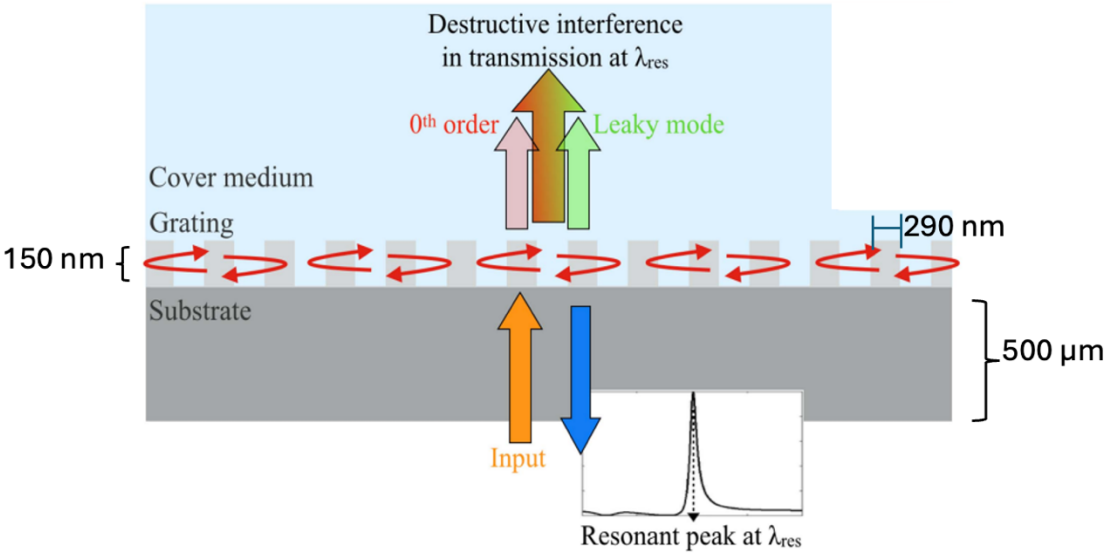

Figure 7: Image depicting excitation of guided mode resonance in wavelength scale gratings. The figure is taken reference from [26] under the Creative Commons Attribution 3.0 Licence.

The guided mode resonance effect is used in various applications, such as transmission filters, solar cells, etc.[140, 141]. It is of great interest in biosensing applications because of its properties, such as narrow and controllable linewidth and high efficiency [142].

2.3.1. Guided mode resonance (GMR) effect for biosensing applications:

Brian T. Cunningham et. al have made significant contributions in the field of development of guided mode resonance-based biosensing devices. One of the early works includes the development of a colorimetric resonant reflection-guided mode resonance-based biosensor as a direct biochemical assay technique by utilising the sharp spectral features of GMR and converting the biological interactions taking place on the surface of the sensor into a visible colour change [143]. Cunningham and coworkers further demonstrated the fabrication of plastic-based colorimetric resonant optical biosensors for multiparallel detection of label-free biochemical interactions, and with that opening the way for mass production of disposable biosensor chips [144]. Chan et al. used guided mode resonance-based sensors to study inhibitors of protein–DNA interactions and provide evidence for label-free screening of small molecule interactions in real time using guided mode resonance-based biosensors [145].

The guided mode resonance-based gratings can be used to sense the external refractive index changes. The resonance occurs when the incident light is coupled into a guided mode in the silicon nitride layer. The standing wave formed inside the grating significantly overlaps with the outside region via its evanescent field formed (as shown in Figure 9) and, hence, is sensitive to changes in the external refractive index. Thus, by monitoring the change in the resonance wavelength, the change in the external refractive index can be tracked. By functionalising the surface with bioreceptors, these gratings can be used for biosensing applications. The bioreceptors are immobilised on the high-index waveguiding layer. The binding of the analyte molecule with the bioreceptor that is immobilised on the surface of the grating results in an increment in optical density on the surface of the surface, which in turn increases the refractive index on the surface. The increment in the refractive index on the surface results in the increment in the effective index of the guided mode and which in turn results in the change of resonance wavelength. This change in the resonance wavelength can be monitored to quantify the binding of the target molecule on the grating surface [26, 146] as shown in Figures 8 and 9.

The sensor is usually designed to detect molecular binding events that occur very close to the surface. Hence, in determining the lowest concentration of analyte, the sensor can detect the surface sensitivity plays an important role. The surface sensitivity of the biosensor is defined as the wavelength shift observed upon the binding of biomolecules with the bioreceptors present on the sensor's surface. The surface sensitivity is determined by various factors and parameters, such as the polarisation of light used and the density or the number of the bioreceptors present on the sensor's surface [26, 146]. The evanescent tail that is utilised for biosensing on the GMR surface, as shown in Figure 9, can be represented in terms of the mode's effective index (n_{eff}) and the refractive index of the cladding (n_1). A simple derivation for the extent of the evanescent tail is as follows.

A wave propagating in a planar waveguide can be represented using this version of the wave equation, considering spatial coordinates only:

$$\nabla^2 E + k_0^2 n^2 E = 0 \quad \text{..... (1)}$$

If only the transverse direction is considered, we can solve this equation as follows, with β the propagation constant of the waveguide mode and n_1 the refractive index of the cladding.

$$E(x) = E_0 e^{-\sqrt{\beta^2 - k_0^2 n_1^2}\,x} \quad \text{..... (2)}$$

The 1/e depth then determines the spatial extent of the mode into the cladding.

The 1/e depth x_0 occurs when

$$\sqrt{\beta^2 - k_0^2 n_1^2}\, x_0 = 1 \quad \text{..... (3)}$$

The equation can be solved further by simplifying it by using.

$$\beta = k_0 n_{eff} \quad \text{..... (4)}$$

$$k_0 \sqrt{n_{eff}^2 - n_1^2}\, x_0 = 1 \quad \text{..... (5)}$$

Solving further gives the equation.

$$x_0 = \frac{\lambda_0}{2\pi} \frac{1}{\sqrt{n_{eff}^2 - n_1^2}} \quad \text{..... (6)}$$

Ideally, the overlap of the evanescent wave with the bioreceptor layer should be maximised to achieve high surface sensitivity [26]. The length of the evanescent wave outside of the grating can be calculated using this equation, depending on the refractive index of the cover medium.

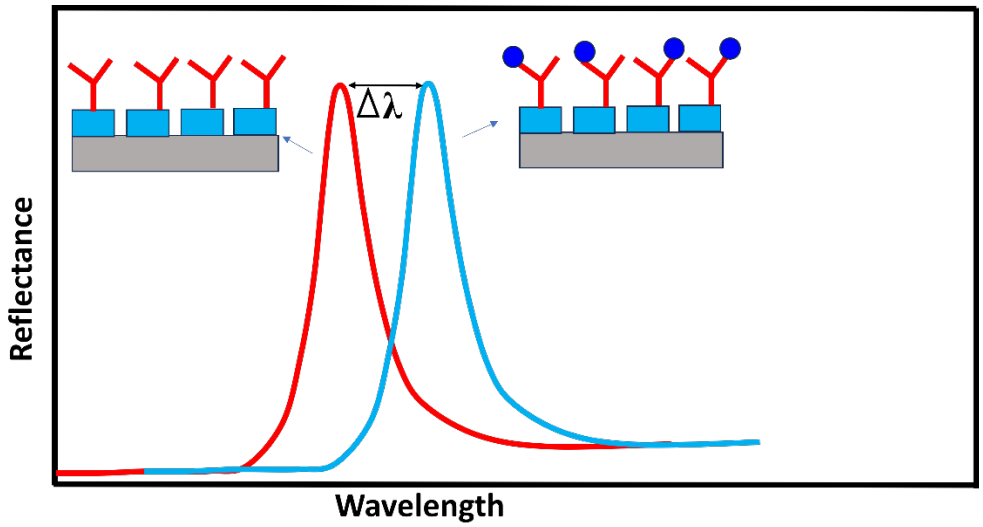

FIGURE 8: Mechanism of biosensing using guided mode resonance-based biosensors. Biological interaction on the surface of the guided-mode resonance biosensor shifts the resonance wavelength.

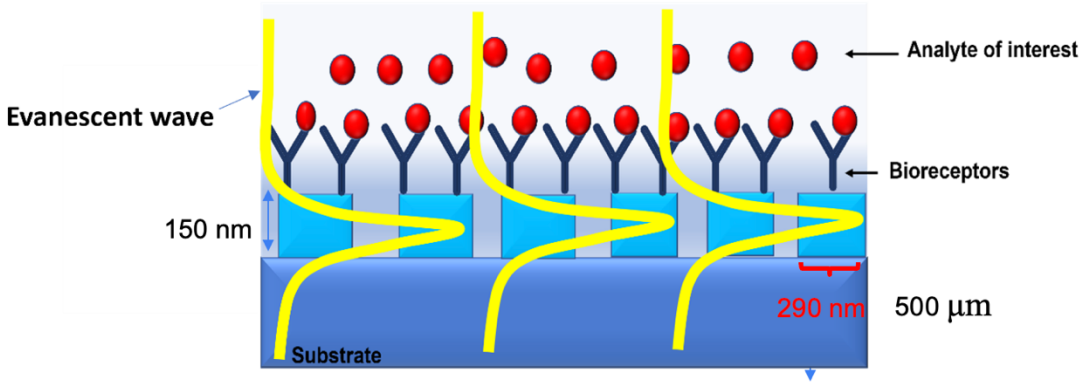

Figure 9: Evanescent wave used by guided mode resonance-based grating sensor for biomolecule detection.

Various studies have reported the use of guided-mode resonance effects for biosensing applications [147-149]. The four major detection methods employed by guided mode resonance-based sensing modalities are the detection of wavelength shift, detection in the angular shift, shift in intensity detection, and detection of phase shift [142].

The transverse-electric (TE) or the transverse-magnetic (TM) polarized quasi-guided modes are excited on the basis of the polarisation of incident light on the surface of the grating. TE and TM modes interact with the surrounding medium differently, which enables differentiation on the basis of polarisation. In the case of TM mode, the direction of the electric field is parallel to the grating vector; on the other hand, in the case of TE mode, the electric field is perpendicular to the grating vector and the Q factor values for both these modes are different. The TM mode exhibits stronger confinement and has better overlap with the surface of the grating and, hence, is more sensitive for the detection of small molecules such as proteins and other biological molecules, while the TE mode is more suitable for the detection of bigger analytes, as the decay length of TE mode is longer than TM mode. In my work, I have therefore focused on using the TM mode [26, 150, 151].

2.3.1. (i) Performance parameters of guided-mode resonance (GMR) based sensors:

- Bulk Limit of Detection: To characterise the performance of the guided-mode resonance sensor, determining the bulk limit of detection is an important parameter. The bulk limit of detection is obtained by dividing the 3 sigma (sigma is noise observed in measurements) values by the sensitivity of the sensor. The slope of the calibration gives the sensitivity of the sensor [26]. Typically, the bulk limit of detection observed for chirped-guided mode resonance-based sensors is around 10^{-4}-10^{-5} RIU [152, 153]. Determining the detection limit for biological analyte detection is complicated, as several other factors, such as surface functionalisation and optimal bioreceptor density, need to be considered [32, 146].

- Q factor: The Q factor is used to describe or explain the sharpness of the resonance peak and is represented as the ratio of the resonance's central wavelength to its full width at half maximum. Sharper peaks correspond to higher Q factors, are easier to track, and make it possible to detect even the smallest change that takes place [26, 146]. However, there are some limitations associated with achieving very high Q factors such as higher Q resonances are more susceptible to scattering loss, resulting in a low resonance amplitude, reducing the sensor's signal-to-noise ratio [154]. The typical field distribution of a TM mode used in my work is shown in Figure 18c.

The GMR-based sensing system is not the most sensitive detection method existing so far in terms of bulk limits of detection. Still, it is easy to bring to practice because of the possibility of large-scale fabrication in a cost-effective manner using techniques such as nanoimprint lithography and easy light coupling. Further, the sensing performance of guided mode resonance sensors can be enhanced by improving the surface sensitivity by designing an efficient biosensing interface.

2.3.2. Chirped guided mode resonance (GMR) based biosensor:

With other types of photonic biosensing modalities being developed, one of the significant limitations associated with miniaturisation is the need for a spectrometer to read the data. Here, we perform the chirping of gratings to eliminate the need for a spectrometer. The gradual or continuous change in period along the length of grating is termed the chirping of guided mode resonance sensors [146] as shown in Figure 10a sketch of the gratings shows the chirping of the grating. Exposing the surface of a chirped guided mode resonance grating with a light results in a narrow portion or band of grating resonating, as shown in Figure 10b. The interaction of biomolecules on the sensor surface results in a shift in the position of this resonance. Thus, the biological interaction on the surface of the sensor can be quantified by monitoring the shift in the position of resonance by taking images at regular intervals, thus eliminating the need for a spectrometer for data readout [146, 153]. The chirping of the grating results in only a narrow strip of grating resonating and thus helps in the conversion of spectral information into spatial information. The grating that I have used in this work for that period varies between 432-440 nm, and the filling factor is 0.7. The gratings are designed for a resonance wavelength at around 650 nm. The reason for choosing this range as the operational wavelength range is because of very negligible absorption or loss exhibited by silicon nitride in the visible light region. Additionally, borosilicate glass is also lossless in the visible range. Therefore, silicon nitride gratings on a borosilicate substrate are appropriate for operation and handling at 650 nm. Further, the introduction of chirping has made it possible to eliminate the need for a large readout instrument, making them comparatively better candidates for lab-on-chip devices.

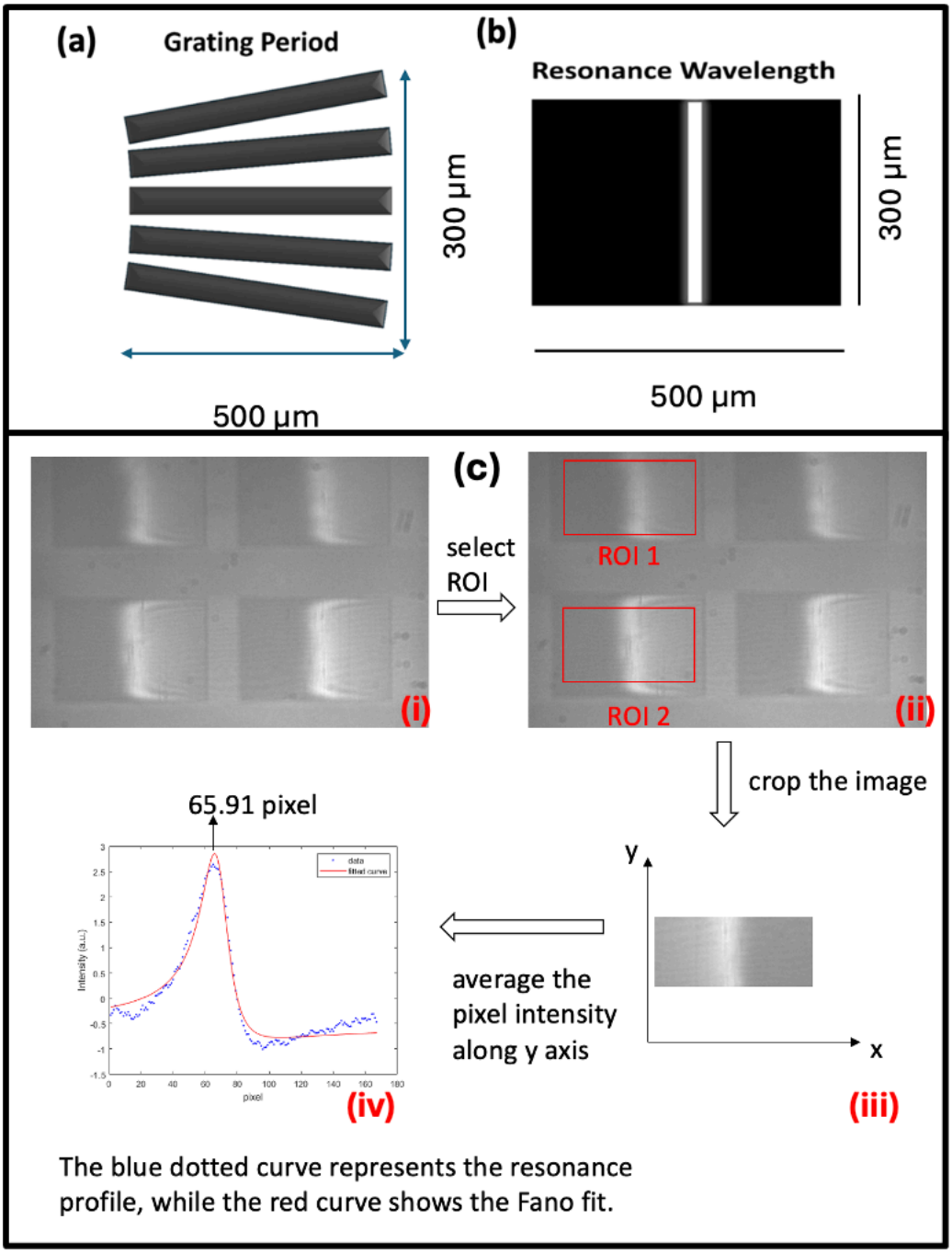

FIGURE 10: (a) Picture depicting the grating design used in the study with period varied along the length of the grating; (b) Only narrow strip resonating on a silicon nitride-based chirped guided mode resonance sensor; (c) Data processing steps to track the change in resonance position in accordance to the refractive index changes on the surface.

2.3.2 (i) Data processing to make graphs of chirped guided mode resonance sensors.

A series of images over time, each indicating and representing the sensor surface's optical properties when exposed to different experimental conditions for example, exposure to proteins, binding and unbinding of biomolecules, washing of the sensor surface with buffers, etc. was taken and saved:

1. Image Acquisition**:** A series of images was captured and collected by employing a camera during the full running duration of the experiment, as shown in one frame in Figure 10c-i.
2. Region of interest selection**:** From a representative frame chosen, two regions of interest were selected, Figure 10c-ii

   Channel 1 is assigned as the reference region and is chosen in an area where no binding activity or biochemical interaction takes place, and hence it is used as a control channel.

   Channel 2 is assigned as the measurement region and is the region where biomolecular interactions or binding events are expected to occur.

   These regions are selected to extract and obtain intensity profiles for further data analysis.
3. For each image in the time series that is captured, the selected regions of interest are extracted and saved. To obtain the accurate location of resonance, firstly, the averaging in the horizontal direction was performed. This was followed by performing the fitting of a curve to the intensity profile that is averaged, as shown in an example in Figure 10c.
4. Peak Detection via Fano Curve Fitting**:** Analysis of each intensity profile was performed to determine the position of maximum intensity, which corresponds to the resonance peak. A Fano-type line shape is fitted to the profile for the precise location of the peak under monitoring. The reason for choosing the fano curve was that the resonance arises from the combined effect of Fabry–Perot resonance in the thin film and Bragg resonance in the grating. The fitting and selection of the peak position is performed using MATLAB, making use of the nonlinear least-squares method. The change in the refractive index on the surface of the grating results in a change in the resonance position correspondingly.

   The fano equation can be presented as equation 7, where *a, b, c, d, e* are fitting parameters, among which *a* depicts the Fano shape, *b* depicts the symmetry of the curve, c depicts the linewidth of the curve, *d* depicts the shift of the curve, *e* depicts the offset. The determination of parameters is done with initial starting points followed by optimisation through a MATLAB built-in nonlinear least squares optimiser.

$$f(x) = a\left(\frac{bc + (x-d)^2}{c^2 + (x-d)^2}\right) + e \quad \text{.....(7)}$$

5. The peak positions from all frames are compiled and put together, and then are plotted as a function of time, which helps in analyzing the biochemical interactions taking place on the sensor surface. The reference channel here acts as a control and provides a baseline, and the measurement channel indicates and reflects the changes due to biochemical events on the sensor surface.
6. The resulting graph obtained typically consists of distinct phases. An increment or decrement in the resonance shift indicates binding or unbinding, respectively, that has taken place on the sensor surface.

2.4. Integration of silicon nitride photonic sensors in miniaturised lab-on-chip systems:

To develop silicon nitride photonic sensors in miniaturised lab-on-chip-based systems for point-of-care applications, silicon nitride-based sensors need to be integrated with microfluidics for sample delivery on the sensing surface, cost-effective light sources and data readout systems, and efficient bioreceptor immobilisation methods for their mass commercialisation and deployment.

2.4.1. Microfluidics for sample delivery:

An efficient microfluidics design is crucial for developing miniaturised lab-on-chip based on silicon nitride sensors. Progression and development in fabrication techniques enable developing micro and nanometre-sized patterns for controlling fluid flow through nanophotonic sensors. By combining microfluidics with together with photonic sensing devices, efficient liquid transport over the sensor surface can be achieved by gaining control over fluid flow, reducing the volume of fluids required for measurements, reducing the analysis times, and making multiplexing possible and amplifying the light-matter interaction, thus enhancing the sensor performance [155-157].

In my work, I have employed polydimethylsiloxane (PDMS) based microfluidic channels to transport biomolecules on the sensor surface. PDMS-based microfluidic channels are widely used to fabricate microfluidic channels because of properties such as biocompatibility, high optical transparency, easy fabrication, and minimal toxicity [158, 159]. The PDMS channels employed in this work are 450 μm wide channels with 100 μm spacing between them, with a channel height of is 100 μm (Figure 11). Although PDMS-based microfluidics has many advantages, but they also suffer from some drawbacks, such as non-specific protein adsorption on the PDMS surface [157, 160]. Hence, there is a further need to explore better materials to fabricate microfluidics for biosensors.

To avoid nonspecific protein attachment on the surface of microfluidics designed using PDMS, we incorporated polyethene glycol polymer into the PDMS mixture to enhance the sensitivity and detection efficiency for protein biomarkers detection.

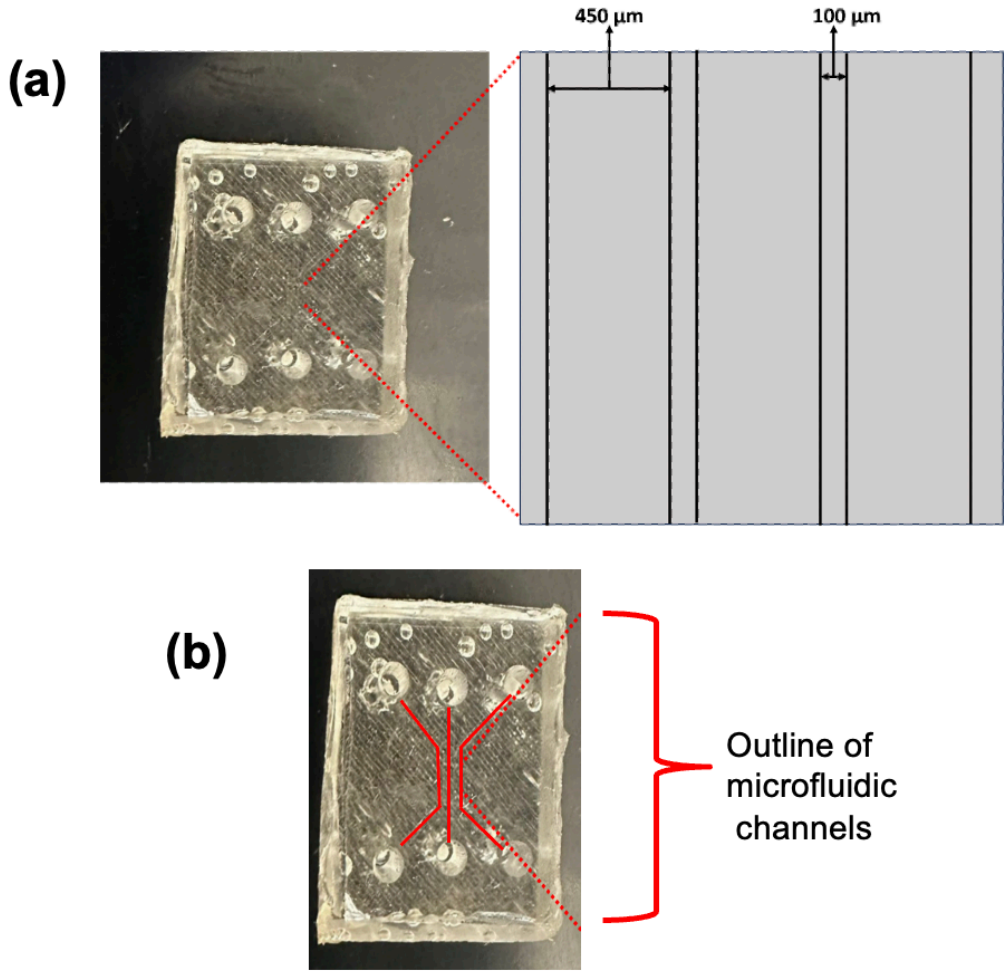

FIGURE 11: (a) Optical image of the polydimethylsiloxane-based microfluidic channels. The width of the channels is 450 µm with 100 µm spacing between them. The height of the channels is 100 µm; (b) Optical image of polydimethylsiloxane microfluidic channels with the outline of microfluidic channels drawn.

2.4.2. Cost-effective light sources and data read-out systems:

Further, for the efficient development of silicon nitride photonic sensors as point-of-care devices, all components, such as light sources and data read-out systems, must be integrated into a chip-based system to develop portable devices for broad deployment. Using Light-emitting diodes and CMOS cameras in place of bulky instruments such as lasers as light sources and spectrometers as read-out systems can be useful in constructing portable silicon nitride photonic biosensors. However, the major challenge that comes with this is achieving the same sensitivity with miniaturised systems as with full-

scale instruments [128, 161]. In addition, developing better data acquisition and data processing methods, such as using machine learning techniques, can further help in increasing the efficiency of lab-on-chip-based biosensors [162].

In our lab, we have successfully miniaturised the GMR-based biosensing system into a miniaturised lab-on-chip type system, as can be seen in Figure 12. The outer box was designed using 3D printing, and the inner setup was designed using cost-effective optical components such as an LED light source and a CMOS camera, as described in detail in the reference [119].

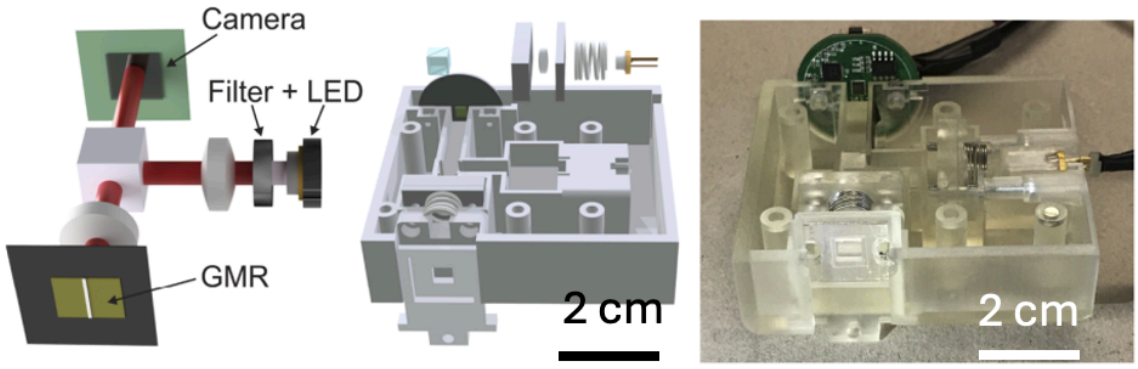

FIGURE 12: Miniaturised guided mode resonance-based sensor setup designed using 3D printing to design the outer box, LED as light source, and CMOS camera for data read out. The figure is reprinted from the reference [119] under the terms of the Creative Commons Attribution 4.0 License.

2.4.3. Biological interface for silicon nitride photonic biosensors:

The biological interface plays an essential role in achieving the sensitivity required in biosensing platforms and enhancing the performance of developed biosensing modalities. For example, Hu et al. reported an increment of five-fold in detection sensitivity and a three-fold decrement in the response time of silicon photonic biosensors by increasing the number of probe molecules on the sensor surface by employing an in-situ probe synthesis technique [163]. Surface-chemistry techniques that employ different types of silanes together with different linkers for biological molecules attachment and biotin-streptavidin-based strategies are utilised to design biological interfaces for silicon-based photonic biosensors. These chemistries are time-consuming and expensive and suffer from several limitations, such as instability in water and air [106, 107]. There is a need and requirement to develop robust and cost-effective surface functionalisation methods, considering the extensive rollout aspect of the biosensor.

I have worked on developing biological interfaces for guided mode resonance-based biosensors using polydopamine surface chemistry, described in detail in Chapter 3.

2.5. Fabrication methods of guided-mode resonance-based sensors:

2.5.1. Electron beam lithography:

Electron beam lithography (EBL) is the commonly used technique for nanoscale pattern fabrication. With the use of EBL, it is possible to pattern high-quality nanoscale features [164]. The EBL method of fabrication employs an accelerated beam of electrons for patterning structures as small as 10 nm in dimensions on the substrates coated with a resist that is sensitive to the electron beam. The properties of resist, such as the solubility, change after getting exposed to the beam of electrons, and thus enabling the selective removal of either the exposed region of the resist or the non-exposed part by placing the sample in a developer solution [165, 166]. Though this method helps in fabricating high-quality structures, it is not a very suitable method when large-scale fabrication is required as the fabrication process is lengthy, and the cost is high with low throughput [164].

2.5.2. Nanoimprint lithography:

Nanoimprint lithography (NIL) is a cost-efficient method for the fabrication of nanostructured patterns at a fast pace with high resolution [164, 167]. As opposed to electron beam lithography, which employs electrons to change the chemical as well as physical properties of the resist coated on the substrate, NIL operates by directly deforming the resist by using a mold, as shown in Figure 13, for pattern transfer. This makes it possible for NIL to go beyond the resolution limitations imposed by the beam scattering [168]. Using NIL, it is possible to pattern 10 nm size features on hard as well as soft substrates [167]. NIL technique can be used to fabricate structures for applications in the field of photonics as well the as biological engineering [169]. For example, the NIL technique can be used for applications such as nanofluidic channel fabrication [170] and biomimetic structures fabrication [171].

2.6. Materials:

Sylgard^{TM} 184 Silicone elastomer kit was purchased from DOW. Dimethylsiloxane (60-70% ethylene oxide) block copolymer was purchased from Gelest. The electron beam resist ARP-13 and charge dissipation layer ARPC-5090 were purchased from ALLResist GmbH (Germany). Microposit^{TM} remover 1165 was obtained from Dupont. Propanol and acetone were purchased from VWR Chemicals. Hydrogen peroxide 35 wt % and sulphuric acid were purchased from ThermoFisher Scientific. Epoxy resin SU-8 2050 was purchased from Kayaku advanced materials. UV PDMS KER-4690 A and UV PDMS KER-4690 B were purchased from Microresist GmbH, and UV-NIL resist mr-NIL213FC-200nm_XP is also from Microresist GmbH. SiN-on-glass substrates were bought from Silson Ltd with 150 nm thick Si_3N_4. Phosphate buffer saline (PBS) tablets were purchased from Sigma Aldrich.

2.7. Methods:

2.7.1. Fabrication protocol of guided-mode resonance (GMR) sensors using nanoimprint lithography:

The first step is to prepare a silicon master using electron beam lithography (the Master was prepared by Dr. Kezheng Li) and reactive ion etching (RIE). Next, place one drop of silane solution in a petri dish in a desiccator and place the Silicon master on another plate for 5 minutes. Next, mix UV PDMS KER-4690 A and UV PDMS KER-4690 B in a 1:1 volume ratio and leave the mixed PDMS in the desiccator for 20-30 minutes until the bubbles disappear. Afterwards, pour the PDMS into the silicon master, then UV expose for 14 minutes, increasing every 7 minutes to check if the PDMS gets harder. If it is soft, then extend for another 7 minutes. This is followed by coating the SiN substrates with the resist called PDMS-compatible UV-NIL resist mr-NIL213FC-200nm_XP by spin-coating at 3000 rpm for 60 s, followed by baking at 60 °C for 3 minutes. The next step was, careful stamping of the PDMS mold to the NIL resist-coated sample, followed by placing the weight on it and UV exposure for 7 minutes. Afterwards, RIE was performed for 10 minutes, followed by placing the sample into an O_2 plasma apparatus powered 100%, and the time was 10 minutes. Lastly, the sample was put into a 98% H_2SO_4 solution for 5 minutes to remove residuals and rinsed with water.

2.7.2. Fabrication protocol of guided mode resonance (GMR) sensors using electron beam lithography:

Start by cleaning the SiN substrate in an acetone ultrasonic bath for 5 min, followed by Isopropyl alcohol (IPA) ultrasonic bath for 3 mins, and then rinse in DI water. Afterwards, apply piranha etch for 5 mins, followed by rinsing in DI water and drying in nitrogen gas. Next, spinning of ARP-13 resist at 5000 rpm for 60 s, followed by a bake at 180 °C for 5 minutes. This is followed by spinning the charge dissipation layer (ARPC 5090) at 2000 rpm for 60s and baking at 90 °C for 2 mins.

The next step is to define the pattern using a Raith Voyager electron-beam lithography tool with an aperture of LC 40 μm, current 130 pA, voltage 50 kV, dose of 145 μC/cm^2, step size 1 nm in x-direction and 4 nm in y-direction. Remove the ARPC layer after the ebeam exposure in DI water for 2 mins, then dry with N_2. Develop in xylene for 2 mins, followed by IPA for 2 mins, then dry with N_2. Then reactive ion etching of the SiN layer for 7 minutes. The recipe for reactive ion etching is a gas mixture of 12.5 sccm CHF_3 and 2 sccm O_2, at 1.8 e-2 mtorr, with a power of 43 W, DC bias 360V. Then remove the resist by placing the sample into 1165 resist remover in an ultrasonic bath at 50% power for 12 mins, then acetone ultrasonic for 5 mins, IPA ultrasonic for 3 mins, rinse in DI water and dry with N_2. The last step is to perform another piranha clean of the sample surface to further remove any residual. The sensors were fabricated by Dr. Kezheng Li.

Dr. Pankaj K. Sahoo fabricated the samples used in the work reported in Chapter 4. The process was mostly similar, with slight differences as described below.

To start, the SiN substrate is cleaned in acetone with an ultrasonic bath for 10 mins, followed by cleaning in an IPA ultrasonic bath for 5 mins and distilled water ultrasonic bath for 2 mins. Next, rinse in distilled water and dry with N_2. Then put the prepared substrates into an oxygen plasma at 200W, 5 sccm O_2 for 5 min. This is followed by coating of the resist ARP13 by spinning on SiN at 5000 rpm for 60 s, after that the substrate is baked at 180 °C for 5 mins. The next step is the coating of a charge dissipation layer ARPC 5090 at 2000 rpm for 60s, then the substrate is baked at 90 °C for 2 mins. This is followed by performing electron-beam lithography using a Raith Voyager tool with parameters as follows: aperture of LC 40 μm, beam current 130 pA, voltage 50 kV to define the GMR with the dose of 145 μC/cm^2, step size 1 nm in x direction and 4 nm in y direction. After performing the electron beam lithography, the removal of ARPC layer is done by placing the substrate in distilled water for 2 mins. Afterwards, the development is performed by placing the substrate in xylene for 2 mins, IPA for 2 mins and drying with N_2. This is followed by performing reactive ion etching for 7 minutes with using a gas mixture of 12.5 sccm CHF_3 and 2 sccm O_2, at 1.8 e^{-2} mtorr, and power at 43 W, DC bias 360V. The resist removal step is performed by placing the sample into 1165 resist remover and ultrasonicating the sample for 12

mins, followed by placing the sample in acetone ultrasonic bath for 3 mins and IPA ultrasonic for 1 min followed by rinse in distilled water and drying with N_2. The last step is to clean the sample in piranha for 5 minutes to remove any remaining residuals.

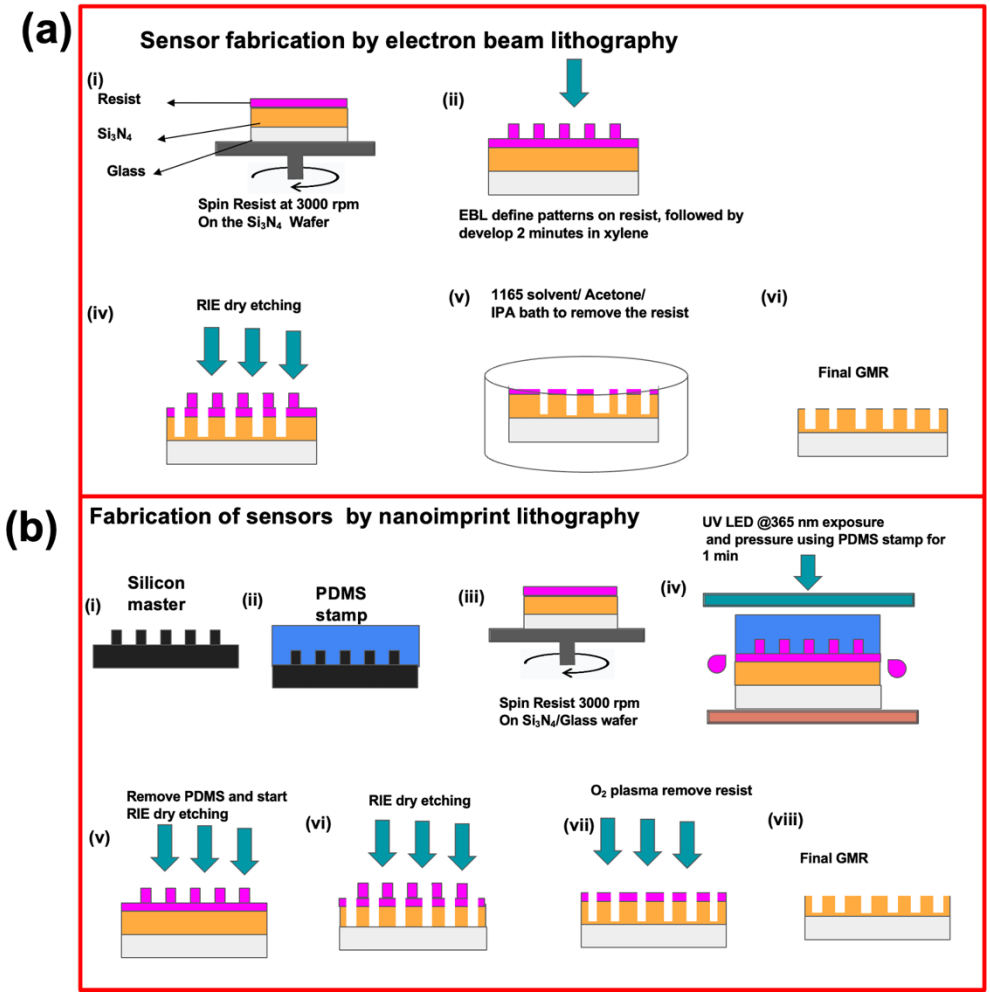

Figure 13: Schematic depicting sensor fabrication steps by (a) Electron beam lithography and (b) Nanoimprint lithography. The image is provided by Dr. Kezheng Li.

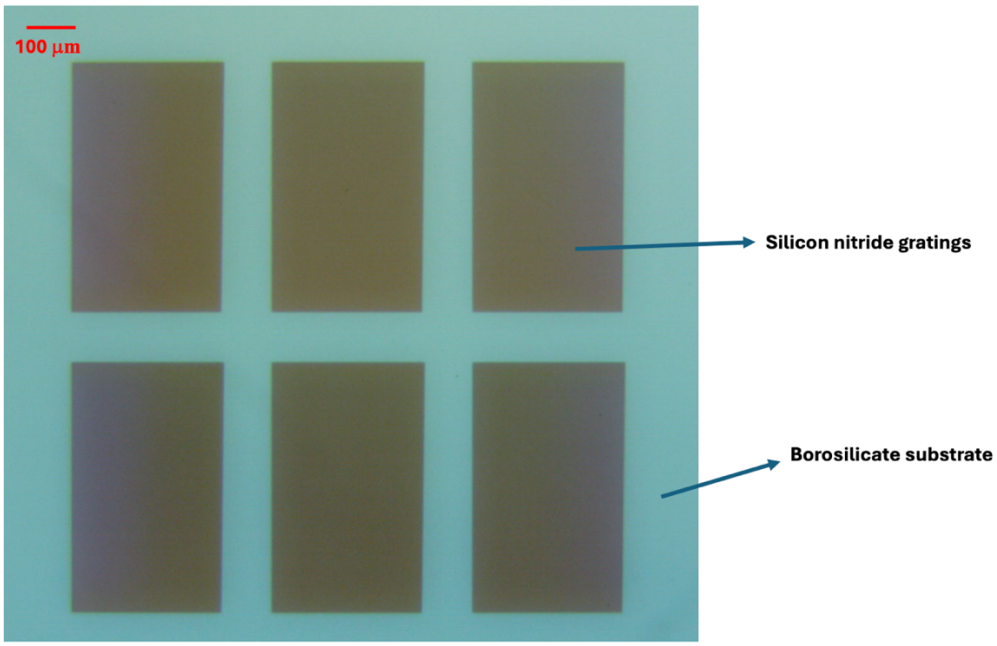

FIGURE 14: Optical Microscope of image six guided mode resonance sensors fabricated with electron beam lithography taken at 4x magnification.

2.7.3. Fabrication of microfluidic circuits:

The various analytes are introduced to the chirped GMR sensor through a microfluidic channel made from a molded polydimethylsiloxane (PDMS) elastomer, which is clamped to the top of the sensor. The mold is fabricated using negative photoresist SU-8 2050 and UV lithography with a direct laser writer (DILASE 650, Kloé). The resist is spin-coated onto a silicon wafer to give a thickness of ~145 µm, followed by soft baking at 65°C for 5 min and 95 °C for 20 min before being exposed to a 375nm UV light, at 65% modulation and 1 mm s^{-1} stage speed. After exposure, the resist is baked again at 65°C for 5 min and 95 °C for 10 min, followed by development in EC-solvent for 15 min. Finally, the mold is rinsed in isopropanol and hard baked at 180 °C overnight. The PDMS elastomer is prepared at a ratio of 7:1 (elastomer: hardener) with 0.5% (w/w) PEG-CO-block-polymer (Dimethylsiloxane (60-70% ethylene oxide) block copolymer, Gelest) added to reduce antigen binding. The mixture was outgassed for 20 minutes, poured into the mold, and cured at 65 °C overnight. Finally, PDMS channels and GMR chip were clamped together in a custom 3D-printed holder to form a watertight seal and provide inlets and outlets for the liquids.

The microfluidic channels used in the study were fabricated by Dr. Casper Kunstmann-Olsen.

2.8. Results and discussion:

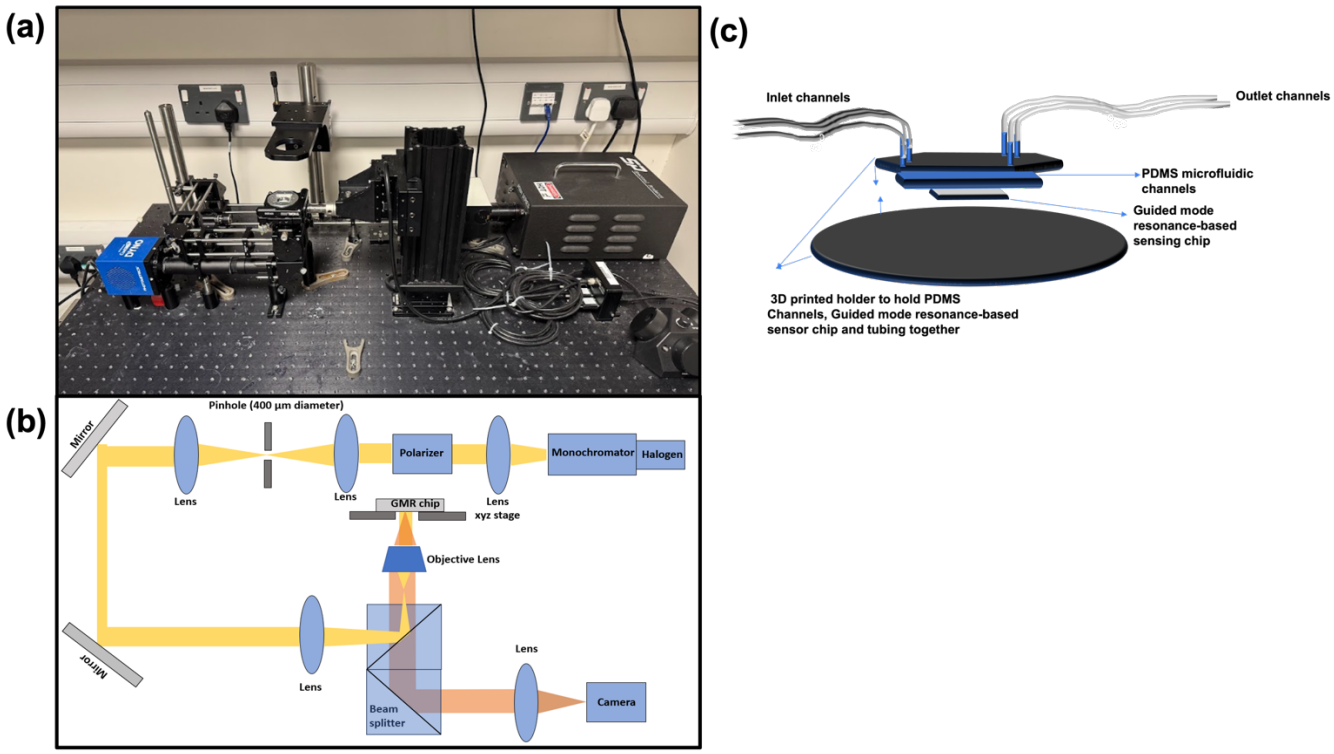

FIGURE 15: (a) Optical image of the setup used for the measurements; (b) Schematic of the optical setup ; (b) Schematic of the microfluidics together with 3D printed holder used to perform experiments.

2.8.1. Characterisation of chirped guided mode resonance (GMR) sensor fabricated using nanoimprint lithography:

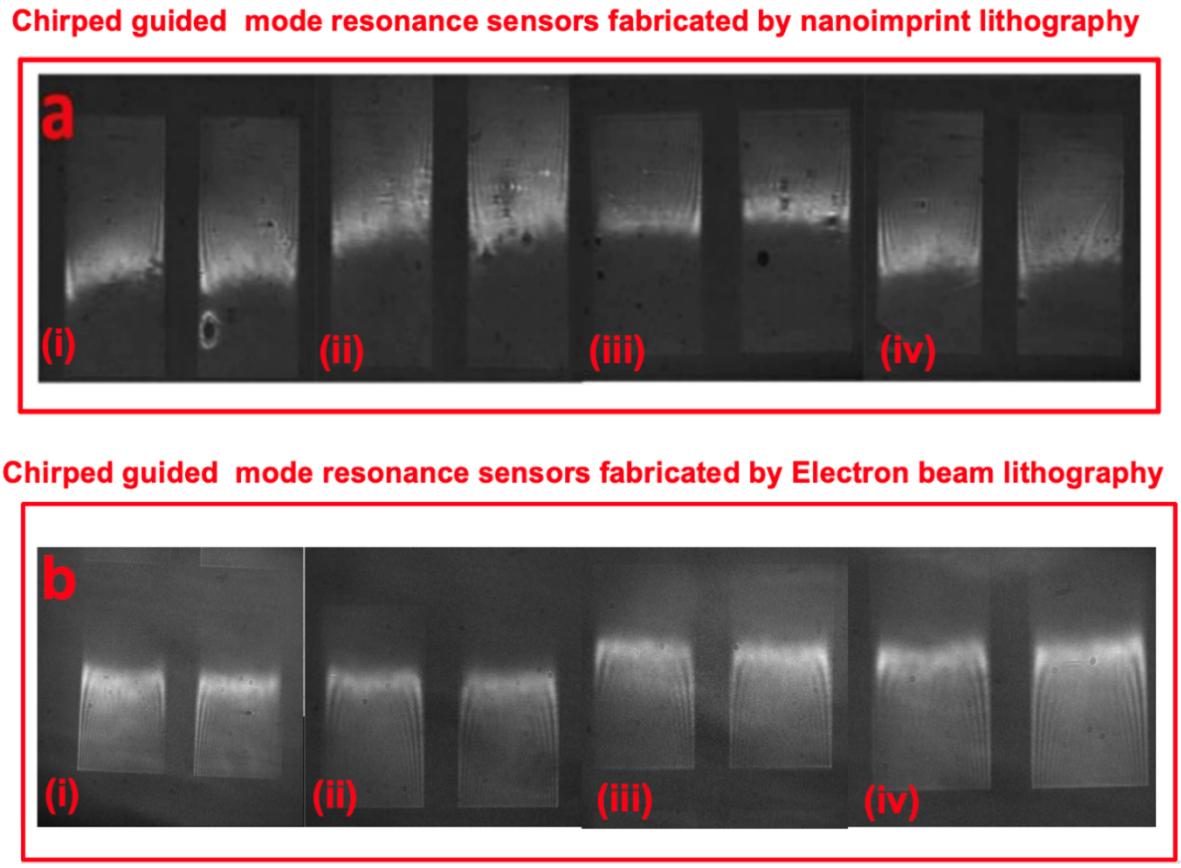

FIGURE 16: (a) Optical images of chirped guided-mode resonance gratings fabricated by nanoimprint lithography showing resonance at 650 nm; (b) Optical images of chirped guided-mode resonance gratings fabricated by electron beam lithography.

Figure 16a shows eight chirped-GMR gratings exhibiting resonance around 650 nm fabricated by nanoimprint lithography, and Figure 16b shows the eight chirped grating sensors fabricated by electron beam lithography. As can be seen in the image, the gratings fabricated by electron beam lithography show sharper resonances as compared to the sensors fabricated by nanoimprint lithography.

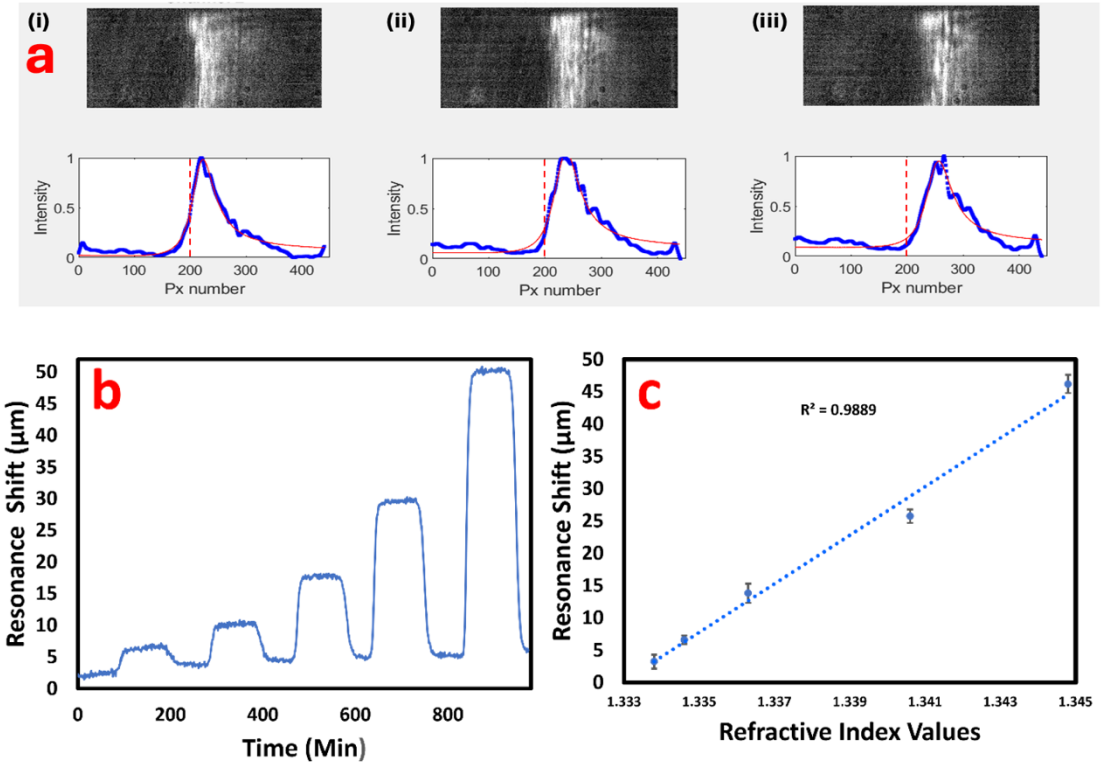

FIGURE 17: (a) Optical images of gratings showing the shifts in resonance position in response to change in refractive index on the surface of the sensor; (b and c) Resonance shifts for different phosphate buffer concentrations that gave different refractive index values in increasing trend as shown in Figure c, giving a bulk limit of detection of around 3.17×10^{-4}. Error bars represent the standard deviation observed from three separate measurements.

Figure 17a shows the change in resonance position on the grating surface when the refractive index on the surface of the sensor changes. To calculate the bulk limit of detection of sensor chips fabricated by nanoimprint lithography different concentrations of phosphate buffer saline solutions were prepared that gave refractive index values in increasing trend (1.3338, 1.3346, 1.3363, 1.3406, 1.3448). The volume of sample used for each measurement was 1mL. The resonance shift observed for each concentration is given in Figures 17b and 17c. The sensitivity of the sensors calculated from curve is 3756.2 µm/RIU. The sensitivity value in nm was calculated to be 75.125 nm/RIU. The bulk limit of detection is calculated using this formula:

$$\text{Bulk limit of detection} = \frac{3\ sigma}{senstivity\ of\ the\ sensor}$$

Sigma here is the noise observed in the measurements, and sensitivity is the slope of the calibration curve. The bulk detection limit of around 3.17×10^{-4} RIU. The bulk limit of detection that we achieve with the sensors fabricated using electron beam lithography is typically 10^{-4} -10^{-5} RIU [152, 153].

Microring resonators and interferometric waveguide-based sensors such as Young interferometers and Mach-Zehnder interferometers, are able to achieve a bulk detection limit in the range of 10^{-7}-10^{-8} refractive index units but suffer from limitations such as relatively large size and the need for precise light coupling when reduced size [26, 139].

The consistency of fabrication of good quality sensors with nanoimprint lithography was not good, and the efficiency of the process was low. The focus of the PhD project was to develop the biological interface for the GMR-based photonic sensors and not to optimise the fabrication process. Hence, I carried forward the work with GMR sensors fabricated using electron beam lithography by Dr Kezheng Li and Dr. Pankaj K. Sahoo.

2.8.2. Chirped guided mode resonance (GMR) sensors fabricated using electron beam lithography:

Figures 18a and 18b show the optical and scanning electron microscope images of GMR sensors fabricated by electron beam lithography. As discussed above, when chirped gratings are illuminated with a light source, only a narrow strip or line exhibits resonance when illuminated with light and imaged on camera Figure 18a. The resonance occurs when the coupling of light into a guided mode in the silicon nitride layer takes place. The standing wave formed inside the grating has a significant overlap with the outside region via its evanescent field (Figure 18c); hence, it is sensitive to changes in the external refractive index. Figure 18c shows the TM-polarized electric field distribution of a GMR sensor. The colour bar represents the normalized electric field strength, referenced to a flat silicon nitride substrate. The structure consists of silicon nitride gratings fabricated on a borosilicate glass substrate, with water as the surrounding medium. The figure is illustrating the evanescent field of the mode, which is decaying exponentially from the surface of the Si_3N_4 with penetrating depth of less than 200 nm, with the main field concentrated within the first 50 nm from the surface, that is enables monitoring of biochemical interactions near the sensor surface.

Thus, by monitoring the resonance position, the change in the external refractive index can be tracked. By functionalising the surface with bioreceptors (Figure 18d), these gratings can then be used for biosensing experiments.

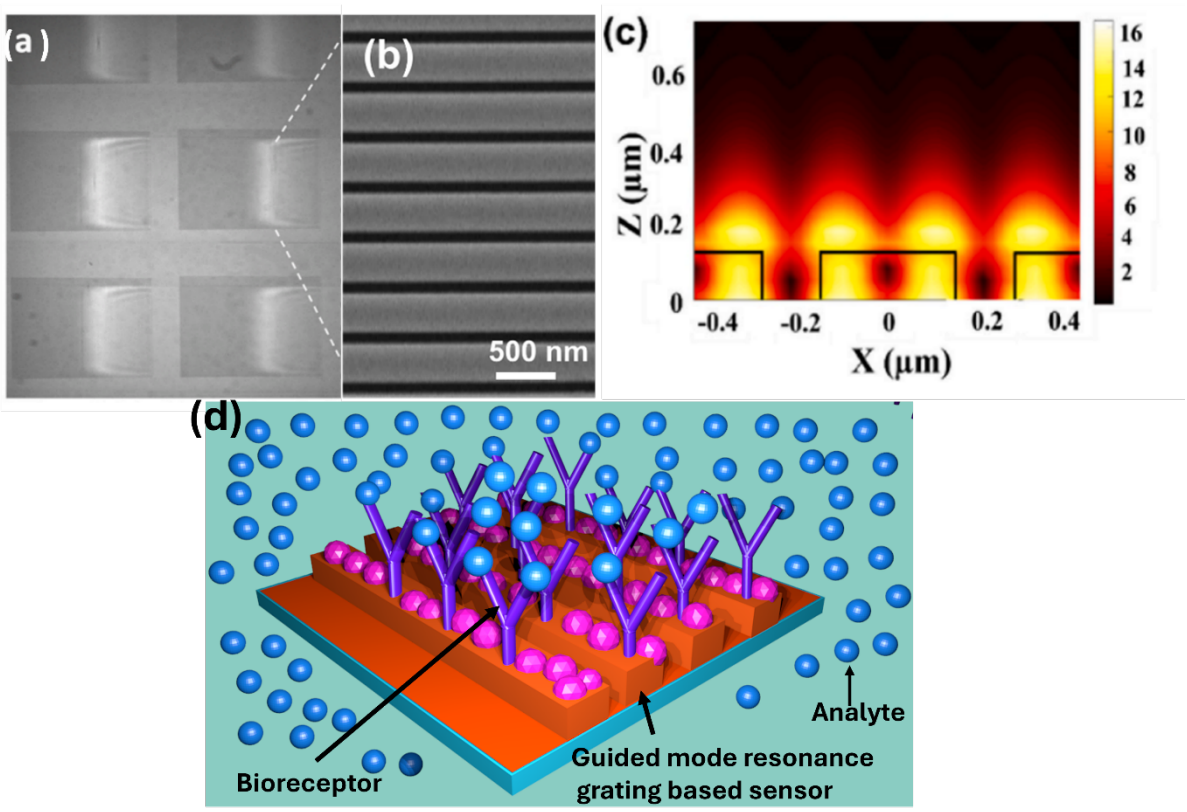

Figure 18: a) Optical micrograph of the resonance on the chirped GMR grating, taken in reflection. The image shows the resonances observed in reflection from chirped GMRs as a typical example; (b) Scanning electron micrograph of the grating. The period varies between 432-440 nm, and the filling factor is 0.7. The gratings are designed for a resonance wavelength around 650 nm; (c) E-field of the GMR on resonance (TM mode), highlighting that the evanescent field of the mode decays exponentially from the surface of the Si_3N_4 and the penetration depth is less than 200 nm, with the main field concentrated within the first 50 nm from the surface. The color bar represents the normalized electric field strength, referenced to a flat silicon nitride substrate. The structure consists of silicon nitride gratings fabricated on a borosilicate glass substrate, with water as the surrounding medium;(d) Bioreceptors immobilised on guided mode resonance based sensor surface for biosensing applications. Image 18c was generated by Dr. Kezheng Li.

Chapter 3. Bio-inspired polydopamine layer as versatile functionalisation protocol for silicon-based photonic biosensors

3.1. Importance of biosensing interface:

The surface chemistry used to functionalise biosensors can play a crucial role in the wide-scale commercialisation of biosensing devices [172]. The final performance of the biosensing device is decided by the combined performance of the bio interface and the transducing system [77]. Many surface functionalisation approaches have been developed for silicon nitride photonic biosensors, yet many of them have serious issues. Here, we explore a simple surface chemistry based on polydopamine and suggest that it may address the need for a simple yet high-performance interface.

3.2. Ideal surface functionalisation strategy:

The bioreceptor immobilisation strategy plays an essential role in determining the sensitivity, i.e., the ability of the biosensor to detect biomarkers at deficient concentrations, and the specificity, i.e., the ability to detect the desired biomarker. The density of immobilised biomolecules, reproducibility, and non-specific adsorption from complex biofluids also depend on the surface functionalisation strategy used. Figure 19 depicts the immobilisation of bioreceptor on a biosensing interface and requirements of an ideal biofunctionalisation protocol.

An ideal surface functionalisation strategy for photonic biosensors has the following qualities:

- It is mild, i.e., it does not cause damage to the bioreceptor and the transducer surface.
- The biofunctionalisation process is short, involving a few steps.
- It is congenial with evanescent field sensing in the case of optical biosensors.
- It provides good biological receptor attachment density and is reproducible.
- Resistant to nonspecific binding.
- It is easy to perform.
- It is compatible with mass manufacturing [107].

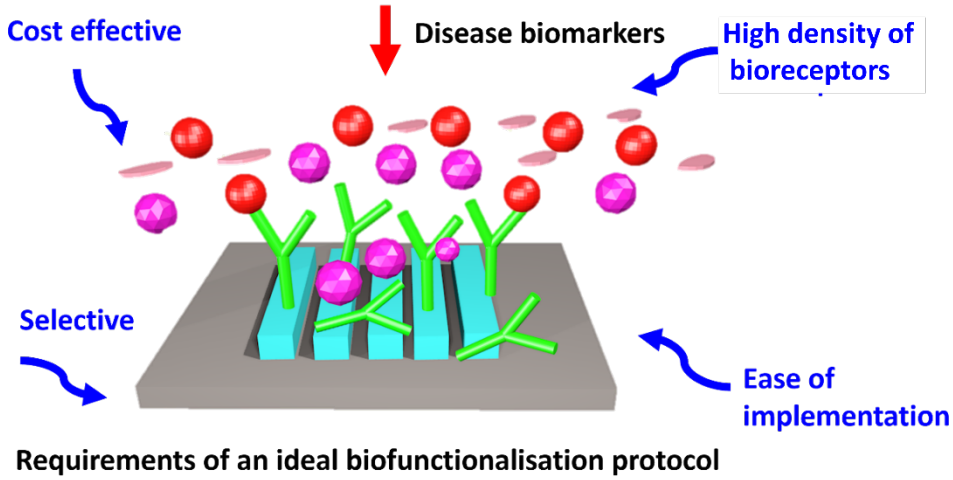

FIGURE 19: General requirements of an ideal surface functionalisation strategy.

3.3. Bioreceptor immobilisation strategies:

3.3.1. Adsorption approach:

The most straightforward approach to immobilise bioreceptors on the transducer surface is using an adsorption approach that utilises weaker forces such as electrostatic, hydrophobic interactions, Van-der-Waal forces, and hydrogen bonding for bioreceptor immobilisation on the transducer surface. Though this is an easy way of bioreceptor immobilisation, but has several limitations such as weak attachment of bioreceptors on the sensor surface, easy desorption of bioreceptors, irreproducibility, and instability. Additionally, this method can also damage the bioreceptors [32, 77, 172]. Figure 20a shows the immobilisation of bioreceptors on the surface by the adsorption process.

3.3.2. Covalent approaches:

Most covalent approaches employ self-assembled monolayers for the covalent immobilisation of bioreceptors on the sensor surface. The self-assembled monolayer formed or developed on the surface of the sensor can be used to covalently conjugate bioreceptors by employing crosslinking with bioreceptor molecules. Some advantages of the covalent approach are hold over the density of immobilised bioreceptors and charge on the surface of the transducer. Self-assembled monolayers for functionalisation are used according to the transducer material, e.g., alkanethiol-based self-assembled monolayers for gold-based surfaces and alkoxysilanes-based self-assembled monolayers for silicon-based surfaces [77, 106, 107].

The use of silane-based self-assembled monolayers for surface modification and bioreceptor immobilisation for silicon-based surfaces has been widely studied. Even though this method is widely

studied, it is a multi-step and complicated process. Many factors impact the final performance of the functionalised surface, such as the time taken for deposition and formation of a self-assembled monolayer on the sensor surface, solvents used in the process to prepare reagents, the temperature at which the process performed, and total water content involved in the process. This method for bioreceptor immobilisation is not well optimised. The common silane-based self-assembled monolayers have amine, thiol, and carboxyl functional groups at the end terminal. These functional groups can be further cross-linked with biomolecules for their covalent immobilisation on the transducer surface [107]. Covalent immobilisation is generally performed together with the N-Hydroxysuccinimide (NHS) activation process. One of the significant drawbacks of NHS-based covalent linking is the hydrolytic nature of NHS esters, which results in reduced conjugation efficiency of bioreceptors [106, 173]. Figure 20b shows the immobilisation of the bioreceptor on the transducer surface using a covalent approach.

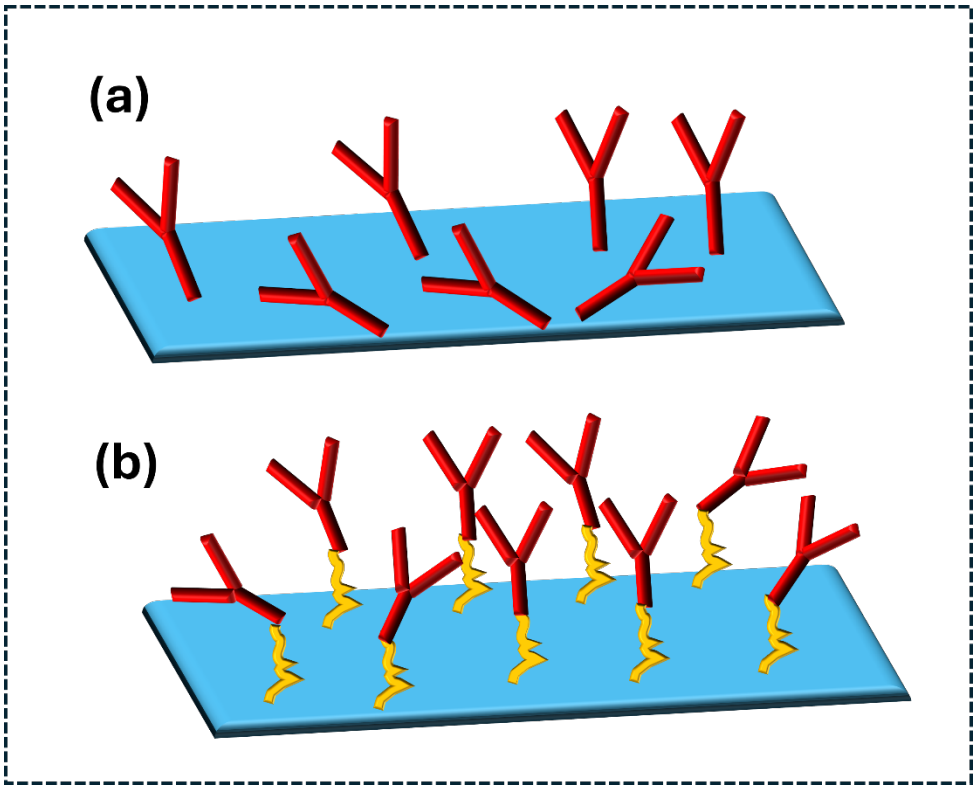

FIGURE 20: (a) Bioreceptor immobilisation on the surface by adsorption method; (b) Bioreceptor immobilisation on the surface by the covalent method using self-assembled monolayers.

3.3.3. Bio-affinity-based approach:

Bio-affinity-based bioreceptor immobilisation strategies are another widely used method for bioreceptor immobilisation. The streptavidin-biotin approach and the use of proteins A and G are bio-affinity-based approaches for bioreceptor immobilisation and are examples of affinity-based approaches for bioreceptor immobilisation. In the case of a biotin-streptavidin-based strategy for bioreceptor, immobilisation, a biotinylated bioreceptor is attached to the streptavidin functionalised surface. This surface chemistry results in the formation of highly stable and strong bonds between biotin and streptavidin and oriented, arranged immobilisation of biotinylated bioreceptor on the sensor surface. Some of the limitations of this approach are the requirement for labelling of the bioreceptors with biotin and interference from biotin that can lead to false positives [172, 174]. Employing proteins A and G for oriented immobilisation of bioreceptors is another example of a bio-affinity-based approach for bioreceptor immobilisation where protein A or G adsorb at the Fc region of antibodies and immobilise antibodies on the transducer surface in an oriented fashion. In the case of proteins A and G, the antibody-protein complex formed might dissociate due to the change in pH and other conditions which is undesirable and can badly impact the performance of biosensors [77, 175]. High cost is also a drawback of the bio-affinity-based approach for bioreceptor immobilisation [172]. Figure 21 shows the schematic bio-affinity-based approaches for bioreceptor immobilisation.

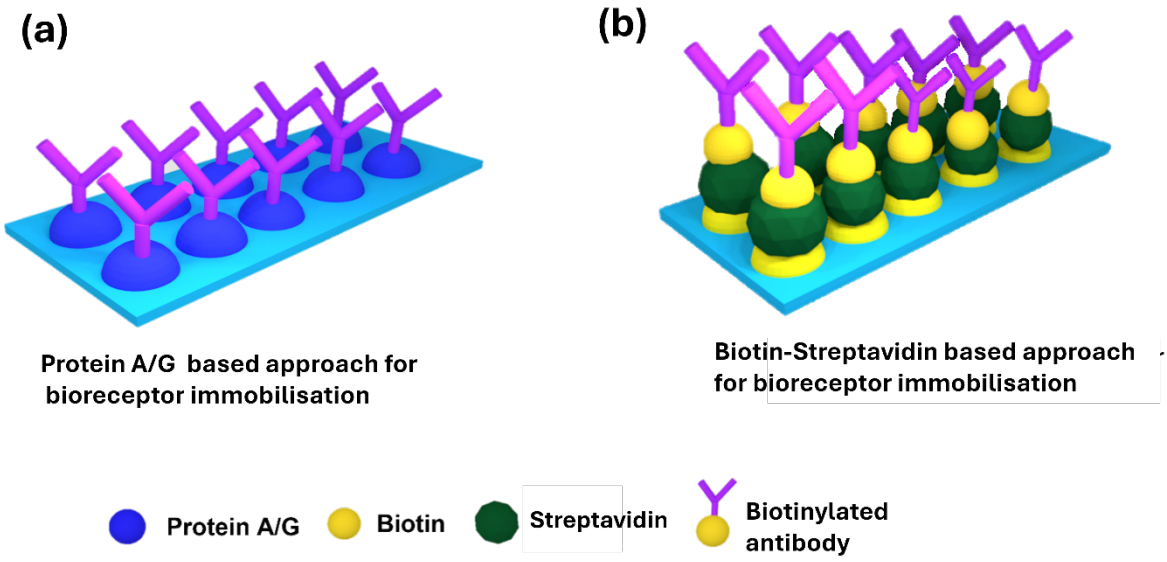

FIGURE 21: (a and b) Affinity-based approaches for bioreceptor immobilisation on the surface.

3.3.4. Polymer layers to immobilise bioreceptors:

Polymers coatings, such as dextran or polyethylene imine layers are used to immobilise bioreceptors on biosensing surfaces [176].

(a) Dextran polymer-based layers are widely used for bioreceptor immobilisation in surface plasmon resonance-based biosensors [177, 178]. For the attachment and immobilisation of biological receptors such as antibodies and proteins, a layer of Carboxymethylated dextran is fabricated on the gold surface [32]. Dextran molecule is a polysaccharide that can form hydrated hydrogel-based layers or films on the surfaces with functional groups present in the layer that interact with the functional groups present in biological receptors. However, this process requires the activation of the sensor surface before the formation of dextran layers, which is an extra step and makes the functionalisation process multi-step. Additionally, the issue of the mass transportation of analytes molecules within the hydrogel layer is also an issue with dextran-based layers for bioreceptor immobilisation on biosensors [179].

(b) Polyethyleneimines (PEIs) are categorised as polycationic polymers and contain repetitive units that can be classified as linear and branched polyethyleneimine chains [180].

The amine functional group in the repeating units makes PEI positive charge that is used to immobilise the biomolecules. For example, carboxyl functional group-containing molecules can form interactions with amine groups in the PEI layer, hence facilitating their immobilisation [181]. The amine-rich cationic nature of PEI plays an important role in forming stable complexes with negatively charged biomolecules or surfaces [182]. For immobilisation, further functionalisation steps such as EDC/NHS crosslinking or the use of biotinylated bioreceptors are required [181, 183].

The chemistries discussed above suffer from limitations such as long processing times, requiring multiple steps, and being expensive, making them less suitable when required for mass manufacturing of photonics-based point-of-care diagnostic systems.

3.4. Mussel-inspired polydopamine (PDA) surface chemistry:

Taking inspiration from the biomolecules found in adhesive proteins found in sea mussels Lee and coworkers presented PDA-based one-step surface chemistry to coat the surfaces with PDA from the aqueous solution of dopamine. Polydopamine surface chemistry is material-independent surface chemistry. Considering the limitations and drawbacks of the above-discussed chemistries, the mussel-inspired PDA coating appears to be a good alternative to the currently developed chemistries because of properties such as simplicity of surface functionalisation and activation, for biological receptor attachment, cost-effective, material-independent surface activation and film formation, biocompatibility, a one-step method for bioreceptor attachment and does not require any coupling agents for biomolecule conjugation. The dopamine molecule undergoes self-polymerisation under oxidative conditions, forming a layer that can attach to any surface without needing any surface modification or preparation of the surface because of the presence of catechol and amine functional groups in high concentrations, as in mussel adhesive proteins. The PDA layer provides a highly chemically reactive surface that can be further used to conjugate biomolecules on the formed PDA film [184-187].

In the last few years, PDA-based coatings have attracted significant interest in various applications such as drug delivery, imaging, etc. [188]. PDA films can act as a linking layer or conjugating layer for the conjugation of biomolecules. The reactive quinone functional groups on the surface of polydopamine act as linker points for further linking of biomolecules. Hence, the covalent immobilisation of biomolecules, such as proteins, deoxyribonucleic acid, etc., can be performed [189-191]. The PDA-based coating has been explored for different applications in the fields of energy, environment and electrochemical biosensors [120]. In one study Toma et al. used PDA thin films as a linker layer to immobilise antibodies on the sensor based on surface plasmon-enhanced fluorescence spectroscopy. The sensor chips functionalised by PDA chemistry exhibited good performance with a detection limit for Interleukin-6 (IL-6) of 2 pg/mL [187]. In short, polydopamine-based surface modification has received great interest since their discovery for a wide range of applications. Here in my work, I have used PDA surface chemistry to design a robust and simple bio-interface for guided mode resonance-based silicon nitride photonic biosensors.

Under the alkaline conditions, the self-polymerisation of dopamine to PDA takes place without any need of elaborate or sophisticated instrumentation [120]. The molecular mechanism that leads to the conversion of dopamine to PDA is still not properly clear and is actively researched because of the formation of various intermediate molecules as the conversion of dopamine molecules to PDA takes

place. One study conducted by Lee et.al indicated that PDA formation takes place via non-covalent self-assembly and covalent polymerisation [192].

The dopamine molecule is composed of a benzene ring with two adjacent hydroxyl groups present and a primary amine group also being there, as, shown in Figure 22, image a. The presence of two reactive functional groups enables dopamine molecule to undergo polymerisation, form polydopamine, and get attached or bind to different types of surfaces. The conversion of the dopamine molecule into the polydopamine molecule involves a series of reactions [120]. Dopamine converts to polydopamine under alkaline conditions. The detailed mechanism involves the following steps:

Step 1: Oxidation of Dopamine: Under slightly basic conditions, oxidation of dopamine-to-dopamine quinone takes place. The oxygen in air oxidises dopamine's catechol group to form dopamine quinone.

Step 2: Dopamine quinone then undergoes an intramolecular cyclisation reaction, resulting in formation of a leucodopaminechrome.

Step 3: This is followed by further oxidation and rearrangement reactions. Leucodopaminechrome undergoes oxidation and rearrangement and forms dopaminechrome, a dark-colored intermediate. These intermediates can further aggregate, rearrange, and crosslink to form oligomers [120].

Step 4: Further polymerisation and crosslinking of these small oxidised and cyclized species takes place through various non-covalent interactions such as cation-π interactions, π-π stacking, Hydrogen bonding and covalent interactions [193], leading to the formation of a highly crosslinked polymer network called polydopamine.

Because PDA has a combination of catechol groups, amine groups, quinone group, crosslinked aromatic structures, these functional groups interact through different mechanisms, depending on the type of surface. Studies have indicated the existence of functional groups, such as catechol or quinone, amino groups, and π-systems, etc., in the formed PDA films, which explains the excellent sticking or attaching ability of PDA films to different kinds of materials [120]. For example, with the presence of quinone and catechol functional groups in the PDA, the PDA film can form coordination bonds with the surface of different substrates, especially metallic surfaces. The PDA film can form a covalent attachment with the surfaces that have nucleophilic functional groups on their surface, thus making strong adhesion with the surface. In addition to these, other attraction forces, such as hydrogen bonding, Van-der-Waals forces, etc., helps in in sticking PDA films on different types of substrates with high strength [194].

The covalent attachment of biomolecules on the PDA film's surface mainly occurs via Michael addition and Schiff base reaction, as shown in Figure 22b. The amine functional groups that are nucleophilic in nature covalently attach to PDA layer via the Schiff base reaction or Michael-addition reaction, while

thiol functional groups side form covalent bonds via the Michael-addition reaction, as shown in Figure 22b. The attachment of biological molecules on the surface of PDA film can take place under gentle conditions. Sophisticated or complicated setups are not required for the reaction to take place. In addition to that, the biomolecule attachment to PDA film is very robust and stable in aqueous environments [120].

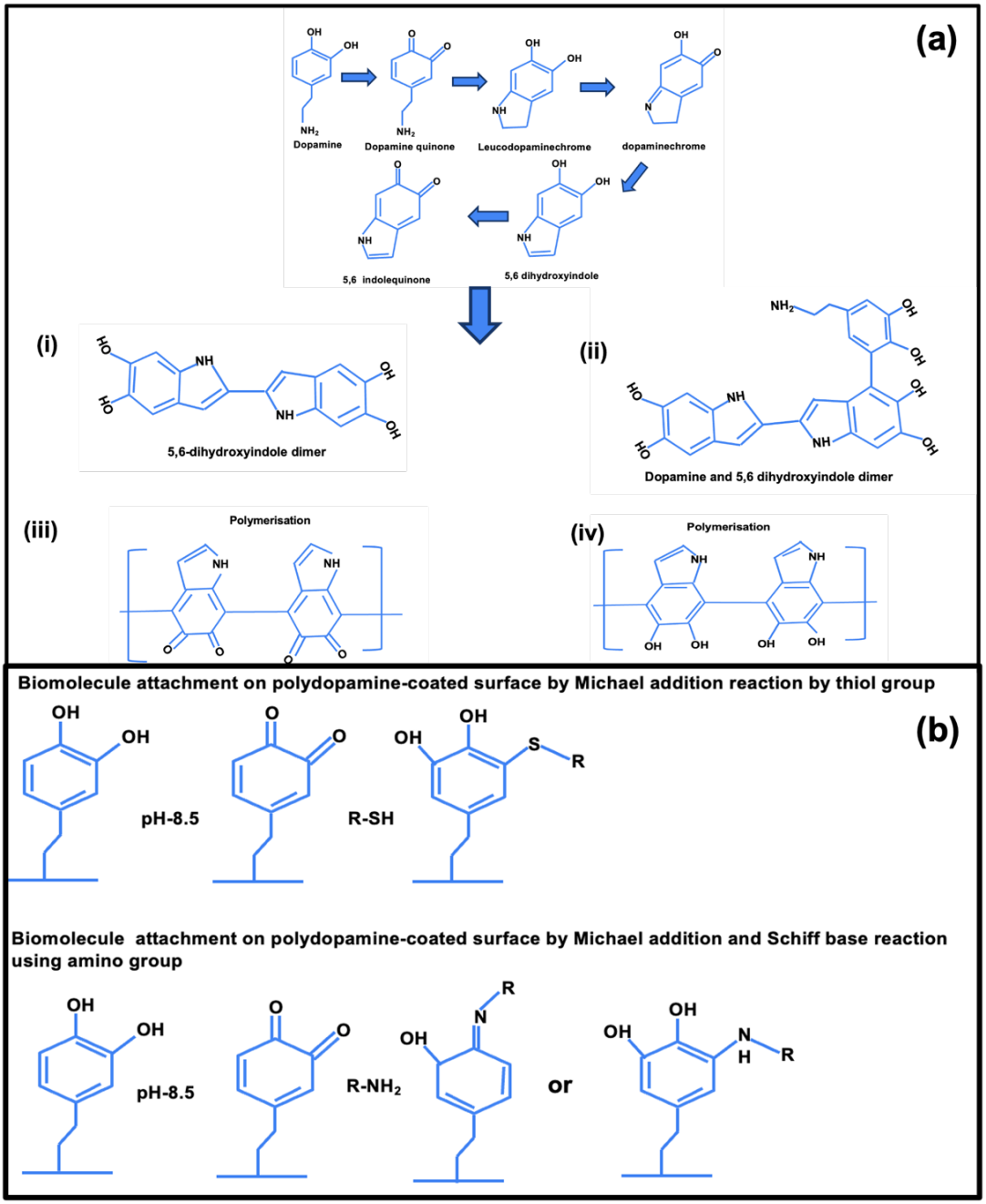

FIGURE 22: (a) Dopamine to polydopamine conversion mechanism; (b) Biomolecule attachment on polydopamine surface via Michael addition and Schiff base reaction. The chemical reactions presented here are according to the mechanism given in the references [120, 195].

3.5. Biosensing in complex biofluids:

Biosensing in complex biofluids, such as blood, is a great challenge that needs to be addressed for the proper utilisation and commercialisation of biosensors. A pool of biological molecules in biofluids causes the matrix effect and non-specific biomolecule attachment to the active sensing area [23]. To avoid non-specific binding from the biological matrix, treatment of the biological interface with surface blockers such as bovine serum albumin [196] or casein [197], or a polyethene glycol layer [198], etc., is performed. For example, Figure 23 shows the avoidance of non-specific binding from fetal bovine serum on the surface blocked using a polyethylene glycol layer. Additionally, Zwitterionic polymers are also now being explored [199] to develop non-fouling surfaces.

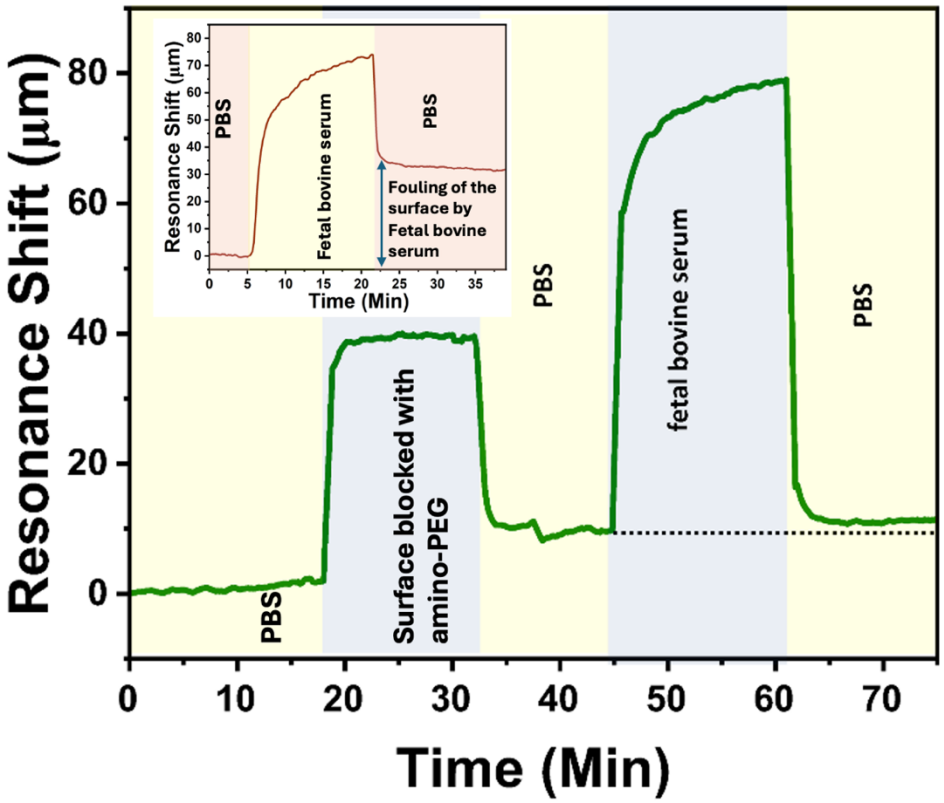

FIGURE 23: Data depicting the antifouling effect of amino-Polyethylene glycol (PEG) functionalised surface as all fetal bovine serum comes off when the washing step is performed with PBS buffer indicating negligible sticking of biomolecules from fetal bovine serum on the sensor surface. Inset image showing an example of fouling of the surface caused by fetal bovine serum when the surface is not blocked using blocker.

In this chapter, I have studied the analytical performance of PDA films as bioreceptor immobilisation chemistry. Chirped-GMR-based photonic sensors were employed to study PDA chemistry for silicon nitride photonic biosensors (Figure 24d-g). First, the PDA surface chemistry was studied using a commercial Quartz crystal microbalance and dissipation (QCM-D) based system. The compatibility of PDA-based surface chemistry with a wide range of antigen-antibody sets was studied using the QCM-D. Additionally, its performance with a silane-NHS linker-based chemistry was compared. The stability of films in aqueous environments was also studied using the QCM-D system. Moving forward, the compatibility of PDA surface chemistry with photonic biosensors here GMR-based sensors was studied, and a dynamic range was established for protein biomarkers Immunoglobulins (IgG), C-Reactive Protein (CRP), and Matrix Metalloproteinase-9 (MMP-9). The suitability of the PDA chemistry for performing measurements in biological fluids here: 10 % human serum was also studied. The application of PDA films as protectant films for silicon-based sensors in cell culture media was also explored as the cell culture media have previously been shown to degrade silicon-based sensors due to their alkaline nature when exposed for longer durations [200].

3.6. Materials:

Dopamine HCl, anti-rabbit-IgG (R2004-1MG), rabbit IgG (I5006-10 MG), sodium hydroxide (NaOH), phosphate buffer saline (PBS) tablets, casein, and mercaptotriethoxy silane (MPTES) were purchased from Sigma Aldrich. Tris buffer 0.5 M was purchased from Alfa Aesar, and NHS-$(PEG)_6$-Maleimide was purchased from ThermoFisher Scientific. Human TNF-alpha antibody (2TNF-H34A) and human TNF-alpha recombinant protein (PHC3011) were purchased from ThermoFisher Scientific, human MMP-9 antibody (AB911) was purchased from R and D systems. Human recombinant MMP-9 protein was bought from Sino Biological (10327-HNAH), Rabbit anti-human interleukin-6 antibody (AHP1040) and recombinant human interleukin 6 (PHP045) protein were purchased from Bio-Rad. C-reactive protein goat polyclonal antibody (GC019) and C-Reactive Protein (C0129) were purchased from Scripps Inc. SiN-on-glass substrates were bought from Silson Ltd with 150 nm thick Si_3N_4. SiO_2-coated quartz QCM-D sensors were purchased from Biolin Scientific. Human serum was purchased from Sigma Aldrich. Goat IgG isotype control (02-6202) antibodies were purchased from Invitrogen**.** Amine functionalised Silica nanoparticles dispersion in water (791342) were purchased from Sigma Aldrich.

3.7. Methods:

The sensors used in the study were fabricated by using the protocol described in Chapter 2, section 2.7.2.

3.7.1. PDA surface functionalisation protocol:

Both QCM-D and GMR-based sensors were employed to characterise the PDA surface chemistry protocol. The sensors were placed horizontally into a petri dish containing 2 mg/mL dopamine solution in tris buffer of pH 8.5 for 30 min to aid the formation of a polydopamine film. We chose an incubation time of 30 min, which results in a typical film thickness of ~2–3 nm [201]. We note that thicker PDA films can be created by extending the incubation period but a thicker film is detrimental to the photonic biosensor performance as it reduces the overlap between the optical mode and the surface molecular layer, thereby reducing the sensitivity of the sensor; it is worth recalling that the photonic sensor uses an evanescent field to interact with the biomolecules, and that the evanescent field only extends 50–100 nm into the analyte. We highlight the limited spatial extent of the optical mode in Figure 18c to illustrate this point. Following PDA film formation, the sensors were rinsed with tris buffer pH-8.5, followed by distilled water, before being dried with nitrogen. Both the QCM-D and guided mode resonance-based sensing experiments were performed at 20° C and with a constant flow rate of 75 µL/min controlled by a peristaltic pump for QCM-D and a syringe pump for guided mode resonance sensing setup. PBS (pH 7.4) was first flowed over the sensor surfaces to establish a stable baseline. Following stabilization, antibodies were introduced at a concentration of 50 µg/mL in PBS, followed by a PBS (pH 7.4) washing step to remove unbound antibodies. A 1% solution of casein in PBS was then used to block unreacted regions of the PDA surface, again followed by a PBS washing step. Finally, the antigen solutions (in PBS) were introduced into the fluidic channels at a range of concentrations before the surface was again rinsed with PBS. The volume the of sample used for the experiments was 1mL.

Schematic depicting the biofunctionalisation of guided mode resonance grating sensors using polydopamine surface chemistry and bioreceptor immobilisation on the functionalised surface.

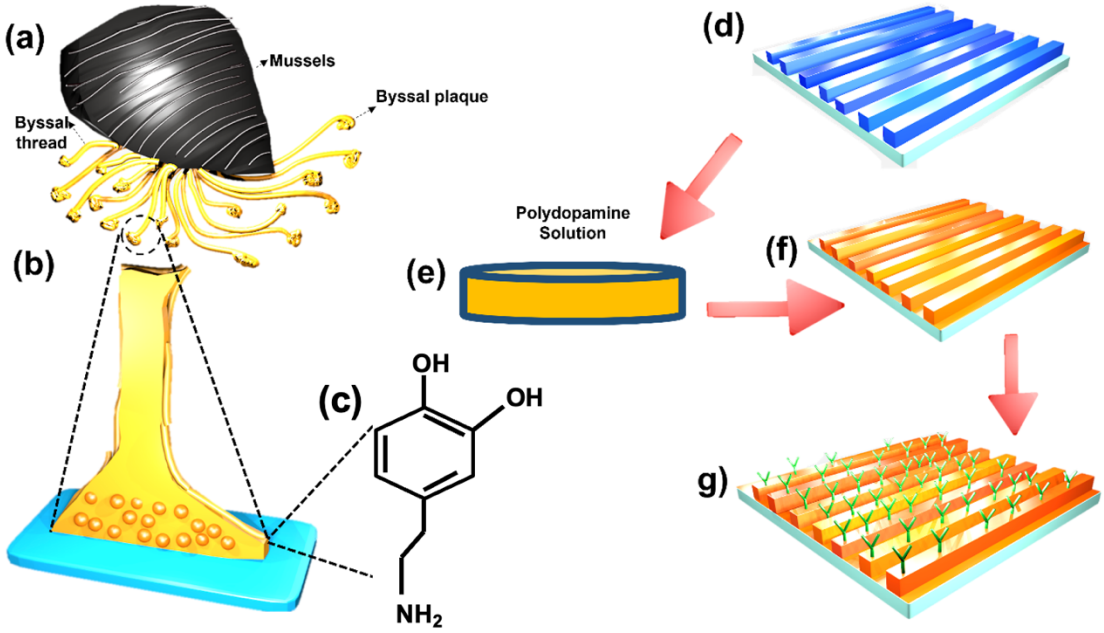

Figure 24: (a) Mussels with adhesive fibres; (b) enlarged image of secreted byssal; (c) chemical structure of the dopamine molecule; (d) sensing surface (here: silicon nitride grating); (e) polydopamine solution in petridish; (f) sensor coated with the polydopamine solution; (g) direct antibody attachment to the polydopamine coated sensing surface.

3.8. Results and discussion:

3.8.1. Quartz crystal microbalance analysis:

To start with, the analytical performance of PDA surface chemistry was studied on the QCM-D system using quartz sensors coated with silicon dioxide. The performance of the PDA chemistry was compared with generally used silane-based chemistries. Here, we used Mercaptotriethoxy silane with maleimide-PEG_6-NHS linker (Silane-NHS linker) described in detail here [152] for comparison. The full immunoassay for anti-IgG and IgG on the PDA-modified sensor on the QCM-D system is shown in Figure 25a. Note that the vibration frequency of quartz crystal sensors decreases as mass attaches to the surface of the sensor, with the decrease being directly proportional to the mass attached to the sensor surface. As shown in Figure. 25a, upon exposure of the PDA-modified sensor surface to a solution of anti-IgG, we observe a shift in resonant frequency, which, after rinsing with PBS, amounts to ≈ 68 Hz, this was followed by blocking of the surface with casein to avoid non-specific binding followed by running IgG solution and a clear binding of IgG with anti-IgG was observed as indicated in Figure 25a. We then compared the PDA protocol with a silane + NHS linker protocol by recording the frequency shifts on QCM-D for the two protocols for different antibody and antigen pairs. The frequency shifts observed for PDA surface chemistry were larger for antibody immobilisation than on silane-NHS linker functionalised sensors (Figure 25c), indicating higher antibody immobilisation density, which in turn gives a higher signal for antigen binding (Figure 25d). The process was performed with five different antibody-antigen pairs (anti-IgG and IgG, anti-TNF-α and TNF-α, anti-CRP and CRP, anti-IL-6 and IL-6, anti-MMP-9 and MMP-9) (Figure 25(c) and 25(d)) to study the compatibility of surface chemistry with a broad range of antigen-antibody pairs. It was observed that the protocol worked well for all the antibodies tested, which suggests the wide applicability of the protocol.

Additionally, the effect of other factors, such as the effect of light shaking while forming polydopamine film on the QCM sensors and increasing the concentration of dopamine to 5 mg/mL was also studied. The frequency shifts observed for anti-IgG (50 µg/mL) immobilisation were -58. 238 Hz ± 1.303 and -60.05 Hz ± 1.373 respectively. The frequency shift observed for IgG (1 µg/mL) attachment were -15.79 hz ± 0.277 and -14.12 Hz ± 0.678, respectively. The incubation time in polydopamine solution was kept constant for 30 min. Since the highest frequency shifts for both antibody and antigen immobilisation were observed for 2 mg/mL of dopamine concentration in tris buffer pH 8.5 with sensors placed horizontally in the solution for 30 min, so this is the recipe I carried forward.

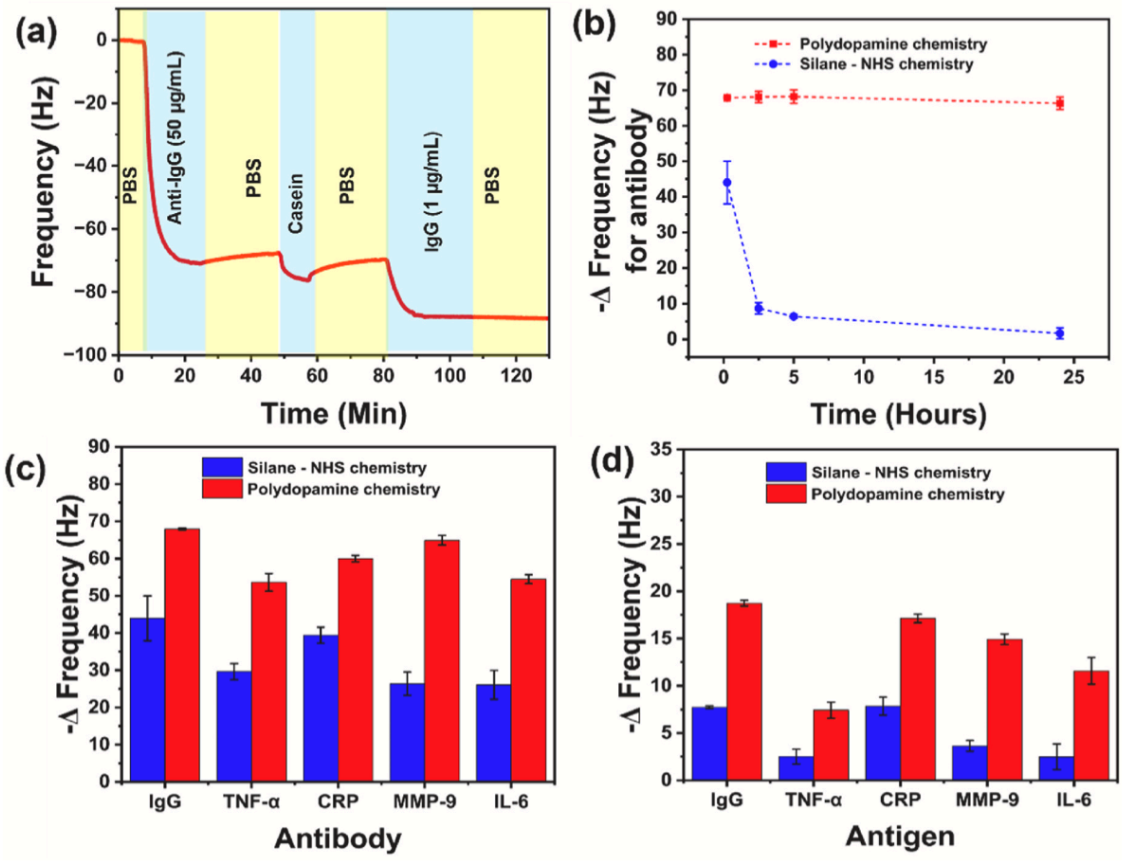

FIGURE 25: (a) IgG immunoassay on a PDA-functionalised silicon dioxide QCM sensor; (b) comparison of chemical reactivity of polydopamine and MPTES + NHS-$(PEG)_6$- maleimide functionalised surfaces after preincubation for up to 24 h in PBS (pH-7.4). The drop in the activity of MPTES + NHS-$(PEG)_6$-maleimide chemistry is observed because of hydrolysis of the NHS ester; (c, d) comparison of the observed frequency shifts for five clinically relevant antibodies (50 µg/mL) (c) and associated antigens (1 µg/mL) (d) for both polydopamine and silane-NHS functionalised sensors (n = 3 ± Standard Deviation (SD)).

To further calculate mass of the proteins attached Sauerbrey equation was used,

$$\Delta m = -C * \frac{\Delta f}{n} \quad \text{..... (8)}$$

Δm = stands for mass change, Δf = stands for frequency change, C = stands for mass sensitivity constant and n stands for harmonic number.

Table 3: Mass of antibodies and antigen attached on the quartz crystal microbalance sensor surface functionalised with polydopamine and silane-NHS chemistry.

Sr. No.	Antibody	Mass immobilised on Silane-NHS functionalised sensor (ng/cm^2)	Mass immobilised on polydopamine functionalised sensor (ng/cm^2)	Antigen	Mass immobilised on Silane-NHS functionalised sensor (ng/cm^2)	Mass immobilised on polydopamine functionalised sensor (ng/cm^2)
1.	Anti-IgG	111.16	171.6	IgG	19.6	47.35
2.	Anti-TNF-α	74.94	135.61	TNF-α	6.35	18.76
3.	Anti-CRP	99.63	151.74	CRP	19.84	43.79
4.	Anti-MMP-9	66.73	164.15	MMP-9	9.8	37.77
5.	Anti-IL-6	65.99	137.69	IL-6	6.30	29.26

It is worth mentioning that the Sauerbrey equation gives an entirely correct value of mass when the film formed on the QCM sensor surface is rigid, thin and firm. In case of protein-based films the Sauerbrey equation might not give exactly correct values of mass of protein immobilised or attached [202] .

The stability of the PDA functionalised surface in aqueous environments was also studied. Instability in aqueous environments is one of the major limitations of chemistries that employ activations of surface using NHS because of the highly hydrolytic nature of NHS ester formed, which reduces the efficiency of the bioconjugation process. We observed that PDA surface chemistry was highly stable in aqueous environments (Figure 25b, red curve) because the frequency shift for anti-IgG immobilisation on PDA functionalised sensors was almost stable even when the sensor was pre-incubated in the aqueous environment for 24 h. In contrast to that, a clear and rapid decrease in the performance of the silane-NHS linker chemistry functionalised sensors was observed because of possible hydrolysis of the NHS ester. The experiments point towards the robustness of the chemistry, which is one of the important requirements for large-scale implementation of photonic biosensors, i.e., efficient, simple, and stable bioreceptor immobilisation chemistry.

3.8.2. Chirped guided mode resonance (GMR) analysis:

Next, the analytical performance of PDA surface chemistry was studied using chirped-GMR sensors. The biomolecular interactions taking place on the surface of the chirped GMR sensor were studied by monitoring the resonance position against time to study the adsorption kinetics of the antibody immobilisation onto the PDA-coated sensor surface and binding kinetics of the antigen to the antibody. A full binding assay for anti-IgG (50 µg/mL) and IgG (0.01 ng/mL), using casein as the blocking agent, is shown in Figure 26a. The resonance shifts observed for a full range of IgG concentrations from 0.01 ng/mL to 10,000 ng/mL are shown in Figure 26b, with an inset image showing binding curves for the same. It was observed that the resonance position reached a steady state after 15-20 mins. The maximum shift was observed for an IgG concentration of 1000 ng/mL. The resonance shift observed for a 0.01ng/mL IgG concentration was approx. 3 µm, which is well above the 3σ (mean 3σ =1.39 µm ± 0.5 µm (n=30 ± SD) value of the system. Going forward the performance of both the protocols was then compared on the chirped GMR sensors by immobilising antibodies (50 µg/mL) on PDA and silane-NHS functionalised GMR sensor chips and binding shift for 10 pg/mL IgG was also observed (Figure 27a and b). The same trend as with the QCM-D studies (Figure 25) was observed i.e. the resonance shifts for the PDA surface chemistry functionalised sensors for anti-IgG immobilisation and IgG detection were higher than for the silane-NHS protocol, further confirming high antibody immobilisation density achieved using PDA surface chemistry. In addition, we also performed specificity studies on the PDA chemistry functionalised GMR sensors. The PDA functionalised GMR sensor surface was immobilised with anti-IgG (50 µg/mL) and challenged with a high concentration of non-specific antigen CRP (10 µg/mL), and TNF-α (10 µg/mL) and as can be seen in Figure 26c and Figure 26d negligible binding for non -specific antigen is observed. In contrast to that for specific antigens i.e. IgG for the concentrations 10 µg/mL and 100 pg/mL, we saw a strong binding signal (Figure 26c and 26d). The dynamic range was also established for two other clinically relevant biomarkers, i.e., CRP and MMP-9, for concentration ranges from 0.01 ng/ml to 10,000 ng/mL, with saturation observed around 1000 ng/mL for both. The robustness of the film was also studied by storing the PDA functionalised sensor in the air for 0.15 h and 24 h (Figure 28a). The resonance shift observed for the antibody binding is very similar for both films placed in the air, thus indicating good stability of PDA film for bioreceptor immobilisation even after being left in the air for around 24 hours. In addition to that, we also experimented to understand the immobilisation mechanism between the antibody and the PDA functionalised sensor surface. For that purpose, a 10 % solution (v/v) of amine-functionalised silica nanoparticles (Figure. 28b) was employed. The binding curve for the silica nanoparticles experimentally confirms one of the possible mechanisms by which biomolecules immobilise on the PDA surface is via the covalent linking of biomolecules via the amine functional group indicating biomolecule attachment to PDA film takes place via Michael addition and Schiff base reaction demonstrated in Figure 22 and discussed above.

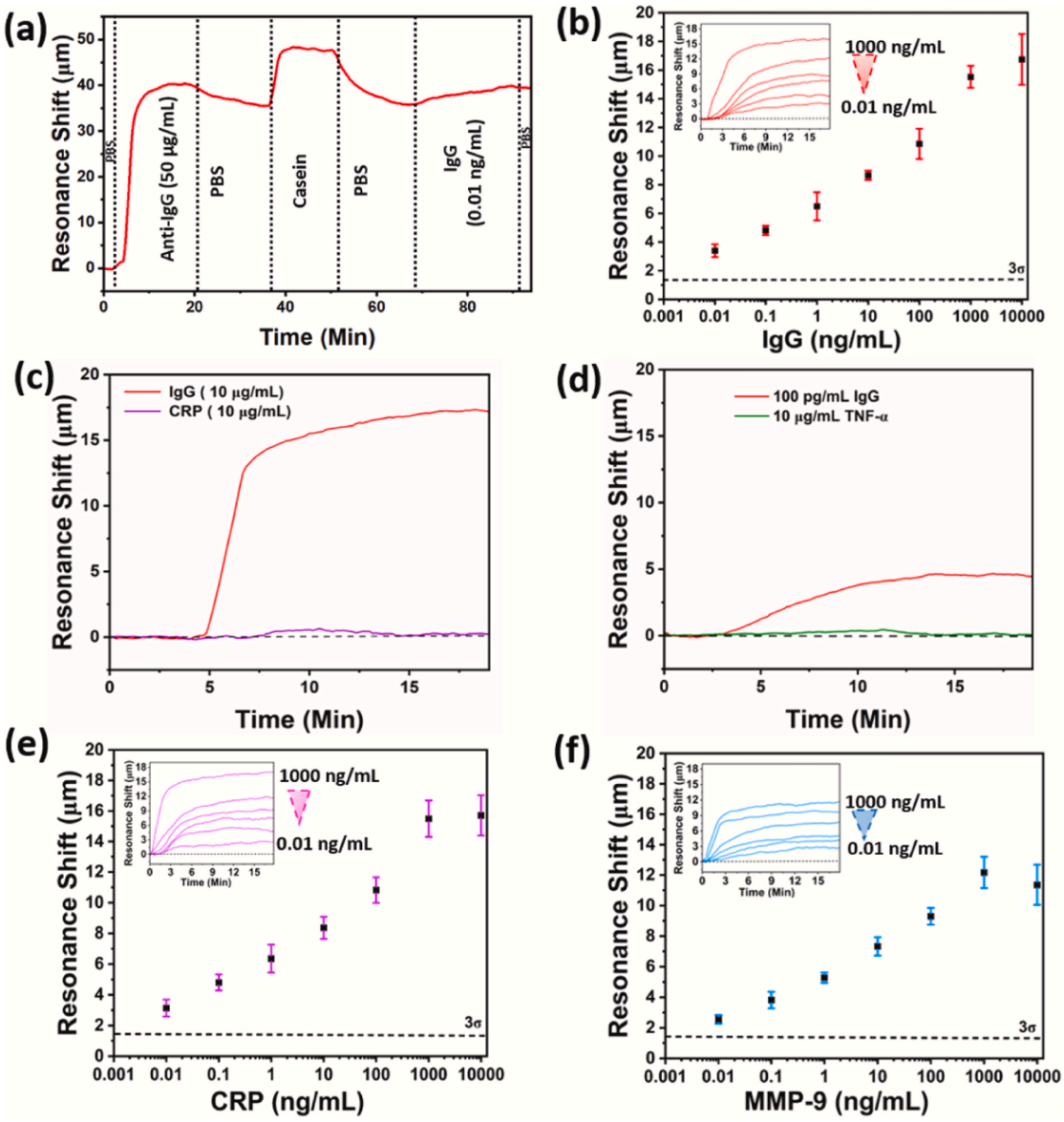

FIGURE 26: (a) IgG immunoassay on PDA-functionalised silicon nitride guided mode resonance grating sensors; b) Resonance shifts observed for an IgG concentration in the range from 0.01 ng/mL to 10,000 ng/mL (n = 3 ± SD). The inset shows the respective binding curves for an IgG concentration ranging from 0.01 ng/mL to 1000 ng/mL; c, d) Selectivity test performed on polydopamine coated silicon nitride GMR grating; c) binding curve for 10 µg/mL of IgG and 10 µg/mL of CRP for a grating functionalised with anti-IgG (50 µg/mL). For 10 µg/mL IgG, a good shift in the resonance position is observed, while for the same concentration of CRP, only negligible non-specific binding is observed; (d) In the second selectivity test, the sensor was functionalised with anti-IgG (50 µg/mL), exposed to 100 pg/mL IgG and 10 µg/mL TNF-α. Again, the specific binding is strong while the non-specific binding is negligible; e and f) Resonance shifts observed for CRP and MMP-9 concentrations in the range from 0.01 ng/mL to 10,000 ng/mL respectively (n = 3 ± SD). The inset shows the respective binding curves for the protein concentrations ranging from 0.01 ng/mL to 1000 ng/mL.

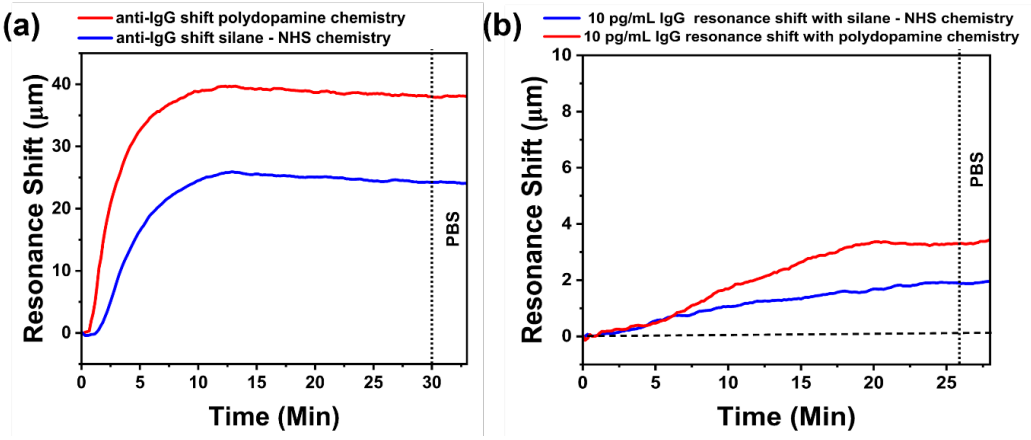

FIGURE 27: (a) Comparison of the resonance shift observed for anti-IgG (50 µg/ml) immobilisation on both polydopamine and silane-NHS functionalised surface; (b) binding curve for 10 pg/mL IgG on both surfaces. 3σ values for these measurements were 0.27 µm.

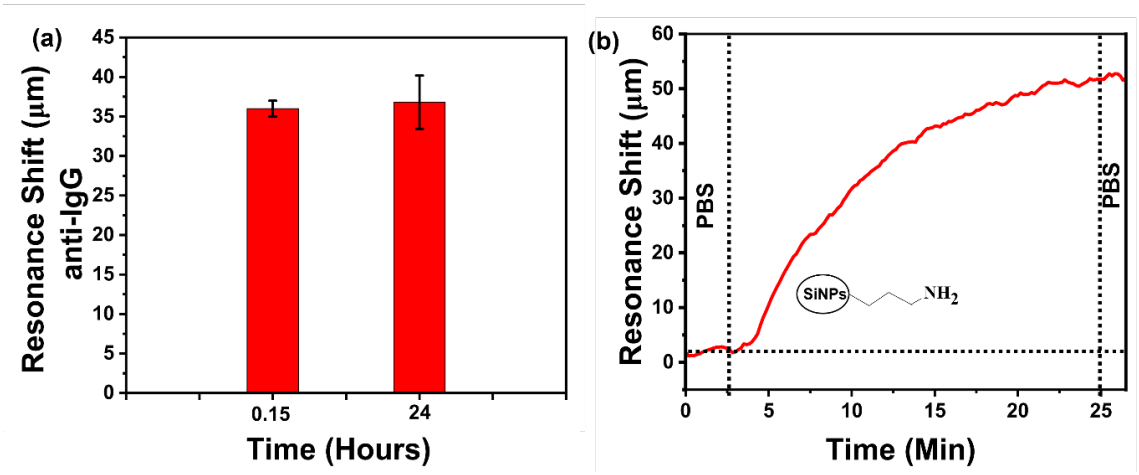

FIGURE 28: (a) Stability test of polydopamine films in the air before protein immobilisation; (b) Binding curve for amine functionalised silica nanoparticles on a polydopamine surface.

The Signal observed above the 3-sigma level is considered important as it gives confidence that the signal obtained is statistically significant and is not because of random noise. The σ represents the natural fluctuation in the baseline signal levels. A signal above 3 sigma confirms that the probability of the signal being due to random fluctuation or noise is very low. In statistics, a 3σ deviation corresponds to a confidence level of 99.7% in a normal distribution and ensures that the detected signal is real and not due to random noise or background signal fluctuations [26].

3.8.3. Biosensing experiments in 10 % human serum:

To study the compatibility of sensors with a human matrix, the bio-detection experiments in 10 % human serum by volume (serum samples were diluted by PBS buffer) were performed. A measurement and a reference channel were employed to perform the measurements in 10 % human serum to account for matrix effect caused by 10 % human serum. The signal channel was functionalised with anti-IgG antibodies, and the reference channel was functionalised with isotype antibodies (Figure 29a) to separate the specific signal from the non-specific signal as the isotype antibodies used to functionalise the reference channel have no specificity for the target antigen. Isotype antibodies do not have specificity for a particular antigen, meaning they do not bind to a specific target molecule, but rather are designed to match the class and subclass of the primary antibody used in an experiment, to assess non-specific binding signals by acting as a negative control. An example of measurement is shown in Figure 29c. After the antibody immobilisation, both channels were blocked with casein protein to block any remaining binding sites and to avoid non-specific binding. Both the channels were exposed to the 10 % human serum spiked with IgG. The resonance shift observed in the measurement channel was higher than that observed in the reference channel because of the specific binding between anti-IgG immobilised in the measurement channel and IgG in serum. After subtracting the shift observed in the reference channel from the shift observed in the measurement channel, the specific signal for IgG binding is obtained as reported in Figure 29b. Figure 29b reports the shifts observed for different IgG concentrations spiked in 10 % human serum. The lowest concentration detected in human serum is 10 ng/mL, which is higher than what I could detect in PBS buffer, but still, the sensitivity is enough to perform the detection of clinically relevant concentrations.

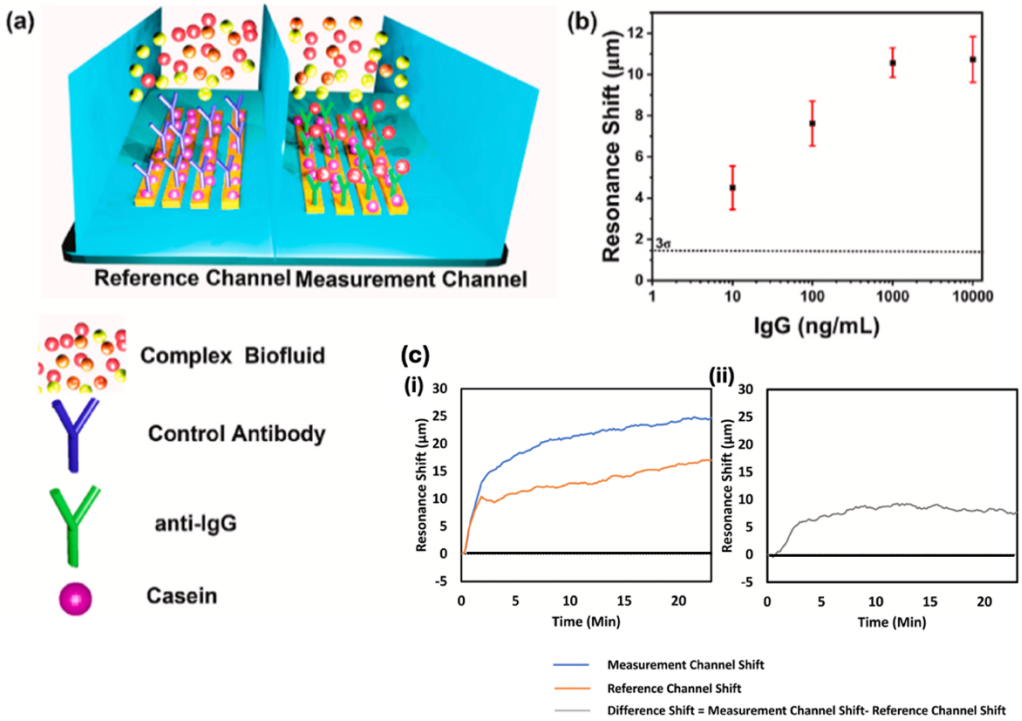

FIGURE 29: a) Working principle of referencing approach to perform measurements in a complex biofluid. The measurement utilises a reference channel immobilised with IgG isotype antibodies and a measurement channel functionalised with specific antibodies (anti-IgG). The spiked human serum is flown through both channels. To remove the matrix effect, the resonance shift in the reference channel is subtracted from the resonance shift in the measurement channel which results in the shift shown in (b). (b) Resonance shift observed for an IgG concentration in the range from 10 ng/mL to 10,000 ng/mL following subtraction of the matrix effect; (c) An example of measurement depicting the reference channel approach for detecting biomarkers in 10 % human serum. The reference channel is prepared by immobilising isotype antibodies and blocked using a casein blocker, while the measurement channel is functionalised with specific antibodies and blocked with a casein blocker; (i) The shift observed in the measurement channel is higher because of the specific binding reaction between the antibody and antigen, while the shift observed in the reference channel is only because of the matrix effect of biological media. The shift for the detection of the biomolecule of interest can be obtained by subtracting the shift observed in the reference channel from the shift observed in the measurement channel; (ii) Difference shift for specific binding of antigen. The curve is obtained after subtracting the shift observed in the reference channel from the shift observed in the measurement channel.

3.8.4. Sensor stability in alkaline solutions:

Another common issue with silicon-based photonic sensors is the slow etching of the photonic nanostructure in alkaline solutions such as cell culture media. For example, cell culture medium or, more generally, alkaline solutions are known to slowly degrade nanostructured silicon surfaces up to 2 nm per hour [200]. The data in Figure 30 exemplifies this effect, showing the degradation of a silicon grating after around 10 hours following immersion in PBS (pH 7.4) and after only 4 hours when exposed to a cell culture medium. When performing the same experiment with the PDA-coated silicon sensors (Figure 30, solid lines), the sensors appear to be much more stable, and we observe the onset of sensor degradation after approx. twice the duration (Figure 30). This observation indicates that the PDA coating forms a protection layer that enables measurements such as cell imaging for extended periods [203], and further polydopamine and polydopamine composite coatings should be explored for the protection of silicon-based surfaces from etching in alkaline solutions.

Dr Isabel Barth performed the effect of PDA coating on protecting degradation of sensor surface experiment.

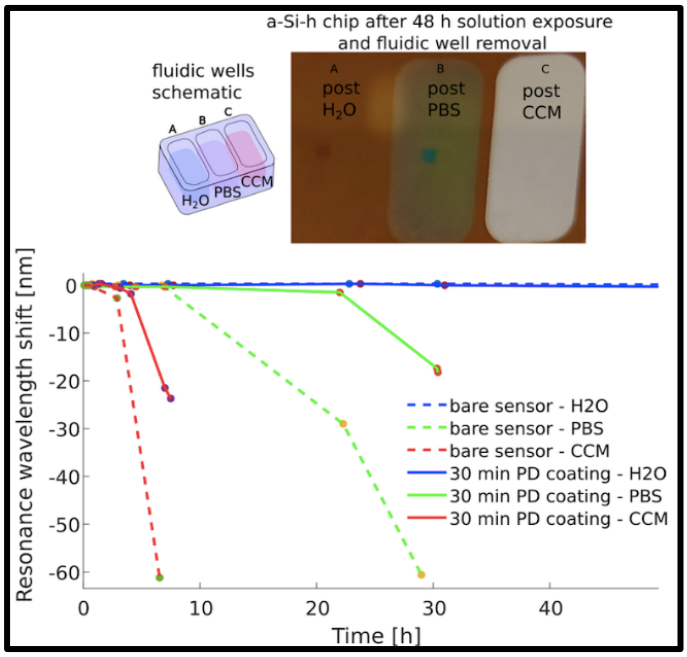

FIGURE 30: Effect of polydopamine coating on the etching of silicon gratings in cell culture medium, PBS (7.4), and water. Note that the PDA coating provides an element of protection from degradation, as it approximately doubles the time that sensors can be used. The CCM here stands for cell culture media.

3.9. Summary of the work reported in this chapter:

In brief, this chapter reports the analytical performance of PDA surface chemistry as one one-step method for bioreceptors immobilisation on silicon nitride-based photonic biosensors. The results indicate that PDA-based surface chemistry has a high bioreceptor immobilisation density. The results also suggest that the PDA film is stable in aqueous and air environments for longer durations and gives bioreceptor immobilisation efficiency similar to freshly formed PDA films. In addition to that, PDA-based surface chemistry is compatible with a wide range of antigen-antibodies based sets. It gives enhanced signals for antigen detection because it helps in achieving high bioreceptor immobilisation density. The protocol is compatible with evanescent wave-based silicon nitride based photonic biosensors and gives good performance for detecting protein-based biomarkers. Additionally, the surface chemistry is robust enough to perform measurements in complex human biofluids such as 10 % human serum. It can also act as a protective layer for silicon photonic sensors when performing measurements in alkaline solutions such as cell culture medium to prevent the etching of silicon devices. Table 4 below compares the dynamic ranges established for IgG detection using different optical sensing modalities.

TABLE 4: Comparison of detection range reported by different optical biosensing devices developed for IgG protein detection.

Sr. No.	Optical sensor	Surface functionalisation	Detection range	Reference
1.	Mach–Zehnder interferometer	Aminopropyl triethoxy silane + glutaraldehyde	0.5-50 µg/mL	[204]
2.	Long period fibre grating	APTS + non imprinted polymer	0.15- 15 µg/mL	[205]
3.	Long period fibre grating	Graphene oxide + EDC/NHS	3-20 µg/mL	[206]
4.	Simple Fibre biosensor	Aminopropyl triethoxy silane + glutaraldehyde	0.1 to 1 mg/mL	[207]
5.	Chirped guided mode resonance biosensor	Polydopamine	0.01 ng/mL-1000 ng/mL	This work

Chapter 4. Nanophotonic and hydrogel-based diagnostic system for the monitoring of chronic wounds

4.1. Chronic wounds:

Chronic wounds come under the category of wounds that take a long time to heal and burden the health care facilities [208]. Some examples of chronic wounds are diabetic foot ulcers, venous leg ulcers, etc. [209]. The problem of chronic wounds puts an immense burden on healthcare facilities due to expensive treatments that cost around two to four percent of the total healthcare budget and deteriorate the patient's quality of life [210]. For example, an estimated number. of patients suffering from chronic wounds in the United States is around 6.5 million and that results in a substantial financial burden of around $25 billion per year on the healthcare system [211]. Managing chronic wounds in the United Kingdom is estimated or calculated to cost the NHS around £5.3 billion per year and which is around 4 percent of the total NHS budget [212]. If timely treatment is not given to these wounds, they can cause serious complications [213]. Improvement in chronic wound management is highly needed, and the development of point-of-care devices can help regularly monitor the wound biomarkers and thus can help in better treatment and management of chronic wounds [214].

4.2. Importance of monitoring biomarkers associated with chronic wounds:

In time, identification of wound conditions is essential for better management of chronic wounds, and studying wounds at the molecular level can be useful for that purpose. Studies have indicated biomarkers can help in studying non-healing and healing wounds as levels of these biomarkers differ in healing and non-healing wounds [215]. A good number of biomarkers are associated with the wound healing problem. For example, cytokines such as Tumour Necrosis factor-α (TNF-α), interleukins (ILs), and enzymes such as matrix metalloproteinases (MMPs) hold great importance in the context of wounds. Elevated levels of these biomarkers are observed in non-healing wounds [215, 216]. Other than protein biomarkers, levels of miRNA-based biomarkers have also been observed to be elevated in the plasma of patients with diabetes foot ulcers [217]. Patient serum and wound fluid are generally used as biological fluids to study and monitor levels of these biomarkers and accordingly give guided

treatment [218]. Table 2 below provides the quantitative analysis of biomarkers in healing and non-healing wounds.

TABLE 5: Concentration of different biomarkers in healing and non-healing wounds.

Biomarker	Healing wound		Nonhealing wound		Reference
	Median	Range	Median	Range	
Interleukin-6 (IL-6)	55185(pg/mL)	24113-119000 (pg/mL)	77762 (pg/mL)	28363-210,000 (pg/mL)	[216]
Tumor Necrosis Factor-α (TNF-α)	1639 (pg/mL)	550-7540 (pg/mL)	4734 (pg/mL)	1030-13257 (pg/mL)	[216]
Interleukin-1 α (IL-1α)	1485 (pg/mL)	257-3186(pg/mL)	6184 (pg/mL)	482-16455 (pg/mL)	[216]
Interleukin-1 β (IL-1β)	7785 (pg/mL)	686-51,205 (pg/mL)	17902 (pg/mL)	7307-72487 (pg/mL)	[216]
Basic Fibroblast growth factor (bFGF)	261 (pg/mL)	44-1267 (pg/mL)	411 (pg/mL)	61-1390 (pg/mL)	[216]
Platelet derived growth factor (PDGF)	133 (pg/mL)	23-244 (pg/mL)	97 (pg/mL)	15-353 (pg/mL)	[216]
Transforming growth Factor- β_1 (TGF- β_1)	12.4 (ng/mL)	4.4-32.4 (ng/mL)	9.2 (ng/mL)	3.9-22.5 9 (ng/mL)	[216]

4.3. Biosensors to monitor wound biomarkers:

As discussed above in Table 5, the levels of biomarkers, differ in healing and non-healing wounds. Also, pH and uric acid levels are also studied to assess the status of wounds [219, 220]. For instance, chronic wounds exhibit an alkaline pH [221]. Currently used methods for biomarker monitoring are performed in specialised laboratories, and the process is time-consuming. Therefore, there is a need to develop more user-friendly devices for quantifying and monitoring wound-related biomarkers. There are some products in the market for this application, but they are not very efficient. For example, Woundchek (https://www.woundcheck.com) has the ability measure one biomarker only and has only limited sensitivity. Another product available is MolecuLight (https://moleculight.com/), which can only sample bacteria using autofluorescence. Biosensors are also being developed for monitoring chronic

wounds [222]. For example, Kim et al. reported a stretchable electrochemical biosensor based on differential pulse voltammetry to detect TNF-α with a limit of detection achieved 100 fM in phosphate buffer saline. The sensing system fabricated developed only showed the detection of one biomarker, and multiplexing ability was lacking [223]. In another work, Rajeev et al. developed a label-free optical TNF-α biosensor based on nanoporous anodic alumina. The detection limit of around 0.13 μg/mL was reported for TNF-α detection, and they also reported the detection of only one wound biomarker [224]. In other work, Gao and coworkers fabricated and developed a flexible, multiplexed device for wound monitoring a range of wound biomarkers such as TNF-α, IL-6, IL-8, and TGF-β1, staphylococcus, temperature and pH [225]. The developed sensor exhibited good performance, but some of the issues with electrochemical biosensing devices have lower stability and show drift with time, which is a major issue when longer-term continuous analyte monitoring is the need and especially here in the case of long-term wound monitoring [54, 226]. Hence, long-term continuous monitoring of chronic wounds in a non-invasive manner is still a challenge. In order to address this problem, there is a need to develop efficient point-of-care devices that can help in achieving long-term continuous monitoring, provide high selectivity and sensitivity for biomarker detection and, most importantly, help in assessing wounds without disturbing the wound bed.

In this work, I have made progress towards developing a nanophotonic test that can detect wound biomarkers in hydrogel-based wound dressings. With the use of hydrogel dressing, the wound biomarkers can be extracted in a non-invasive manner without causing any disturbance to the wound bed, and their quantification can be performed using the chirped-GMR-based optical test (Figure 31).

4.4. Hydrogel-based wound dressings:

Hydrogel-based wound dressings are now being developed and studied for wound applications. Hydrogels are composed of hydrophilic polymers and possess good biocompatibility [227]. The high water-holding capacity of hydrogels contributes to maintaining a moist environment around the wound [228]. Hydrogel-based wound dressings can act as a transitory skin that makes a protective wall, hence reducing the infection risk and enhancing wound healing by starting cell migration. Additionally, hydrogel-based wound dressings, because of their inherent water-absorbing properties, can absorb a wound exudate leaking around the wound and hence prevent its leakage [229]. Furthermore, it is possible to load hydrogel-based wound dressings with therapeutic drugs and other biological molecules that help promote the wound healing process. Also, customisation of the hydrogel-based wound according to specific wounds is possible by considering the size and location of the wound [230].

This chapter reports the application of chirped-GMR-based biosensors for monitoring chronic wound biomarkers. The biological interface was optimised to perform the detection of chronic wound biomarkers in hydrogel absorbed with human matrix and wound exudate. Neotherix Limited has designed a hydrogel-based system that can be used to extract the wound fluid without causing disruption to the wound bed [https://www.neotherix.com, US 10,687,790]. The principle that allows non-disruptive and non-invasive sampling of wound exudate is the thermosensitive nature of the gel, which has low viscosity at low temperatures and becomes gel at body temperatures, forming solid gel-based dressing over the wound and the dressing can absorb the wound fluid released into the environment as shown in schematic Figure 31. The challenge we address here is to demonstrate the detection and quantification of biomarkers relevant to the progression and trajectory of wound healing at clinically relevant levels in this hydrogel-containing wound exudate.

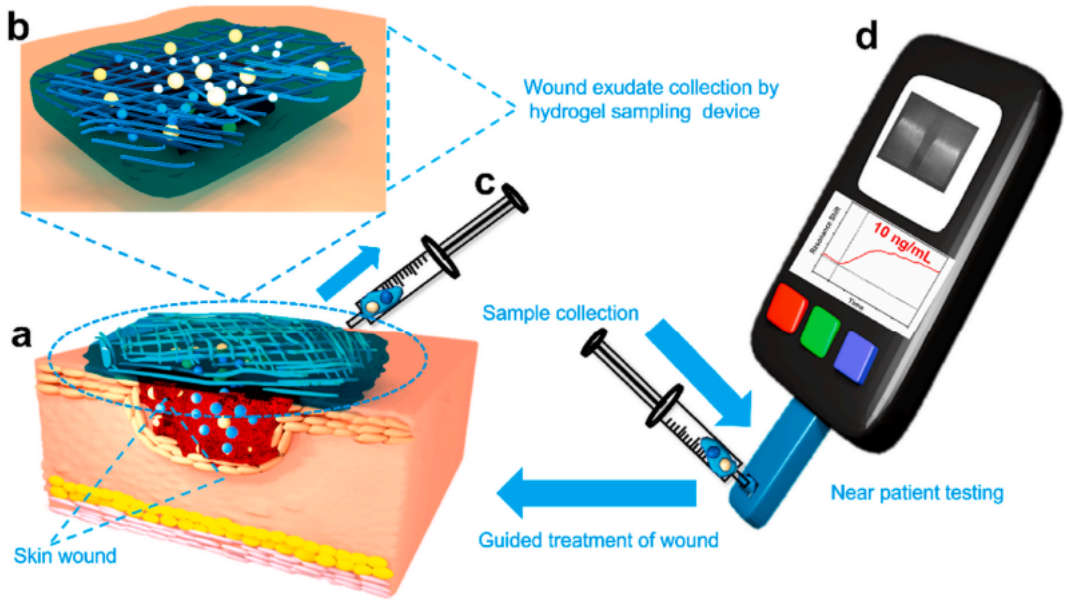

FIGURE 31: Schematic of the proposed diagnostic system for monitoring chronic wounds. The hydrogel based dressing enables non-destructive sampling of the wound exudate for analysis to inform treatment; (a) Hydrogel wound dressing based sampling device placed on skin wound; (b) Magnified image showing wound fluid absorbed in hydrogel based dressing placed on skin wound; (c) Wound fluid absorbed dressing collection from skin wound; (d) Near patient testing device to detect wound biomarkers in wound fluid absorbed dressing.

4.5. Materials:

Except the hydrogel dressing, Human plasma, and the clinical wound exudate, the sources of all other materials used to perform the work described in this chapter are reported in Chapter 2 and Chapter 3. Human plasma was purchased from Sigma Aldrich. The proprietary hydrogel dressing was provided by Neotherix. Clinical wound exudate samples were obtained under research ethics committee approval 19/NE/0150. Samples were collected from Hull Royal Infirmary. Samples were collected with complete, informed patient consent.

4.6. Methods:

The fabrication protocol of guided mode resonance-based sensors used in the study is described in Chapter 2, section 2.7.2. Dr. Pankaj K. Sahoo fabricated the sensors used in this study. The surface chemistry protocol to functionalise the sensor surface is described in Chapter 3, section 3.7.1.

4.6.1. Human matrix capture by hydrogel dressing experiment:

In order to study the volume of human matrix that is captured by the hydrogel, 1 mL of hydrogel dressing was spread in a petri dish with 1 mL of human matrix (50: 50) mixture of human serum and human plasma placed onto it and left in an incubator at 37°C for 2 hours. After 2 hours the remaining wound exudate was collected by pipette, which amounted to 900 µL; hence we conclude that 1 mL of hydrogel captures around 100 µL of wound exudate.

4.6.2. Bio-recognition assay in phosphate buffer saline (PBS):

A range of concentrations of TNF-α and IL-6 were prepared in PBS buffer to generate the dynamic range data. The functionalised sensors were mounted in a microfluidic circuit and the antibody solutions were then introduced at a concentration of 50 µg/mL made in PBS (pH 7.4) and were flown through at a flow rate of 75 µL/ min. This was followed by the washing step in PBS buffer, blocking of the surface with 1 % casein solution in PBS (pH 7.4), followed by another washing step in PBS before the various concentrations of TNF- α and IL-6 were introduced.

4.6.3. Biorecognition assay in hydrogel containing human matrix and clinical wound exudate:

The hydrogel was diluted to 70 % v/v (i.e., 7 parts hydrogel and 3 parts PBS buffer) to ensure sufficiently low viscosity and compatibility with microfluidic handling. For the data in Figure 34, we prepared human matrix as a 50:50 mix of human serum and human plasma [224]. The sample for measurements was then prepared as follows: 1 mL of dressing with 100 µL of human matrix was spiked with the antigen of interest followed by dilution to 70 % v/v giving the final concentration of biomarkers (TNF-α and IL-6) used in the measurements shown in Figure 34b and 34c. Similar process was repeated with clinical wound exudate samples that is 100 µL of wound exudate was absorbed in 1 mL of hydrogel wound dressing followed with spiking with antigen of interest and thereafter dilution to 70 % v/v of mixture was performed.

4.7. Results and discussion:

4.7.1. Detection of Tumor Necrosis Factor-α (TNF-α) and Interleukin-6 (IL-6) in PBS buffer:

To start with, we first establish the detection range of the sensor for the detection of TNF-α and IL-6 in PBS. The PDA layer was used to functionalise the sensors and immobilise the antibodies onto the sensor surface. Anti-TNF-α and anti-IL-6 antibodies were first immobilised on the sensor surface, followed by blocking of the surface using casein to block the non-specific binding sites. The functionalised sensors were then exposed to TNF-α and IL-6 with concentrations ranging from 0.01 ng/mL to 1µg/mL. The shift of the resonance position is shown in Figures 32c and 32d for different concentrations of TNF-α and IL-6. The insets show binding curves for the different concentrations. The shifts observed for the lowest concentration, i.e. 0.01 ng/mL of TNF-α and IL-6, are ~0.07 nm and ~0.09 nm, respectively, both of which are above the 3σ value of the system, which is 0.028 nm ± 0.003 (n=10).

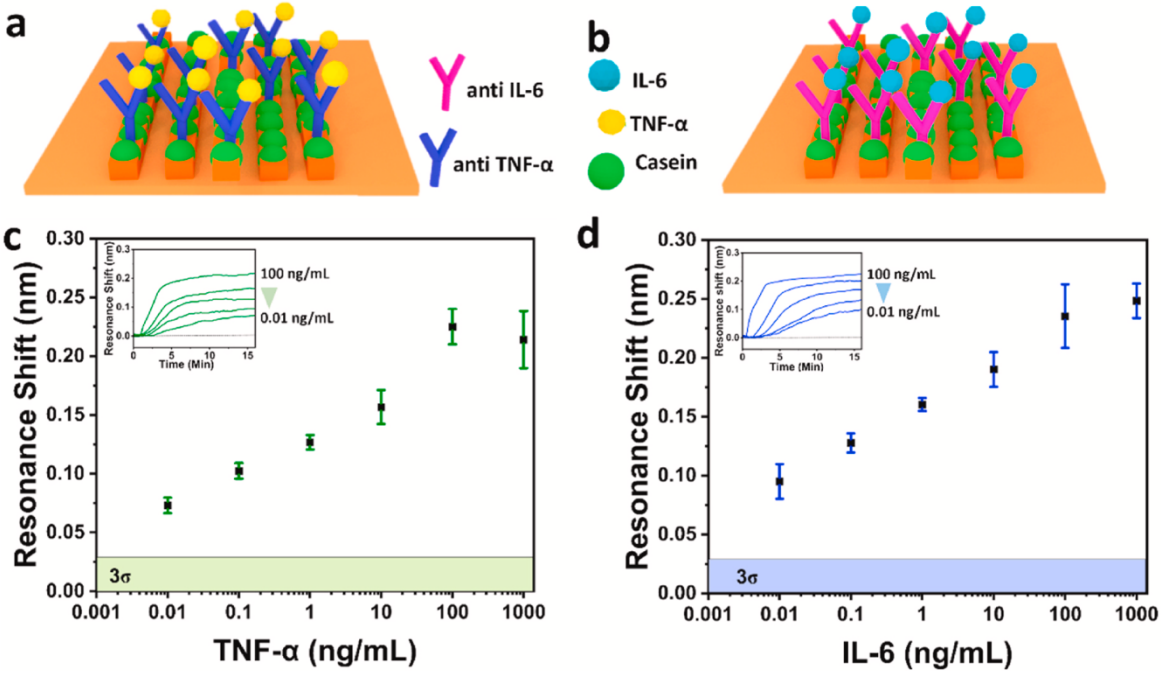

FIGURE 32: Surface chemistry and characterisation of the GMR biosensor for TNF-α and IL-6 detection. (a and b) Polydopamine surface chemistry was used for the anti-TNF-α and anti-IL-6 immobilisation on GMR sensors, followed by the blocking of remaining sites with casein in order to observe selective binding and to minimise fouling; (c) Resonance shifts observed for TNF-α concentrations ranging from 0.01 ng/mL to 1 µg/mL. The inset shows the binding curves for the same. (d) Resonance shift for IL-6 protein in PBS buffer at concentrations ranging from 0.01 ng/mL to 1 µg/mL. The binding curves for the same are shown in the inset. The error bars correspond to the standard deviation for three separate experiments for each concentration.

4.7.2. Wound biomarker detection in hydrogel:

Next, we studied the effect of a hydrogel-based matrix on antigen-antibody binding. As hydrogel is composed of long polymeric chains, it was interesting to check if these chains cause any interference with the binding of antigens with antibodies and whether the bulk change in the refractive index would mask the effect of binding of antigens with antibodies (Figure 33). The experiment was performed using the following steps to study all these effects. First, the sensor chip was functionalised with the PDA chemistry, and anti-TNF-α antibodies were immobilised on the sensor surface followed by blocking the sensor surface with casein and washing step to get rid of unbound casein. Then, the blank hydrogel was introduced into the channel to quantify the shift in resonance due to the mass refractive index change caused by the hydrogel (Figure 33a-i and 33b-ii). This was followed by running the hydrogel spiked with antigen over the sensor surface (Figures 33a-ii and 33b-iii) to see if the hydrogel interfered with the binding between antigen and antibody. A clear binding curve for antigen is observed when hydrogel spiked with antigen is flown over the surface of the functionalised sensor, as seen in Figure 33b -iii. An example of the full assay is given in Figure 35. The resonance shifts observed for different TNF-α concentrations spiked in hydrogel are comparable with the shifts observed in PBS buffer containing TNF-α (compare Figure 32c and 33c) within the experimental error; this confirms that the hydrogel does not interfere with binding and that the refractive index shift it causes can be subtracted. This shows that our biosensing interface design is sufficiently robust to perform measurements in the hydrogel diluted to 70 % (v/v).

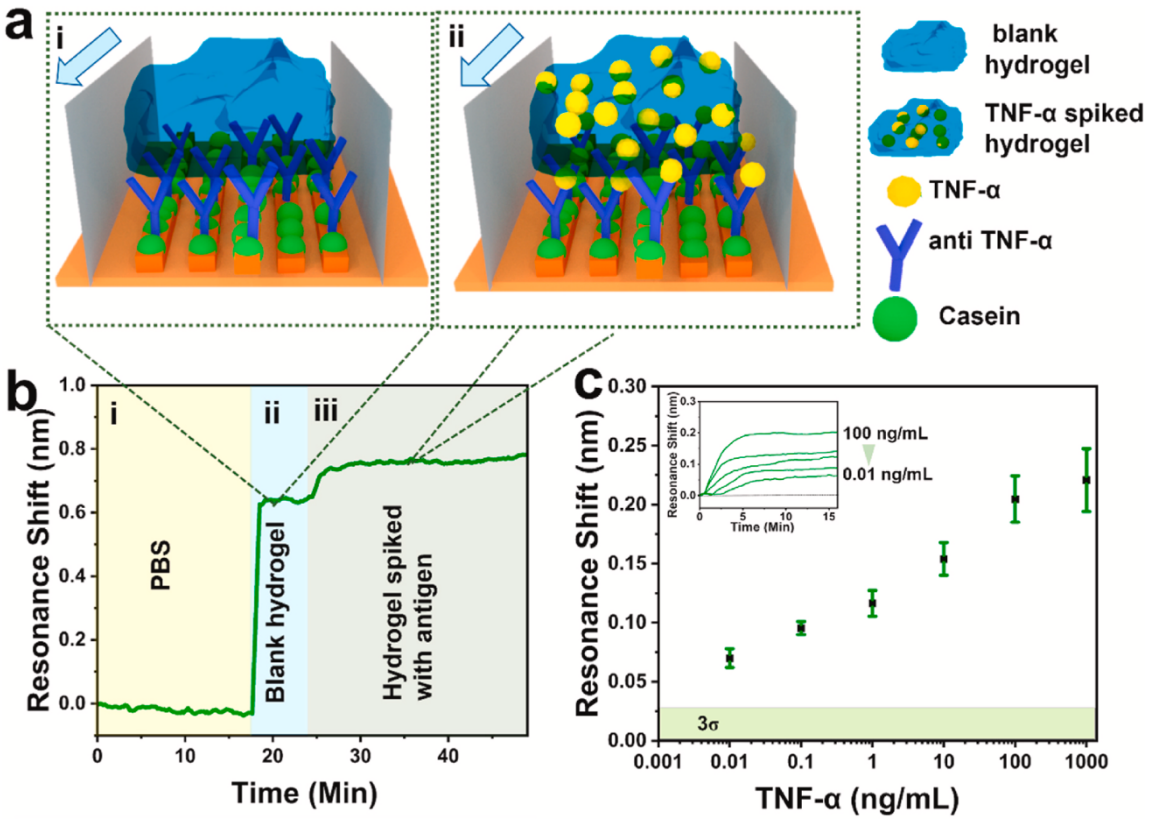

FIGURE 33: a) Schematic of the experiment, illustrating that blank hydrogel is introduced first, followed by spiked hydrogel. The arrows representing the direction of flow of sample in microfluidic channel; b) Biorecognition assay performed in hydrogel. Firstly, blank hydrogel (ii) is introduced into the channel to quantify the resonance shift caused by the refractive index of the hydrogel solution. This is followed by introducing hydrogel spiked with antigen (10 ng/mL) (iii) to obtain the shift caused by the antibody-antigen binding; (c) Resonance shifts observed for TNF-α of concentrations ranging from 0.01 ng/mL to 1 µg/mL. The inset shows the binding curves for different concentrations. The error bars correspond to the standard deviation derived from three separate experiments for each concentration.

4.7.3. Biomarker detection in hydrogel dressing absorbed with human matrix and clinical wound exudate:

The final experiment was performed with hydrogel absorbed with human matrix and clinical wound exudate and spiked with different concentrations of TNF-α and IL-6. A reference channel-based approach was used to perform measurements in such a complicated matrix, whereby the measurement channel was functionalised with the specific antibodies and blocked with casein to avoid non-specific binding. In contrast, the reference channel was blocked with casein only to prevent non-specific protein adsorption. The specific binding signal for antigen binding was then obtained by subtracting the shift observed in the reference channel from the shift observed in the signal channel, an example shown in Figure 36. The corresponding wavelength shifts are shown in Figures 34b and 34c. Critically, the resonance shifts observed in Figures 32 and 34 are comparable, indicating the system's robustness in measuring complex matrices such as wound fluid absorbed in hydrogel-based dressings. In addition, due to the limited amount of clinical wound exudate, the detection of TNF-α and IL-6 was performed in hydrogel dressing containing clinical wound exudate and spiked at a concentration of 1 ng/mL for both antigens. This concentration was chosen as clinically relevant value for both these biomarkers in the context of wound healing is above this value. The results for the clinical wound exudate absorbed hydrogel dressings are shown in Figures 34d and 34e. The results indicate that the developed biosensing interface was robust enough to perform measurements in complex clinical matrices.

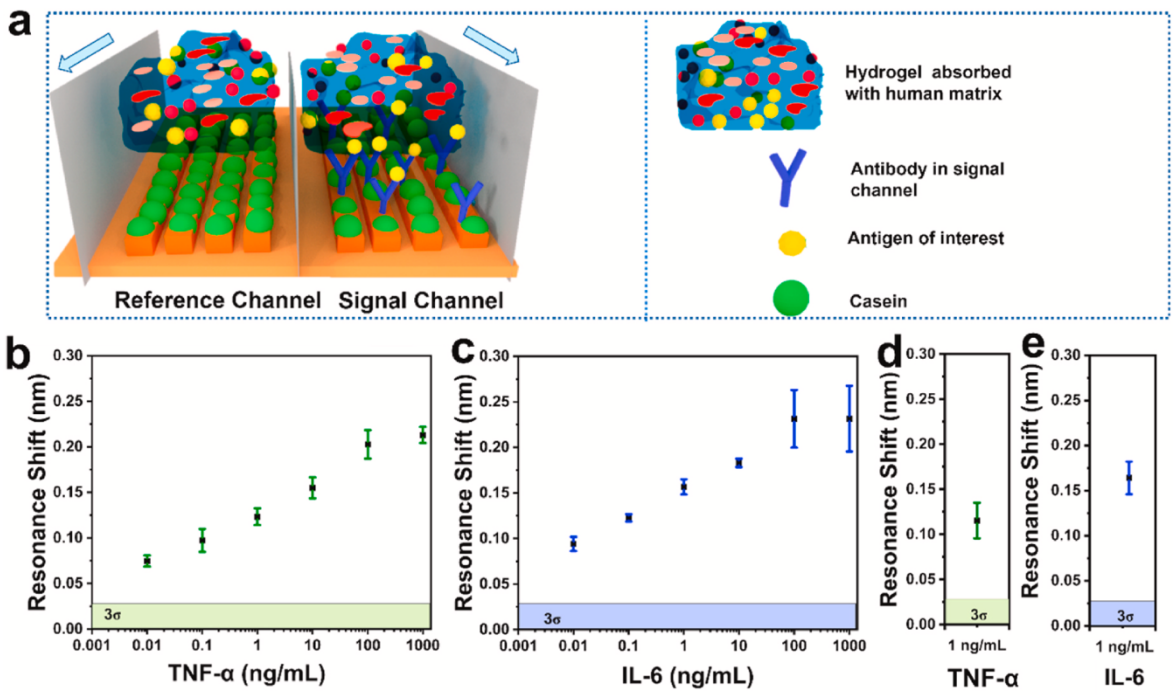

FIGURE 34: (a) Schematic of the biorecognition assay used to detect TNF-α and IL-6 on both the signal and the reference channels. The arrow in Figure 34a represents the direction of flow of sample in microfluidic channel; b) and c) Differential resonance shifts obtained by subtracting the shift observed in reference channel from the shift observed in signal channel for TNF-α and IL-6 binding, spiked into human matrix absorbed dressings for concentrations varying from 0.01 ng/mL to 1 µg/mL; (d) and (e) Resonance shifts observed for the 1 ng/mL TNF-α and IL-6 spiked in the hydrogel dressing absorbed with clinical wound exudate acquired from the hospital. The error bars correspond to the standard deviation derived from three separate experiments for each concentration.

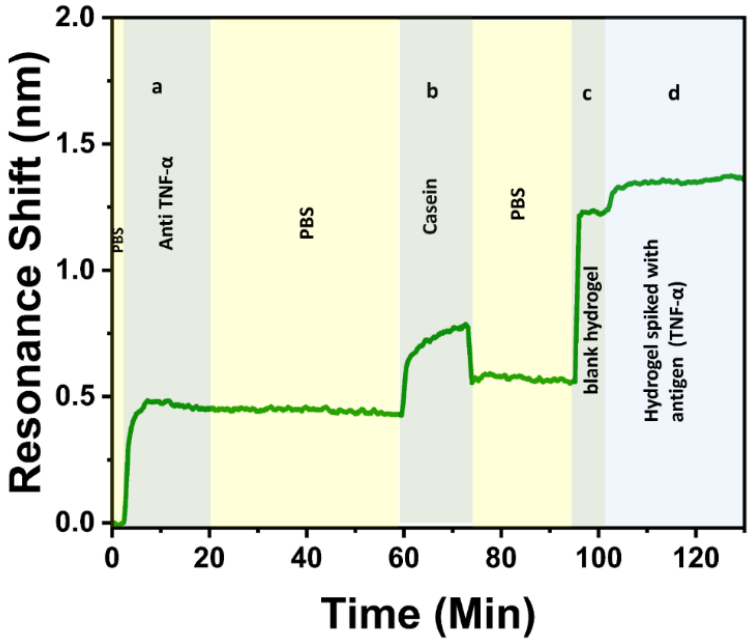

FIGURE 35: Full assay to perform antigen (TNF-α) detection in hydrogel-based dressing. The polydopamine functionalised surface is a) immobilised with anti-TNF-α (50 µg/mL) followed by a washing step with phosphate buffer saline and b) blocking of the surface with casein to block remaining sites, followed by another washing step in PBS c) The blank hydrogel is introduced, which causes an obvious refractive index shift followed by d), the hydrogel spiked with the antigen of interest is introduced, here TNF-α and clear binding curve for antigen binding is observed.

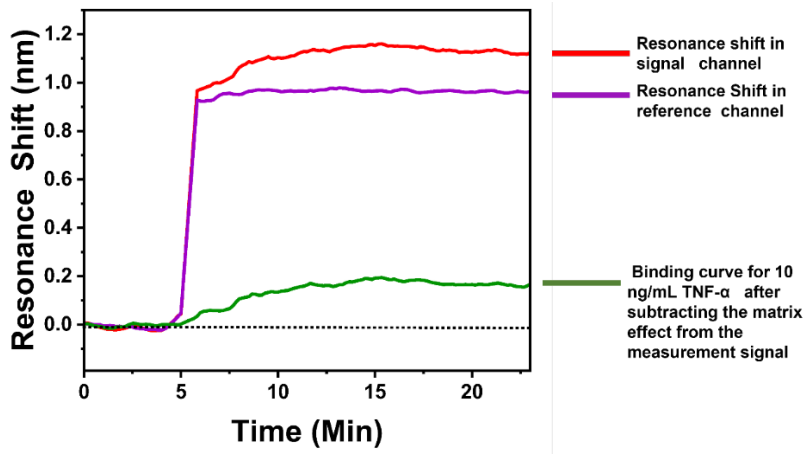

FIGURE 36: The resonance shift for antigen detection in the human matrix /hydrogel mixture was determined by subtracting the shift observed in the reference channel from the shift observed in the signal channel. The reference channel was blocked with casein.

4.8. Summary of the work reported in the chapter:

In this chapter, I have reported the development of a nanophotonic-based diagnostic element of a novel theranostic system that can sample wound biomarkers in a non-invasive manner without harming the wound bed and the quantification of the biomarkers can be performed using chirped guided mode resonance-based sensors. Hence, it can be deployed for longer-term monitoring of chronic wounds in a non-invasive manner. The detection of two wound biomarkers i.e., IL-6 and TNF-α, in human matrix and clinical wound exudate absorbed hydrogel dressing using chirped guided mode resonance-based sensing modalities at clinically relevant concentrations is performed. Achieving high sensitivity and wide dynamic range are important in the context of the clinical relevance of the developed sensing system. Also, the presence of hydrogel in the biological matrix employed here for the measurements could have played an important role in achieving high performance for biomarker detection because of the antifouling properties of hydrogels [231-233].

Chapter 5. Nanophotonic platform for highly sensitive detection of trypsin enzyme in human urine

5.1. Enzymes:

Enzymes are the biological catalysts that increase the rate of biochemical reactions occurring in living entities [234]. The enzyme structure is made up of complex proteins molecules [235]. The word enzyme was first given by German physiologist Wilhelm Kühne in 1878 while presenting his work demonstrating the production of alcohol from sugars by yeast [234]. Though earlier it was believed that enzymes consist of mostly proteins, later it was found that ribonucleic acid molecules also possess catalytic properties and are termed ribozymes and play an essential role in gene expression [234, 236]. For applications such as drug screening and discovery, enzyme bioassays can be beneficial [237]. Generally, enzymes are usually classified based on the reaction they are involved in catalysing and have a suffix at the end, such as oxidase, dehydrogenase, etc. Additionally, enzymes are also classified, addressed or identified on the basis of their substrate that they catalyse, for example, glucose oxidase, alcohol dehydrogenase, etc. [234].

5.2. Protease enzymes:

Proteases are the class of enzymes that came into existence in the very early stages of protein evolution and were required for protein catalysis in the earliest organisms [238]. Protease enzymes are responsible for the catalysis of the proteolysis reaction of proteins into smaller polypeptide units or single amino acid units [239]. Protease enzymes are responsible for many important biological processes such as digestion, cell proliferation of the cell, fertility, etc. Cancer and neurodegenerative disorders can occur when the protease enzymes are not functioning properly [240]. Besides biological applications, protease enzymes are widely used in other food industries and drug discovery [241, 242]. Protease enzymes are also employed in wastewater management [243].

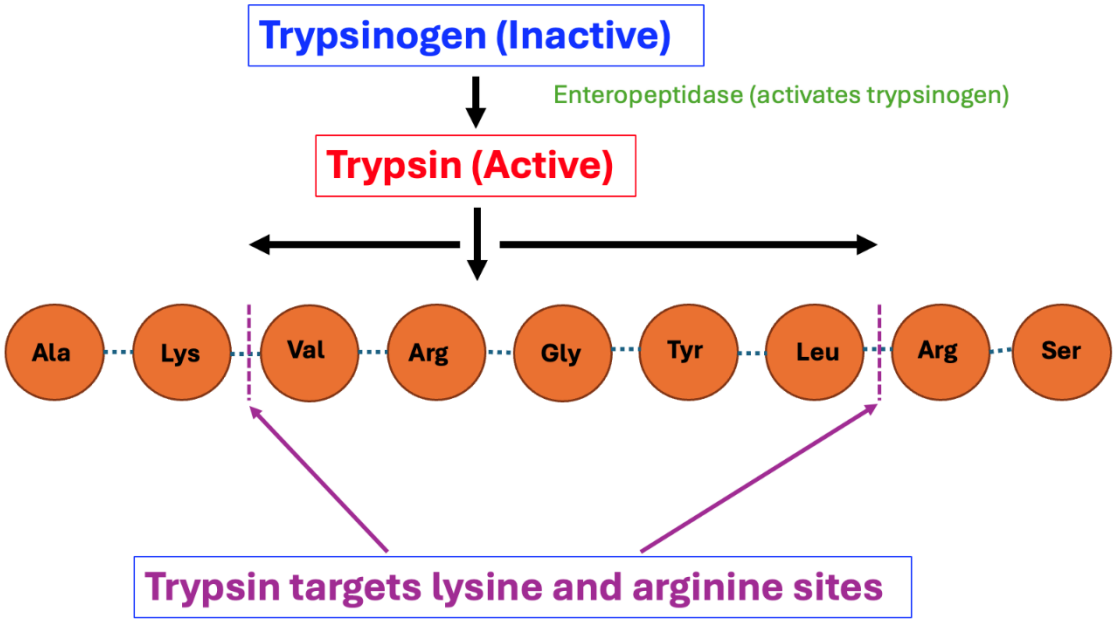

FIGURE 37: Mechanism of action of trypsin enzyme on proteins.

Trypsin, a serine protease secreted by the pancreas, is required for the hydrolysis of protein molecules into shorter peptide segments to enhance and increase their absorption [244, 245]. Trypsin enzyme is secreted as a trypsinogen molecule in the pancreas, which is its inactive or unfunctional form and is converted into trypsin, its active form in the duodenum by the enzyme named enteropeptidase and this enzyme acts on arginine and lysine sites via carboxyl functional group of proteins to break down the protein into smaller units, as shown in Figure 37 [245, 246]. Abnormal trypsin levels such as elevated or decreased, can indicate or refer to various conditions and diseases, such as cancer [247], metabolic disorders [248], cystic fibrosis [249], etc.

Pancreatic diseases affect a significant number of people worldwide [250, 251]. For example, pancreatitis is one of the most common pancreas diseases in the UK, resulting in 12000 hospital admissions per year [252], and the problem is rapidly increasing worldwide [253]. Trypsin is an important biomarker for monitoring pancreatic diseases [254].

General techniques or methods utilised for trypsin detection are Enzyme-linked immunosorbent assay [255], mass spectrometry [256], gel electrophoresis [257], fluorescence-based biosensors [258, 259] , etc. The requirement for labelling and bulky complicated read-out instruments complicates all these methods. Few studies have reported label-free sensors for trypsin detection to address this complication. For example, Nemati and coworkers developed a nanoporous anodic alumina-based optical sensor for trypsin detection [260]. The limit of detection reported in the study is 0.025 mg/mL for trypsin detection,

and biofluid testing was not performed. In another work, Tabrizi et al. used a nanoporous anodic alumina-based method to detect trypsin with a limit of detection achieved of 0.06 μg/mL [261].

There is no trypsin found or present in the urine of healthy people. However, in the urine of patients who have performed pancreas transplants contains high levels of trypsin, i.e. concentrations on the order of 10's of μg/ mL [262, 263]. To perform effective trypsin monitoring, robust and highly sensitive biosensors that can be cost-effectively deployed and can exhibit a wide dynamic range are required for the purpose.

This chapter reports the development of a biological interface for a chirped-guided mode resonance-based nanophotonic platform to detect trypsin in clinical human urine samples.

5.3. Materials:

β-casein was purchased from Sigma Aldrich and trypsin from the porcine pancreas was purchased from Sigma Aldrich

Human urine samples were collected from 13 healthy adults recruited from within the University of York. Before utilisation, the urine samples underwent filter sterilisation using 0.22 μm syringe filters to eliminate any cells present. Subsequently, the urine samples were pooled to create a combined human urine sample. This was followed by the aliquotation of urine samples, and then samples were stored at a −80 °C freezer. The urine samples were collected and handled according to procedures approved by the University of York's Department of Biology Ethics Committee and in obedience with the UK Concordat to Support Research Integrity (2019). Consent with full knowledge was obtained from all the people who donated urine sample donors.

All other materials that were used in the work, the sources are reported in chapters 2,3 and 4.

5.4. Methods:

5.4.1. Trypsin detection experiments in phosphate buffer saline (PBS):

Guided mode resonance sensors used for the experiments were fabricated by electron beam lithography, as described in Chapter 2, section 2.7.2. Following the functionalisation of the sensors with PDA chemistry, as described in Chapter 3, microfluidics was placed together with the sensors, and the sensor was clamped to a custom-made 3D-printed holder. First, the PBS solution was flown over the sensor surface with a flow rate of 75 μL/min controlled by a syringe pump to achieve a stable baseline. Then, a 100 μg/mL of β-Casein solution prepared in PBS was flown over the sensor surface, followed by the washing step to remove any unbound β-Casein. The temperature for the experiments was maintained at 20°C. Finally, the trypsin solutions (in PBS) were introduced into the fluidic channels at a range of concentrations from 0.1 ng/mL to 1000 ng/mL.

5.4.2. Trypsin detection experiments in human urine:

The enzyme detection experiments in human urine were performed at 20°C. A syringe pump controlled the flow rate at 75 µL/min. After immobilising the sensor surface with β-Casein and washing off any unbound β-casein, as described in section 5.4.1, unspiked human urine was first introduced into the fluidic channels. Then urine spiked with trypsin was introduced into the fluidic channels at a range of concentrations from 0.1 ng/mL to 1000 ng/mL.

5.5. Results and discussion:

A stable surface functionalisation method ensures sensitive detection of the analytes of interest from a complex matrix. Figure 38 (a -d) describes the sensors' biological interface preparation to detect trypsin. PDA surface chemistry was used to functionalise the sensor surface for biomolecule immobilisation, as described in Chapter 3. The immobilisation of substrate β-casein molecules on the functionalised sensor surface was performed in flow. Figure 38c shows the sensor surface immobilised with β-casein molecules, and Figure 38d illustrates the trypsin action on the sensor.

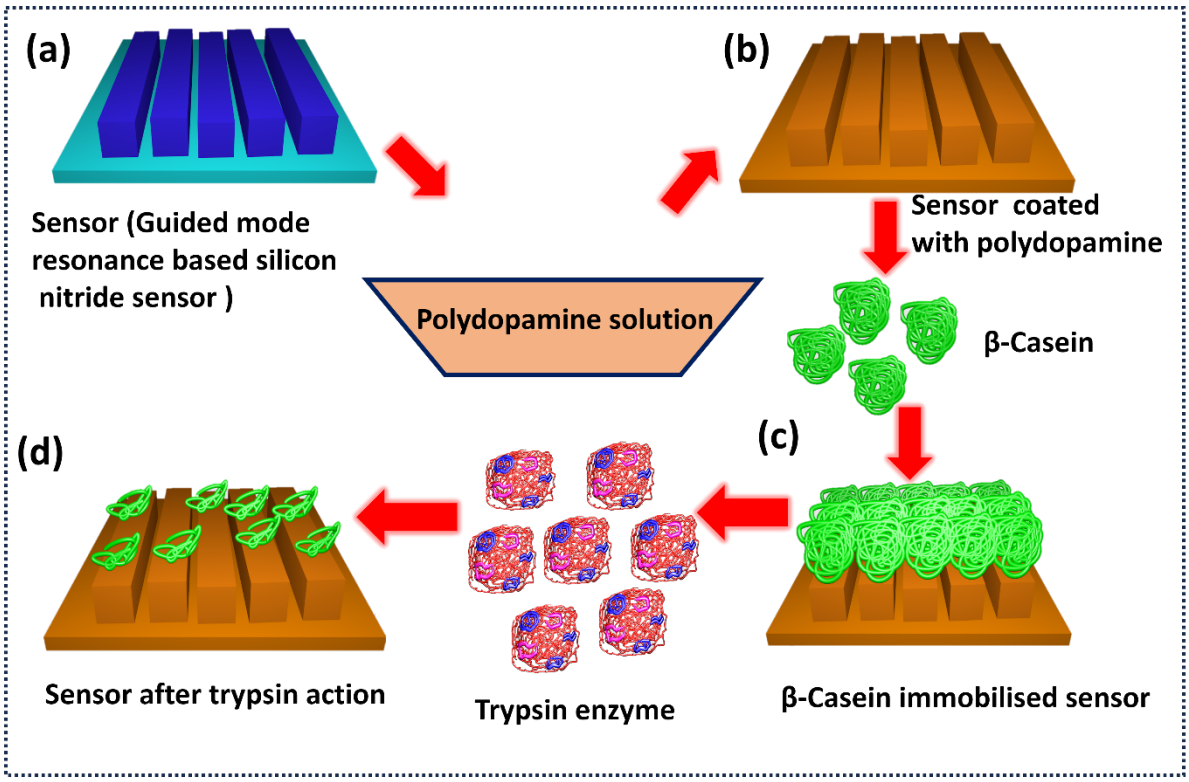

FIGURE 38: Structure of the sensor and biological interface for the detection of trypsin: (a) Sketch of the silicon nitride-based grating sensor; (b) coating of the sensor surface with polydopamine surface chemistry; (c) in-flow immobilisation of β-casein on the coated sensor surface; (d) sensor surface after the action of the enzyme.

5.5.1. Detection of trypsin using guided mode resonance-based sensors in PBS:

To start with, first, the detection of trypsin was performed in PBS. GMR sensors typically exhibit an increase in resonance wavelength when proteins bind to the sensor surface. This occurs because the bound material increases the refractive index of the cladding, thereby affecting the effective index of the mode. In contrast, since trypsin digests the β-casein and breaks it into smaller peptides, we observe a mass loss on the sensor surface. Hence, a reduction in resonance wavelength is observed. By tracking the resonance position over time, the kinetics of unbinding by digestion of the β-casein layers from the sensor surface is monitored. Figure 39b shows the full assay for trypsin detection in PBS using β-casein as substrate.

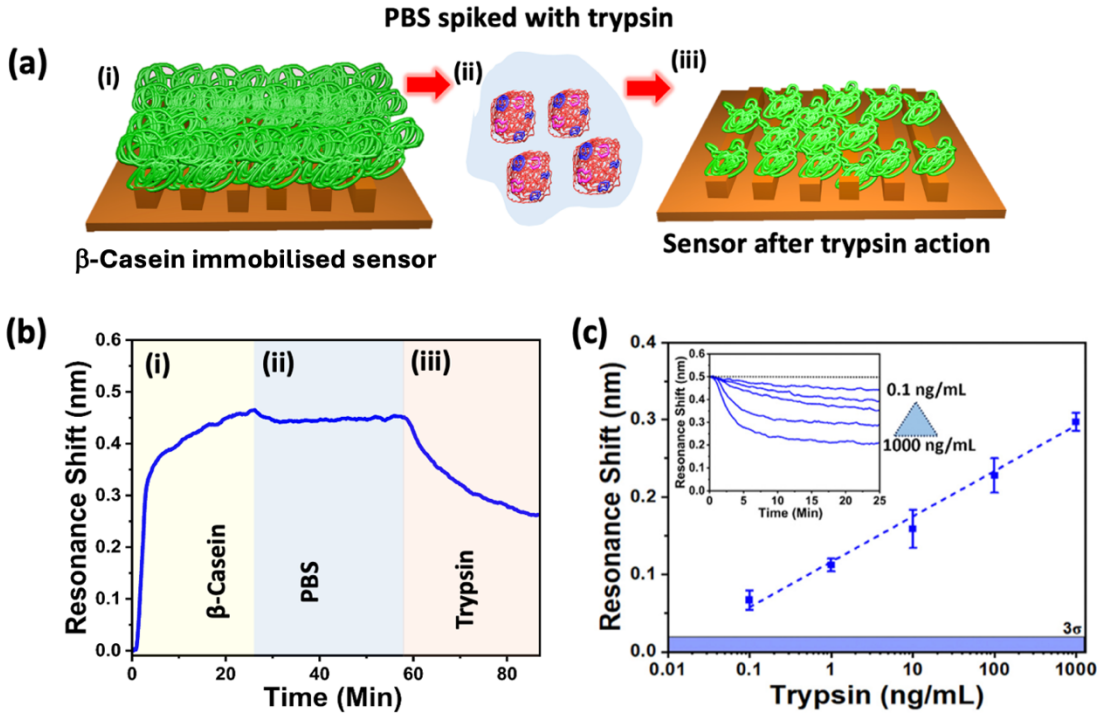

FIGURE 39: (a) Schematic illustrating the detection of trypsin enzyme in PBS; (b) Full assay for the detection of trypsin in PBS; (c) dynamic range graph for trypsin detection between 0.1 ng/mL and 1000 ng/mL. The inset shows the unbinding curves for the different trypsin concentrations between 0.1 ng/mL-1000 ng/mL as the enzyme digests the β-casein.

Figure 39c shows the dynamic range for different trypsin concentrations, varying from 0.1 ng/mL to 1000 ng/ mL. The resonance shift observed for a concentration of 0.1 ng/mL is~0.066 nm, which is well above the 3σ (mean 3σ = 0.019 nm ± 0.01 nm (n = 31 ± SD)) value of the system. For the higher concentrations up to 1000 ng/mL, we observe a linear trend with an R^2 value of 0. 99383 indicating that the sensor is very suitable for quantifying different trypsin concentrations. The inset in Figure 39c displays the individual unbinding curves for different concentrations ranging from 0.1 ng/mL to 1000 ng/mL of trypsin. To study the effect of interfering molecules in human urine on trypsin detection, urea and glucose were as interferents and added into PBS. The resonance shift for 100 ng/mL of trypsin in PBS was observed to be 0.228 ± 0.02 nm (n=3). The resonance shift observed for 100 ng/mL of trypsin in PBS buffer with 2% urea in it was 0.231± 0.01 nm (n=3), and the resonance shift for 100 ng/mL of trypsin in PBS buffer with 100 ug/mL of glucose in it the shift observed was 0.232± 0.03 nm (n=3). As the resonance shift observed for all three buffer types is comparable, it can be concluded that interferents added in the PBS buffer had a negligible effect on trypsin detection.

5.5.2. Detection of trypsin in undiluted human urine:

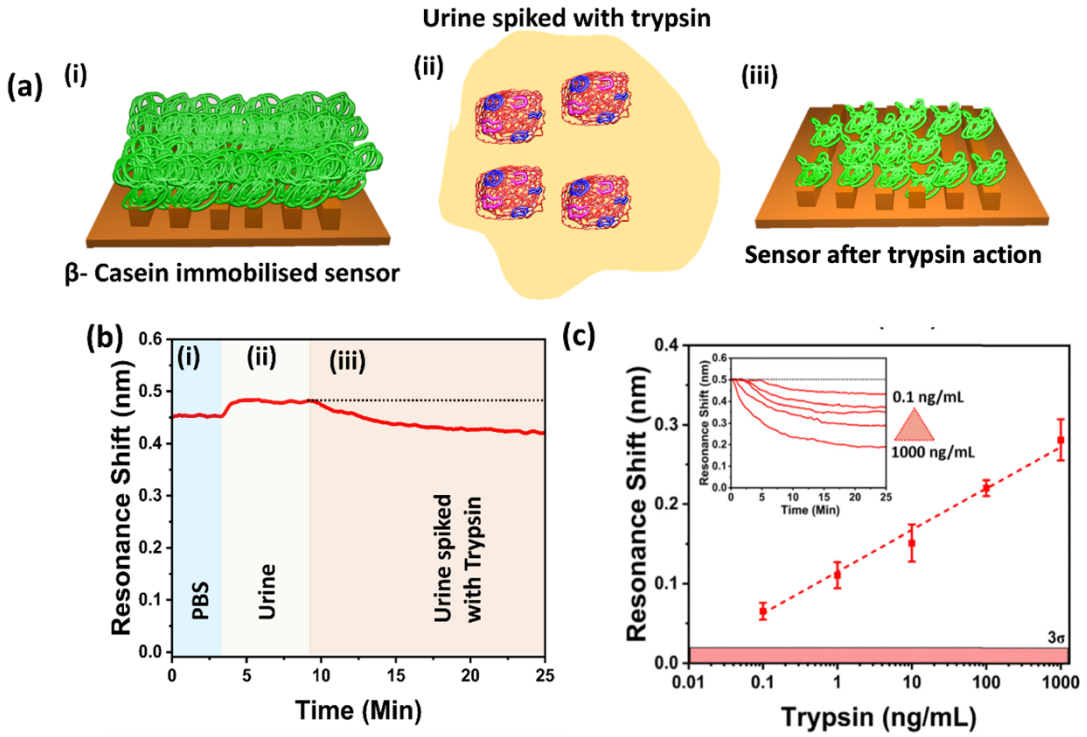

FIGURE 40: (a) Schematic of the detection of trypsin in human urine; (b) Detection of trypsin in undiluted human urine; (c) Dynamic range data for the detection of different trypsin concentrations in undiluted human urine, ranging from 0.1 ng/mL to 1000 ng/mL. The inset shows the digestion of β-casein by different concentrations of trypsin spiked in human urine for concentrations from 0.1 ng/mL to 1000 ng/mL.

To assess the suitability of our sensor for enzyme detection in human biofluids, we conducted enzyme detection measurements using undiluted human urine. The schematic in Figure 40a illustrates the application of human urine spiked with trypsin to a layer of β-casein immobilised on the sensor surface. The functionalised sensor surface is first immobilised with β-casein molecules, and a washing step with PBS buffer is performed, which is the same as shown in Figures 39b-i and 39b-ii. The β-casein immobilised sensor surface is then exposed to undiluted human urine Figure 40b-ii to observe if any other enzymes or biomolecules presented in undiluted clinical human urine cause any reaction on the sensor surface. A small resonance shift is observed because of the higher refractive index of urine Figure 40b-ii. We then flowed the urine spiked with trypsin across the sensor Figure 40b-iii, and a clear unbinding curve was observed, indicating the specificity of the trypsin detection. We used the same concentration range as for PBS, i.e., 0.1 ng/mL to 1000 ng/mL of trypsin spiked in undiluted human

urine, and Figure 40c shows the corresponding resonance shifts for the different concentrations of trypsin spiked in undiluted human urine. The average shift observed for 0.1 ng/mL is approx. 0.065 nm, which is above the 3-sigma values of the systems. As before, we observe a linear trend with a high R^2 value of 0.99469. The inset in Figure 40c shows unbinding curves of β-casein layers by trypsin enzyme spiked in undiluted human urine.

5.6. Summary of the work reported in this chapter:

Overall, we optimised the biological interface for chirped-GMR sensor chips for the detection of the trypsin enzyme in human urine. The sensor surface is functionalised with β-casein layers via PDA film. The trypsin detection was performed via hydrolysis of β-casein layers by trypsin enzyme. The amount of hydrolysis of β-casein layers is directly proportional to the concentration of the trypsin enzyme. The trypsin detection assay was performed in phosphate buffer saline and undiluted human urine. The lowest concentration detected in phosphate buffer saline and human urine was 0.1 ng/mL, with a linear trend observed for trypsin detection from 0.1 ng/mL to 1000 ng/mL trypsin.

Considering the important biological functions that trypsin enzymes perform, developing efficient biosensing platforms for the detection of trypsin and monitoring its activity can play an important role in the efficient management of pancreatic and other diseases. Developing label-free and sensitive biosensing devices that perform well in biological fluids for trypsin detection and have the potential for commercialisation and wide-scale deployment. In brief, biosensors for trypsin detection can contribute significantly to medical diagnostics, pharmaceutical research, food safety, and environmental monitoring.

Table 6 compares the performance of the label-free sensing system developed for trypsin detection with the other label-free sensors reported for trypsin detection in the literature.

Table 6: Label-free biosensors for detection of trypsin enzyme.

Sr. No.	Sensor type	Lowest concentration detection reported	Substrate used	Tested in biofluid	Reference
1.	Nanoporous anodic alumina	0.025 mg/mL	Gelatin	-	[260]
2.	Nanoporous Anodic Alumina	0.06 μg/mL	Urease and fluorescein 5(6)-isothiocyanate	2 μg/mL concentration detected in human urine with 86 % recovery	[261]
3.	Electrical detection nanochannels	5 ng/mL	Polylysine	-	[264]
4.	Quartz crystal microbalance	8.5 ng/mL	Au nanoparticles functionalised with mercaptoacetic acid coupled to peptide chain immobilised on the sensor surface.	-	[265]
5.	Guided mode resonance-based sensor	Lowest concentration detected is 0.1 ng/mL in PBS and human urine	β-Casein	Range of concentrations detected in undiluted human urine from 0.1 ng/mL to 1000 ng/mL	This work

6. Objectives achieved and Conclusions:

The thesis makes progress towards the development of an efficient bio-interface for silicon nitride-based guided mode resonance-based photonic sensing chips by studying polydopamine-based surface chemistry as a one-step method to immobilise bioreceptors. Polydopamine (PDA), inspired by the adhesive properties of mussel foot proteins, offers a versatile and universal surface functionalisation route. The thesis demonstrates that PDA forms a stable, reactive coating on silicon and silicon nitride-based surfaces, allowing efficient one-step and robust immobilisation of bioreceptors.

Progress made towards each objective mentioned in the introduction:

1. To evaluate the performance of polydopamine-based surface chemistry for the immobilisation of various bioreceptors using chirped guided mode resonance biosensors and stability of polydopamine surface chemistry in different environmental conditions.
2. To investigate the analytical performance of the functionalised chirped guided mode resonance-based biosensors in detecting a range of clinically relevant protein biomarkers (IgG, CRP, MMP-9, TNF-α, IL-6) and study the suitability of the polydopamine-based interface to perform measurements in complex human biofluids**.**

The work reported in Chapter 3 reports the progress towards objectives 1 and 2. Conclusions and future work are discussed below

6.1. Conclusions Chapter 3-Bioinspired polydopamine layer as versatile functionalisation protocol for silicon-based photonic biosensor:

We have studied a bio-inspired polydopamine (PDA) based surface functionalisation protocol for silicon-based sensors and have shown that it can be used as a simple, single-step method for the immobilisation of functional bioreceptors on the sensor surface. The polydopamine based protocol provides a higher surface density of immobilised biomolecules when compared to more familiar surface chemistries based on surface silanisation and NHS crosslinkers and bioreceptor conjugation using crosslinkers. We believe that this improvement is partially due to the insensitivity of the PDA film to hydrolysis but also to its simplicity and the brevity of the process. Further, when tested on GMR biosensors, we observe a wide dynamic range for the detection of IgG, CRP and MMP-9 biomarkers. In addition, we also verified the compatibility of the protocol with complex biofluids (diluted human serum) and were able to successfully perform measurements to ng/mL sensitivity. We also tested the integrity of the film by exposing coated and uncoated sensors to alkaline media and observed a delay in the onset of degradation, thus highlighting the high quality of the film and its ability to provide additional functionality by protecting the sensor surface. Overall, we suggest that the wider adoption of

this protocol should improve the consistency of photonic immunoassays and that its simplicity will encourage researchers to engage more widely with surface functionalisation and the addition of biorecognition elements to their experiments.

6.1.1. Future Work:

Future work in this area should involve studying other mussel-inspired chemistries, such as poly levodopa and polynorepinephrine films, comparing their efficiency with the polydopamine films in terms of bioreceptor immobilisation density and signal observed for the analyte detection. In addition, it will be interesting to develop better antifouling strategies in combination with mussel-inspired chemistries to perform analyte detection in undiluted human biofluids such as human serum.

3. To develop a bio-interface for the detection of wound biomarkers and perform the detection of wound biomarkers in phosphate buffer, hydrogel-based wound dressings, and clinical wound fluid-absorbed hydrogel dressings.
   The results reported in Chapter 4 demonstrated the progress made towards the Objective 3 by developing a biointerface for the detection of wound biomarkers**.**

6.2. Conclusions Chapter 4-Nanophotonic and hydrogel-based diagnostic system for the monitoring of chronic wounds:

We report progress towards the development of a nanophotonic theranostic system for the non-invasive monitoring and improved management of chronic wounds by developing a diagnostic element of the system. We demonstrate the successful detection of two important wound biomarkers, i.e., TNF-α and IL-6 in a clinically relevant matrix. Remarkably, we observe very similar resonance shifts for antigens spiked into phosphate buffer saline (PBS), hydrogel and human matrix absorbed hydrogel dressings. We have also studied the applicability of this system with clinical wound sample acquired from the hospital and observed the similar resonance shifts for 1 ng/mL of TNF-α and IL-6 as we in the other above-mentioned matrix. This similarity highlights the high quality and the robustness of the biosensing interface we have developed. Both the sensitivity and the dynamic range are essential for the clinical relevance of the developed test to account for variations between patients and for assessing different stages of wound healing.

6.1.2. Future work:

The developed diagnostic system must be tested and validated with more clinical samples. Also, the biological interface needs to be developed and tested with other biomarkers, such as proteases, cytokines, enzymes, and microbes, to better monitor and predict the status of chronic wounds.

Furthermore, a larger-scale patient study is required to better understand the correlation between biomarker concentration and the wound healing process and to inform the clinically actionable outcome. With these future improvements, we believe that our approach can be used with a wide range of hydrogel-based wound dressings and form the basis of a low-cost near-patient theranostic wound healing system.

4. To develop biointerface for detection of enzyme as analyte in phosphate buffer saline and clinical urine using chirped guided mode resonance based biosensors.

   Chapter 5 reports the development toward the objective 4 that is bio interface was optimised on chirped guided mode resonance sensors using PDA chemistry for detection of enzymes.

6.2. Conclusions Chapter 5-Nanophotonic platform for the highly sensitive detection of trypsin enzyme in human urine:

In this work, we developed a guided mode resonance-based nanophotonic test for the highly sensitive detection of the trypsin enzyme in human urine. The biological interface we developed using β-casein layers immobilised on the polydopamine surface chemistry helped to detect a range of trypsin concentrations from 0.1ng/mL to 1000 ng/mL in phosphate buffer saline and human urine. The test can be used for the screening and timely treatment of diseases such as cystic fibrosis, pancreatitis, and pancreatic cancer. In addition, the advancement of label-free nanophotonic-based approaches opens up novel avenues for detecting enzyme activity at extremely low concentrations.

6.2.1. Future work:

The future work in this project should involve optimising the biological interface for more sensitive detection by developing more sensitive guided-mode resonance sensor chips and biological interfaces. We should explore other substrates, perform trypsin detection using different substrates, and compare the sensitivities for the biological interface side. In addition, it would be interesting to optimise the biological interface to detect trypsin enzymes in other biological fluids, such as human serum. The development of the biological interface for the detection of other enzyme classes (e.g. proteases) of clinical significance would be of great interest.

This thesis demonstrates that polydopamine surface chemistry, when integrated with chirped guided mode resonance-based sensors, enables a simplified, reproducible and high-performance platform for detection of biomarkers of clinical interest.

- The polydopamine surface chemistry helps in achieving bioreceptor immobilisation on the sensor surface via a single-step functionalisation without loss of sensitivity.

- It is solid and robust enough to perform detection in clinical matrices such as serum, urine, and wound fluid absorbed by hydrogel dressings.
- It is possible to detect different types of biomarkers, such as antibodies, cytokines and enzymes etc.

The work reported in this thesis helps in bridging the gap by a studying simple to perform polydopamine surface chemistry to prepare a bio interface for the detection of a range of biomarkers in different type of biofluids. These results make the way for broader translation of chirped guided mode resonance-based biosensors into clinical and near-patient tests.

6. References:

[1] D. Bhatia, S. Paul, T. Acharjee, S.S. Ramachairy, Biosensors and their widespread impact on human health, Sensors International, 5 (2024) 100257.
[2] S. Sharma, J. Zapatero-Rodriguez, P. Estrela, R. O'Kennedy, Point-of-Care Diagnostics in Low Resource Settings: Present Status and Future Role of Microfluidics, Biosensors (Basel), 5 (2015) 577-601.
[3] O. Pashchenko, T. Shelby, T. Banerjee, S. Santra, A Comparison of Optical, Electrochemical, Magnetic, and Colorimetric Point-of-Care Biosensors for Infectious Disease Diagnosis, ACS Infectious Diseases, 4 (2018) 1162-1178.
[4] S. Mostufa, B. Rezaei, S. Ciannella, P. Yari, J. Gomez-Pastora, R. He, K. Wu, Advancements and Perspectives in Optical Biosensors, ACS Omega, 9 (2024) 24181-24202.
[5] E.H. Yoo, S.Y. Lee, Glucose biosensors: an overview of use in clinical practice, Sensors (Basel), 10 (2010) 4558-4576.
[6] N. Bhalla, P. Jolly, N. Formisano, P. Estrela, Introduction to biosensors, Essays in Biochemistry, 60 (2016) 1-8.
[7] S. Mummareddy, S. Pradhan, A.K. Narasimhan, A. Natarajan, On Demand Biosensors for Early Diagnosis of Cancer and Immune Checkpoints Blockade Therapy Monitoring from Liquid Biopsy, Biosensors (Basel), 11 (2021) 500.
[8] A. Chougale, S. Vedante, G. Kulkarni, S. Patnawar, Recent Progress on Biosensors for the Early Detection of Neurological Disorders, ChemistrySelect, 7 (2022) e202203155.
[9] J. Cheon, J. Qin, L.P. Lee, H. Lee, Advances in Biosensor Technologies for Infection Diagnostics, Accounts of Chemical Research, 55 (2022) 121-122.
[10] J. Kim, A.S. Campbell, B.E. de Avila, J. Wang, Wearable biosensors for healthcare monitoring, Nature Biotechnology, 37 (2019) 389-406.
[11] R. Uddin, I. Koo, Real-Time Remote Patient Monitoring: A Review of Biosensors Integrated with Multi-Hop IoT Systems via Cloud Connectivity, Applied Sciences, 14 (2024) 1876.
[12] A.I. Zamaleeva, G. Despras, C. Luccardini, M. Collot, M. de Waard, M. Oheim, J.M. Mallet, A. Feltz, FRET-Based Nanobiosensors for Imaging Intracellular Ca(2)(+) and H(+) Microdomains, Sensors (Basel), 15 (2015) 24662-24680.
[13] C. Meliana, J. Liu, P.L. Show, S.S. Low, Biosensor in smart food traceability system for food safety and security, Bioengineered, 15 (2024) 2310908.
[14] C.W. Huang, C. Lin, M.K. Nguyen, A. Hussain, X.T. Bui, H.H. Ngo, A review of biosensor for environmental monitoring: principle, application, and corresponding achievement of sustainable development goals, Bioengineered, 14 (2023) 58-80.
[15] M. Pohanka, Current Trends in the Biosensors for Biological Warfare Agents Assay, Materials (Basel), 12 (2019) 2303.
[16] X. Lu, M. Cui, Q. Yi, A. kamrani, Detection of mutant genes with different types of biosensor methods, TrAC Trends in Analytical Chemistry, 126 (2020) 115860.
[17] M. Ngoepe, Y.E. Choonara, C. Tyagi, L.K. Tomar, L.C. du Toit, P. Kumar, V.M. Ndesendo, V. Pillay, Integration of biosensors and drug delivery technologies for early detection and chronic management of illness, Sensors (Basel), 13 (2013) 7680-7713.
[18] W.S. Liang, B. Beaulieu-Jones, S. Smalley, M. Snyder, L.H. Goetz, N.J. Schork, Emerging therapeutic drug monitoring technologies: considerations and opportunities in precision medicine, Frontiers in Pharmacolgy, 15 (2024) 1348112.
[19] P. Mehrotra, Biosensors and their applications - A review, Journal of Oral Biology and Craniofacial Research, 6 (2016) 153-159.
[20] V. Naresh, N. Lee, A Review on Biosensors and Recent Development of Nanostructured Materials-Enabled Biosensors, Sensors (Basel), 21 (2021) 1109.
[21] X. Wang, J. Zhou, H. Wang, Bioreceptors as the key components for electrochemical biosensing in medicine, Cell Reports Physical Science, 5 (2024) 101801.
[22] E.O. Polat, M.M. Cetin, A.F. Tabak, E. Bilget Guven, B.O. Uysal, T. Arsan, A. Kabbani, H. Hamed, S.B. Gul, Transducer Technologies for Biosensors and Their Wearable Applications, Biosensors (Basel), 12 (2022) 385.

[23] J.F. Masson, Consideration of Sample Matrix Effects and "Biological" Noise in Optimizing the Limit of Detection of Biosensors, ACS Sensors, 5 (2020) 3290-3292.
[24] K.E. Mach, P.K. Wong, J.C. Liao, Biosensor diagnosis of urinary tract infections: a path to better treatment?, Trends in Pharmacological Sciences, 32 (2011) 330-336.
[25] N. De Acha, A.B. Socorro-Leranoz, C. Elosua, I.R. Matias, Trends in the Design of Intensity-Based Optical Fiber Biosensors (2010-2020), Biosensors (Basel), 11 (2021) 197.
[26] G. Pitruzzello, T.F. Krauss, Photonic crystal resonances for sensing and imaging, Journal of Optics, 20 (2018) 073004.
[27] R. Guider, D. Gandolfi, T. Chalyan, L. Pasquardini, A. Samusenko, C. Pederzolli, G. Pucker, L. Pavesi, Sensitivity and Limit of Detection of biosensors based on ring resonators, Sensing and Bio-Sensing Research, 6 (2015) 99-102.
[28] I. Molina-Fernandez, J. Leuermann, A. Ortega-Monux, J.G. Wanguemert-Perez, R. Halir, Fundamental limit of detection of photonic biosensors with coherent phase read-out, Optics Express, 27 (2019) 12616-12629.
[29] W.J. Peveler, M. Yazdani, V.M. Rotello, Selectivity and Specificity: Pros and Cons in Sensing, ACS Sensors, 1 (2016) 1282-1285.
[30] R. Dubey, R. Bhushan, Specificity versus selectivity: twin aims of aptasensors in bioanalysis, Bioanalysis, 10 (2018) 1549-1551.
[31] B. Katey, I. Voiculescu, A.N. Penkova, A. Untaroiu, A Review of Biosensors and Their Applications, ASME Open Journal of Engineering, 2 (2023) 020201.
[32] M. Soler, L.M. Lechuga, Biochemistry strategies for label-free optical sensor biofunctionalization: advances towards real applicability, Analytical and Bioanalytical Chemistry, 414 (2022) 5071-5085.
[33] G. Kalaiyarasan, J. Joseph, Processes in biosensor design, development, and validation parameters, Health and Environmental Applications of Biosensing Technologies 2024, 27-49.
[34] M. Song, X. Lin, Z. Peng, S. Xu, L. Jin, X. Zheng, H. Luo, Materials and Methods of Biosensor Interfaces With Stability, Frontiers in Materials, 7 (2021).
[35] A. Fernandez Gavela, D. Grajales Garcia, J.C. Ramirez, L.M. Lechuga, Last Advances in Silicon-Based Optical Biosensors, Sensors (Basel), 16 (2016) 285.
[36] A.K. Singh, M. Anwar, R. Pradhan, M.S. Ashar, N. Rai, S. Dey, Surface plasmon resonance based-optical biosensor: Emerging diagnostic tool for early detection of diseases, Journal of Biophotonics, 16 (2023) e202200380.
[37] G. Rajeev, B. Prieto Simon, L.F. Marsal, N.H. Voelcker, Advances in Nanoporous Anodic Alumina-Based Biosensors to Detect Biomarkers of Clinical Significance: A Review, Advanced Healthcare Materials, 7 (2018) 1700904.
[38] R. Vercauteren, A. Leprince, J. Mahillon, L.A. Francis, Porous Silicon Biosensor for the Detection of Bacteria through Their Lysate, Biosensors (Basel), 11 (2021) 27.
[39] K. Sankar, U. Kuzmanovic, S.E. Schaus, J.E. Galagan, M.W. Grinstaff, Strategy, Design, and Fabrication of Electrochemical Biosensors: A Tutorial, ACS Sensors, 9 (2024) 2254-2274.
[40] I.H. Cho, D.H. Kim, S. Park, Electrochemical biosensors: perspective on functional nanomaterials for on-site analysis, Biomaterials Research, 24 (2020) 6.
[41] K. Cali, E. Tuccori, K.C. Persaud, Gravimetric biosensors, Methods in Enzymology, 642 (2020) 435-468.
[42] N. Alanazi, M. Almutairi, A.N. Alodhayb, A Review of Quartz Crystal Microbalance for Chemical and Biological Sensing Applications, Sensing and Imaging, 24 (2023) 10.
[43] H.J. Lim, T. Saha, B.T. Tey, W.S. Tan, C.W. Ooi, Quartz crystal microbalance-based biosensors as rapid diagnostic devices for infectious diseases, Biosensors and Bioelectronics, 168 (2020) 112513.
[44] T.T. Nguyen, C.M. Nguyen, M.A. Huynh, H.H. Vu, T.K. Nguyen, N.T. Nguyen, Field effect transistor based wearable biosensors for healthcare monitoring, Journal of Nanobiotechnology, 21 (2023) 411.
[45] T. Sakata, Signal transduction interfaces for field-effect transistor-based biosensors, Communications chemistry, 7 (2024) 35.
[46] D. Sadighbayan, M. Hasanzadeh, E. Ghafar-Zadeh, Biosensing based on field-effect transistors (FET): Recent progress and challenges, Trends in Analytical Chemistry, 133 (2020) 116067.
[47] M. Yakovleva, S. Bhand, B. Danielsson, The enzyme thermistor-a realistic biosensor concept. A critical review, Analytica Chimica Acta, 766 (2013) 1-12.

[48] S. Patel, R. Nanda, S. Sahoo, E. Mohapatra, Biosensors in Health Care: The Milestones Achieved in Their Development towards Lab-on-Chip-Analysis, Biochemistry Research International, 2016 (2016) 3130469.
[49] S. Akgönüllü, A. Denizli, Recent advances in optical biosensing approaches for biomarkers detection, Biosensors and Bioelectronics: X, 12 (2022) 100269.
[50] Y. Ye, M. Xie, J. Tang, J. Ouyang, Highly sensitive and tunable terahertz biosensor based on optical Tamm states in graphene-based Bragg reflector, Results in Physics, 15 (2019) 102779.
[51] X. Fan, I.M. White, S.I. Shopova, H. Zhu, J.D. Suter, Y. Sun, Sensitive optical biosensors for unlabeled targets: a review, Analytica Chimica Acta, 620 (2008) 8-26.
[52] Divya, D.S. Dkhar, R. Kumari, S. Mahapatra, R. Kumar, P. Chandra, Ultrasensitive Aptasensors for the Detection of Viruses Based on Opto-Electrochemical Readout Systems, Biosensors (Basel), 12 (2022) 81.
[53] W.-Z. Jia, K. Wang, X.-H. Xia, Elimination of electrochemical interferences in glucose biosensors, TrAC Trends in Analytical Chemistry, 29 (2010) 306-318.
[54] R. Laref, E. Losson, A. Sava, M. Siadat, Empiric Unsupervised Drifts Correction Method of Electrochemical Sensors for in Field Nitrogen Dioxide Monitoring, Sensors (Basel), 21 (2021) 3581.
[55] A. Afzal, A. Mujahid, R. Schirhagl, S. Bajwa, U. Latif, S. Feroz, Gravimetric Viral Diagnostics: QCM Based Biosensors for Early Detection of Viruses, Chemosensors, 5 (2017) 7.
[56] R. Hao, L. Liu, J. Yuan, L. Wu, S. Lei, Recent Advances in Field Effect Transistor Biosensors: Designing Strategies and Applications for Sensitive Assay, Biosensors (Basel), 13 (2023) 426.
[57] Z. Zheng, H. Zhang, T. Zhai, F. Xia, Overcome Debye Length Limitations for Biomolecule Sensing Based on Field Effective Transistors, Chinese Journal of Chemistry, 39 (2021) 999-1008.
[58] N.L. Henry, D.F. Hayes, Cancer biomarkers, Molecular Oncology, 6 (2012) 140-146.
[59] V.K. Sarhadi, G. Armengol, Molecular Biomarkers in Cancer, Biomolecules, 12 (2022) 1021.
[60] Y.Y. Broza, X. Zhou, M. Yuan, D. Qu, Y. Zheng, R. Vishinkin, M. Khatib, W. Wu, H. Haick, Disease Detection with Molecular Biomarkers: From Chemistry of Body Fluids to Nature-Inspired Chemical Sensors, Chemical Reviews, 119 (2019) 11761-11817.
[61] X. Zhang, B. Yao, Q. Hu, Y. Hong, A. Wallace, K. Reynolds, C. Ramsey, A. Maeder, R. Reed, Y. Tang, Detection of biomarkers in body fluids using bioprobes based on aggregation-induced emission fluorogens, Materials Chemistry Frontiers, 4 (2020) 2548-2570.
[62] C. Ozyurt, I. Uludag, B. Ince, M.K. Sezginturk, Lab-on-a-chip systems for cancer biomarker diagnosis, Journal of Pharmaceutical and Biomedical Analysis, 226 (2023) 115266.
[63] J.F. Rusling, C.V. Kumar, J.S. Gutkind, V. Patel, Measurement of biomarker proteins for point-of-care early detection and monitoring of cancer, Analyst, 135 (2010) 2496-2511.
[64] M.H. Son, S.W. Park, H.Y. Sagong, Y.K. Jung, Recent Advances in Electrochemical and Optical Biosensors for Cancer Biomarker Detection, BioChip Journal, 17 (2022) 44-67.
[65] D. Chen, Biomarkers navigate drug development: Pharmacology, effectiveness and safety, Medicine in Drug Discovery, 21 (2024) 100174.
[66] R.M. Califf, Biomarker definitions and their applications, Experimental Biology and Medicine, 243 (2018) 213-221.
[67] B. Holmstrom, M. Johansson, A. Bergh, U.H. Stenman, G. Hallmans, P. Stattin, Prostate specific antigen for early detection of prostate cancer: longitudinal study, BMJ, 339 (2009) b3537.
[68] T.S. Zabka, J. Burkhardt, W.J. Reagan, J.C. Gautier, W.E. Glaab, M. Guffroy, J. Harding, D. Brees, E. McDuffie, L. Ramaiah, A.E. Schultze, J.D. Smith, A. Wolfreys, D.A. Dalmas, The use of emerging safety biomarkers in nonclinical and clinical safety assessment - The current and future state: An IQ DruSafe industry survey, Regulatory Toxicology and Pharmacology, 120 (2021) 104857.
[69] B.R. Griffin, S. Faubel, C.L. Edelstein, Biomarkers of Drug-Induced Kidney Toxicity, Therapeutic Drug Monitoring, 41 (2019) 213-226.
[70] A. Bodaghi, N. Fattahi, A. Ramazani, Biomarkers: Promising and valuable tools towards diagnosis, prognosis and treatment of Covid-19 and other diseases, Heliyon, 9 (2023) e13323.
[71] K. Sechidis, K. Papangelou, P.D. Metcalfe, D. Svensson, J. Weatherall, G. Brown, Distinguishing prognostic and predictive biomarkers: an information theoretic approach, Bioinformatics, 34 (2018) 3365-3376.
[72] M.G. Davey, S.O. Hynes, M.J. Kerin, N. Miller, A.J. Lowery, Ki-67 as a Prognostic Biomarker in Invasive Breast Cancer, Cancers (Basel), 13 (2021) 4455.

[73] B.D. Malhotra, M.A. Ali, Nanomaterials in Biosensors, Nanomaterials for Biosensors 2018, 1-74.
[74] B. Byrne, E. Stack, N. Gilmartin, R. O'Kennedy, Antibody-based sensors: principles, problems and potential for detection of pathogens and associated toxins, Sensors (Basel), 9 (2009) 4407-4445.
[75] H.W. Schroeder, Jr., L. Cavacini, Structure and function of immunoglobulins, Journal of Allergy Clinical Immunology, 125 (2010) 41-52.
[76] S. Sharma, H. Byrne, R.J. O'Kennedy, Antibodies and antibody-derived analytical biosensors, Essays in Biochemistry, 60 (2016) 9-18.
[77] M.J. Ugarte-Orozco, G.A. López-Muñoz, A. Antonio-Pérez, K.M. Esquivel-Ortiz, J. Ramón-Azcón, High-throughput biointerfaces for direct, label-free, and multiplexed metaplasmonic biosensing, Current Research in Biotechnology, 5 (2023) 100119.
[78] S. Tombelli, M. Minunni, M. Mascini, Analytical applications of aptamers, Biosensors and Bioelectronics, 20 (2005) 2424-2434.
[79] B. Sequeira-Antunes, H.A. Ferreira, Nucleic Acid Aptamer-Based Biosensors: A Review, Biomedicines, 11 (2023) 3201.
[80] B.D. Wilson, H.T. Soh, Re-Evaluating the Conventional Wisdom about Binding Assays, Trends in Biochemical Sciences, 45 (2020) 639-649.
[81] Q. Liu, P. Wang, Cell-based biosensors: principles and applications, Artech House, 2009.
[82] N. Gupta, V. Renugopalakrishnan, D. Liepmann, R. Paulmurugan, B.D. Malhotra, Cell-based biosensors: Recent trends, challenges and future perspectives, Biosensors and Bioelectronics, 141 (2019) 111435.
[83] S.D. Wijayanti, L. Tsvik, D. Haltrich, Recent Advances in Electrochemical Enzyme-Based Biosensors for Food and Beverage Analysis, Foods, 12 (2023) 3355.
[84] A. Mulchandani, K.R. Rogers, Enzyme and microbial biosensors : techniques and protocols, 1998.
[85] H.H. Nguyen, S.H. Lee, U.J. Lee, C.D. Fermin, M. Kim, Immobilized Enzymes in Biosensor Applications, Materials (Basel), 12 (2019) 121.
[86] C.I.L. Justino, A.C. Freitas, R. Pereira, A.C. Duarte, T.A.P. Rocha Santos, Recent developments in recognition elements for chemical sensors and biosensors, TrAC Trends in Analytical Chemistry, 68 (2015) 2-17.
[87] K. Groff, J. Brown, A.J. Clippinger, Modern affinity reagents: Recombinant antibodies and aptamers, Biotechnology Advances, 33 (2015) 1787-1798.
[88] A. Hasan, M. Nurunnabi, M. Morshed, A. Paul, A. Polini, T. Kuila, M. Al Hariri, Y.K. Lee, A.A. Jaffa, Recent advances in application of biosensors in tissue engineering, BioMed Research International, 2014 (2014) 307519.
[89] I. Bazin, S.A. Tria, A. Hayat, J.L. Marty, New biorecognition molecules in biosensors for the detection of toxins, Biosensors and Bioelectronics, 87 (2017) 285-298.
[90] B. Strehlitz, N. Nikolaus, R. Stoltenburg, Protein Detection with Aptamer Biosensors, Sensors (Basel), 8 (2008) 4296-4307.
[91] D. Sakhuja, H. Ghai, R.K. Rathour, P. Kumar, A.K. Bhatt, R.K. Bhatia, Cost-effective production of biocatalysts using inexpensive plant biomass: a review, 3 Biotech, 11 (2021) 280.
[92] M.A. Morales, J.M. Halpern, Guide to Selecting a Biorecognition Element for Biosensors, Bioconjugate Chemistry, 29 (2018) 3231-3239.
[93] S. Sang, Y. Wang, Q. Feng, Y. Wei, J. Ji, W. Zhang, Progress of new label-free techniques for biosensors: a review, Critical Reviews in Biotechnology, 36 (2016) 465-481.
[94] Y. Wang, E.C. Alocilja, Gold nanoparticle-labeled biosensor for rapid and sensitive detection of bacterial pathogens, Journal of Biological Engineering, 9 (2015) 16.
[95] M.L. Sin, K.E. Mach, P.K. Wong, J.C. Liao, Advances and challenges in biosensor-based diagnosis of infectious diseases, Expert Review of Molecular Diagnostics, 14 (2014) 225-244.
[96] A. Koyappayil, M.H. Lee, Ultrasensitive Materials for Electrochemical Biosensor Labels, Sensors (Basel), 21 (2020) 89.
[97] A. Chieng, Z. Wan, S. Wang, Recent Advances in Real-Time Label-Free Detection of Small Molecules, Biosensors (Basel), 14 (2024) 80.
[98] A.V. Kabashin, V.G. Kravets, A.N. Grigorenko, Label-free optical biosensing: going beyond the limits, Chemical Society Reviews, 52 (2023) 6554-6585.
[99] A. Syahir, K. Usui, K.Y. Tomizaki, K. Kajikawa, H. Mihara, Label and Label-Free Detection Techniques for Protein Microarrays, Microarrays (Basel), 4 (2015) 228-244.

[100] V.R. Samuel, K.J. Rao, A review on label free biosensors, Biosensors and Bioelectronics: X, 11 (2022) 100216.
[101] B.G. Andryukov, N.N. Besednova, R.V. Romashko, T.S. Zaporozhets, T.A. Efimov, Label-Free Biosensors for Laboratory-Based Diagnostics of Infections: Current Achievements and New Trends, Biosensors (Basel), 10 (2020) 11.
[102] Y. Wu, R.D. Tilley, J.J. Gooding, Challenges and Solutions in Developing Ultrasensitive Biosensors, Journal of the American Chemical Society, 141 (2019) 1162-1170.
[103] G. Liu, Grand Challenges in Biosensors and Biomolecular Electronics, Frontiers in Bioengineering and Biotechnology, 9 (2021) 707615.
[104] H. Yoo, H. Jo, S.S. Oh, Detection and beyond: challenges and advances in aptamer-based biosensors, Materials Advances, 1 (2020) 2663-2687.
[105] M.M. Shanbhag, G. Manasa, R.J. Mascarenhas, K. Mondal, N.P. Shetti, Fundamentals of bio-electrochemical sensing, Chemical Engineering Journal Advances, 16 (2023) 100516.
[106] M. Oliverio, S. Perotto, G.C. Messina, L. Lovato, F. De Angelis, Chemical Functionalization of Plasmonic Surface Biosensors: A Tutorial Review on Issues, Strategies, and Costs, ACS Applied Material & Interfaces, 9 (2017) 29394-29411.
[107] M.J. Banuls, R. Puchades, A. Maquieira, Chemical surface modifications for the development of silicon-based label-free integrated optical (IO) biosensors: a review, Analytica Chimica Acta, 777 (2013) 1-16.
[108] J. Leuermann, V. Stamenkovic, P. Ramirez-Priego, A. Sánchez-Postigo, A. Fernández-Gavela, C.A. Chapman, R.C. Bailey, L.M. Lechuga, E. Perez-Inestrosa, D. Collado, R. Halir, Í. Molina-Fernández, Coherent silicon photonic interferometric biosensor with an inexpensive laser source for sensitive label-free immunoassays, Optics Letters, 45 (2020) 6595-6598.
[109] D. Martens, P. Ramirez-Priego, M.S. Murib, A.A. Elamin, A.B. Gonzalez-Guerrero, M. Stehr, F. Jonas, B. Anton, N. Hlawatsch, P. Soetaert, R. Vos, A. Stassen, S. Severi, W. Van Roy, R. Bockstaele, H. Becker, M. Singh, L.M. Lechuga, P. Bienstman, A low-cost integrated biosensing platform based on SiN nanophotonics for biomarker detection in urine, Analytical Methods, 10 (2018) 3066-3073.
[110] A. Ksendzov, Y. Lin, Integrated optics ring-resonator sensors for protein detection, Optics Letters, 30 (2005) 3344-3346.
[111] K.D. Vos, I. Bartolozzi, E. Schacht, P. Bienstman, R. Baets, Silicon-on-Insulator microring resonator for sensitive and label-free biosensing, Optics Express, 15 (2007) 7610-7615.
[112] C. Liu, Q. Cai, B. Xu, W. Zhu, L. Zhang, J. Zhao, X. Chen, Graphene oxide functionalized long period grating for ultrasensitive label-free immunosensing, Biosensors and Bioelectronics, 94 (2017) 200-206.
[113] P. Biswas, F. Chiavaioli, S. Jana, N. Basumallick, C. Trono, A. Giannetti, S. Tombelli, A. Mallick, F. Baldini, S. Bandyopadhyay, Design, fabrication and characterisation of silica-titania thin film coated over coupled long period fibre gratings: Towards bio-sensing applications, Sensors and Actuators B: Chemical, 253 (2017) 418-427.
[114] S. Schulze, M. Wehrhold, C. Hille, Femtosecond-Pulsed Laser Written and Etched Fiber Bragg Gratings for Fiber-Optical Biosensing, Sensors (Basel), 18 (2018) 2844.
[115] S. Sridevi, K.S. Vasu, S. Asokan, A.K. Sood, Sensitive detection of C-reactive protein using optical fiber Bragg gratings, Biosensors and Bioelectronics, 65 (2015) 251-256.
[116] M.J. McGrath, C.N. Scanaill, Regulations and Standards: Considerations for Sensor Technologies, Sensor Technologies: Healthcare, Wellness, and Environmental Applications, Apress, Berkeley, CA, 2013,115-135.
[117] L. Soleymani, F. Li, Mechanistic Challenges and Advantages of Biosensor Miniaturization into the Nanoscale, ACS Sensors, 2 (2017) 458-467.
[118] H. Vaisocherova, E. Brynda, J. Homola, Functionalizable low-fouling coatings for label-free biosensing in complex biological media: advances and applications, Analytical and Bioanalytical Chemistry, 407 (2015) 3927-3953.
[119] A. Drayton, K. Li, M. Simmons, C. Reardon, T.F. Krauss, Performance limitations of resonant refractive index sensors with low-cost components, Optics Express, 28 (2020) 32239-32248.
[120] Y. Liu, K. Ai, L. Lu, Polydopamine and its derivative materials: synthesis and promising applications in energy, environmental, and biomedical fields, Chemical Reviews, 114 (2014) 5057-5115.

[121] Y. Abdiche, D. Malashock, A. Pinkerton, J. Pons, Determining kinetics and affinities of protein interactions using a parallel real-time label-free biosensor, the Octet, Analytical Biochemistry, 377 (2008) 209-217.
[122] M. Soler, M.C. Estevez, M. Cardenosa-Rubio, A. Astua, L.M. Lechuga, How Nanophotonic Label-Free Biosensors Can Contribute to Rapid and Massive Diagnostics of Respiratory Virus Infections: COVID-19 Case, ACS Sensors, 5 (2020) 2663-2678.
[123] H. Altug, S.H. Oh, S.A. Maier, J. Homola, Advances and applications of nanophotonic biosensors, Nature Nanotechnology, 17 (2022) 5-16.
[124] C.S. Huertas, O. Calvo-Lozano, A. Mitchell, L.M. Lechuga, Advanced Evanescent-Wave Optical Biosensors for the Detection of Nucleic Acids: An Analytic Perspective, Frontiers in Chemistry, 7 (2019) 724.
[125] D. Capelli, V. Scognamiglio, R. Montanari, Surface plasmon resonance technology: Recent advances, applications and experimental cases, TrAC Trends in Analytical Chemistry, 163 (2023) 117079.
[126] H.H. Nguyen, J. Park, S. Kang, M. Kim, Surface plasmon resonance: a versatile technique for biosensor applications, Sensors (Basel), 15 (2015) 10481-10510.
[127] G.I. Janith, H.S. Herath, N. Hendeniya, D. Attygalle, D.A.S. Amarasinghe, V. Logeeshan, P.M.T.B. Wickramasinghe, Y.S. Wijayasinghe, Advances in surface plasmon resonance biosensors for medical diagnostics: An overview of recent developments and techniques, Journal of Pharmaceutical and Biomedical Analysis Open, 2 (2023) 100019.
[128] M. Soler, O. Calvo-Lozano, M.C. Estevez, L.M. Lechuga, Nanophotonic Biosensors: Driving Personalized Medicine, Optics and Photonics News, 31 (2020) 24-31.
[129] J. Jatschka, A. Dathe, A. Csáki, W. Fritzsche, O. Stranik, Propagating and localized surface plasmon resonance sensing -A critical comparison based on measurements and theory, Sensing and Bio-Sensing Research, 7 (2016) 62-70.
[130] K. Yang, Y. Chen, S. Yan, W. Yang, Nanostructured surface plasmon resonance sensors: Toward narrow linewidths, Heliyon, 9 (2023) e16598.
[131] S. Romero-García, F. Merget, F. Zhong, H. Finkelstein, J. Witzens, Silicon nitride back-end optics for biosensor applications, Proceedings SPIE, 8781 (2013).
[132] W. Muhammad, J. Song, S. Kim, F. Ahmed, E. Cho, H. Lee, J. Kim, Silicon-Based Biosensors: A Critical Review of Silicon's Role in Enhancing Biosensing Performance, Biosensors (Basel), 15 (2025) 119.
[133] T. Sharma, J. Wang, B.K. Kaushik, Z. Cheng, R. Kumar, Z. Wei, X. Li, Review of Recent Progress on Silicon Nitride-Based Photonic Integrated Circuits, IEEE Access, 8 (2020) 195436-195446.
[134] J. Wang, Z. Yao, A.W. Poon, Silicon-Nitride-Based Integrated Optofluidic Biochemical Sensors Using a Coupled-Resonator Optical Waveguide, Frontiers in Materials, 2 (2015).
[135] M. Antoniou, D. Tsounidi, P.S. Petrou, K.G. Beltsios, S.E. Kakabakos, Functionalization of silicon dioxide and silicon nitride surfaces with aminosilanes for optical biosensing applications, Medical Devices & Sensors, 3 (2020) e10072.
[136] Q. Liu, X. Tu, K.W. Kim, J.S. Kee, Y. Shin, K. Han, Y.J. Yoon, G.Q. Lo, M.K. Park, Highly sensitive Mach–Zehnder interferometer biosensor based on silicon nitride slot waveguide, Sensors and Actuators B: Chemical, 188 (2013) 681-688.
[137] M.R. Bryan, J.N. Butt, J. Bucukovski, B.L. Miller, Biosensing with Silicon Nitride Microring Resonators Integrated with an On-Chip Filter Bank Spectrometer, ACS Sens, 8 (2023) 739-747.
[138] L.S. Puumala, S.M. Grist, J.M. Morales, J.R. Bickford, L. Chrostowski, S. Shekhar, K.C. Cheung, Biofunctionalization of Multiplexed Silicon Photonic Biosensors, Biosensors (Basel), 13 (2022) 53.
[139] C. Ciminelli, F. Dell'Olio, D. Conteduca, M.N. Armenise, Silicon photonic biosensors, IET Optoelectronics, 13 (2019) 48-54.
[140] M. Shyiq Amin, J. Woong Yoon, R. Magnusson, Optical transmission filters with coexisting guided-mode resonance and Rayleigh anomaly, Applied Physics Letters, 103 (2013) 131106.
[141] T. Khaleque, H.G. Svavarsson, R. Magnusson, Fabrication of resonant patterns using thermal nano-imprint lithography for thin-film photovoltaic applications, Optics Express, 21 (2013) A631-641.
[142] Y. Zhou, B. Wang, Z. Guo, X. Wu, Guided Mode Resonance Sensors with Optimized Figure of Merit, Nanomaterials (Basel), 9 (2019) 837.

[143] B. Cunningham, B. Lin, J. Pepper, Colorimetric resonant reflection as a direct biochemical assay technique, Senors and Actuators B: Chemical, 81 (2002) 316-328.
[144] B. Cunningham, J. Qiu, P. Li, J. Pepper, B. Hugh, A plastic colorimetric resonant optical biosensor for multi-parallel detection of label-free biochemical interactions, Sensors and Actuators B: Chemical, 85 (2002) 219-226.
[145] L. L. Chan, M. Paneda, J. T. Heeres, P. J. Hergenrother, B. T. Cunningham, A General method for discovering inhibitors of protein DNA interactions using photonic crystal biosensors ACS Chemical Biology, 3 (2008) 437-448.
[146] A. Drayton, I. Barth, T.F. Krauss, Guided mode resonances and photonic crystals for biosensing and imaging, Semicondcutors and Semimetals 2019, 115-148.
[147] H. Shafiee, E.A. Lidstone, M. Jahangir, F. Inci, E. Hanhauser, T.J. Henrich, D.R. Kuritzkes, B.T. Cunningham, U. Demirci, Nanostructured optical photonic crystal biosensor for HIV viral load measurement, Scientific Reports, 4 (2014) 4116.
[148] Y.K. Tu, M.Z. Tsai, I.C. Lee, H.Y. Hsu, C.S. Huang, Integration of a guided-mode resonance filter with microposts for in-cell protein detection, Analyst, 141 (2016) 4189-4195.
[149] M.Z. Tsai, C.T. Hsiung, Y. Chen, C.S. Huang, H.Y. Hsu, P.Y. Hsieh, Real-time CRP detection from whole blood using micropost-embedded microfluidic chip incorporated with label-free biosensor, Analyst, 143 (2018) 503-510.
[150] Q. Wang, D. Zhang, H. Yang, C. Tao, Y. Huang, S. Zhuang, T. Mei, Sensitivity of a label-free guided-mode resonant optical biosensor with different modes, Sensors (Basel), 12 (2012) 9791-9799.
[151] R. Magnusson, D. Wawro, S. Zimmerman, Y. Ding, Resonant photonic biosensors with polarization-based multiparametric discrimination in each channel, Sensors (Basel), 11 (2011) 1476-1488.
[152] A. Kenaan, K. Li, I. Barth, S. Johnson, J. Song, T.F. Krauss, Guided mode resonance sensor for the parallel detection of multiple protein biomarkers in human urine with high sensitivity, Biosensors and Bioelectronics, 153 (2020) 112047.
[153] G.J. Triggs, Y. Wang, C.P. Reardon, M. Fischer, G.J.O. Evans, T.F. Krauss, Chirped guided-mode resonance biosensor, Optica, 4 (2017) 229-234.
[154] D. Conteduca, G.S. Arruda, I. Barth, Y. Wang, T.F. Krauss, E.R. Martins, Beyond Q: The Importance of the Resonance Amplitude for Photonic Sensors, ACS Photonics, 9 (2022) 1757-1763.
[155] J. Fritzsche, D. Albinsson, M. Fritzsche, T.J. Antosiewicz, F. Westerlund, C. Langhammer, Single Particle Nanoplasmonic Sensing in Individual Nanofluidic Channels, Nano Letters, 16 (2016) 7857-7864.
[156] J. Wang, S.A. Maier, A. Tittl, Trends in Nanophotonics-Enabled Optofluidic Biosensors, Advanced Optical Materials, 10 (2022) 2102366.
[157] E. Luan, H. Shoman, D.M. Ratner, K.C. Cheung, L. Chrostowski, Silicon Photonic Biosensors Using Label-Free Detection, Sensors (Basel), 18 (2018) 3519.
[158] A. Shakeri, S. Khan, T.F. Didar, Conventional and emerging strategies for the fabrication and functionalization of PDMS-based microfluidic devices, Lab on a Chip, 21 (2021) 3053-3075.
[159] J. Friend, L. Yeo, Fabrication of microfluidic devices using polydimethylsiloxane, Biomicrofluidics, 4 (2010) 026502.
[160] Y. Wang, S. Chen, H. Sun, W. Li, C. Hu, K. Ren, Recent progresses in microfabricating perfluorinated polymers (Teflons) and the associated new applications in microfluidics, Microphysiological Systems, 2 (2018).
[161] D. Lange, C.W. Storment, C.A. Conley, G.T.A. Kovacs, A microfluidic shadow imaging system for the study of the nematode Caenorhabditis elegans in space, Sensors and Actuators B: Chemical, 107 (2005) 904-914.
[162] F. Cui, Y. Yue, Y. Zhang, Z. Zhang, H.S. Zhou, Advancing Biosensors with Machine Learning, ACS Sensors, 5 (2020) 3346-3364.
[163] S. Hu, Y. Zhao, K. Qin, S.T. Retterer, I.I. Kravchenko, S.M. Weiss, Enhancing the Sensitivity of Label-Free Silicon Photonic Biosensors through Increased Probe Molecule Density, ACS Photonics, 1 (2014) 590-597.
[164] C. Li, P. Yu, Y. Huang, Q. Zhou, J. Wu, Z. Li, X. Tong, Q. Wen, H.C. Kuo, Z.M. Wang, Dielectric metasurfaces: From wavefront shaping to quantum platforms, Progress in Surface Science, 95 (2020) 100584.

[165] A.S. Gangnaik, Y.M. Georgiev, J.D. Holmes, New Generation Electron Beam Resists: A Review, Chemistry of Materials, 29 (2017) 1898-1917.
[166] M. Altissimo, E-beam lithography for micro-nanofabrication, Biomicrofluidics, 4 (2010) 026503.
[167] J.Y. Woo, S. Jo, J.H. Oh, J.T. Kim, C.S. Han, Facile and precise fabrication of 10-nm nanostructures on soft and hard substrates, Applied Surface Science, 484 (2019) 317-325.
[168] L.J. Guo, Nanoimprint Lithography: Methods and Material Requirements, Advanced Materials, 19 (2007) 495-513.
[169] M.C. Traub, W. Longsine, V.N. Truskett, Advances in Nanoimprint Lithography, Annual Review of Chemical and Biomolecular Engineering, 7 (2016) 583-604.
[170] E. Abad, S. Merino, A. Retolaza, A. Juarros, Design and fabrication using nanoimprint lithography of a nanofluidic device for DNA stretching applications, Microelectronic Engineering, 85 (2008) 818-821.
[171] J.K. Kim, S.J. Park, S. Kim, H.H. Park, K.D. Kim, J.H. Choi, J. Lee, D.G. Choi, K.Y. Suh, J.H. Jeong, Fabrication of ZrO_2 nanopatterns for biomimetic antireflection by thermal nanoimprint lithography, Microelectronic Engineering, 100 (2012) 12-15.
[172] S. Liebana, G.A. Drago, Bioconjugation and stabilisation of biomolecules in biosensors, Essays in Biochemistry, 60 (2016) 59-68.
[173] L. S. Wong, F. Khan, J. Micklefield, Selective Covalent Protein Immobilization: Strategies and Applications, Chemical Reviews 109 (2009) 4025–4053.
[174] A.H.A. Balzer, C.B. Whitehurst, An Analysis of the Biotin-(Strept)avidin System in Immunoassays: Interference and Mitigation Strategies, Current Issues in Molecular Biology, 45 (2023) 8733-8754.
[175] S. Gao, J.M. Guisan, J. Rocha-Martin, Oriented immobilization of antibodies onto sensing platforms - A critical review, Analytica Chimica Acta, 1189 (2022) 338907.
[176] S. Löfås, B. Johnsson, A novel hydrogel matrix on gold surfaces in surface plasmon resonance sensors for fast and efficient covalent immobilization of ligands, Journal of the Chemical Society, Chemical Communications, (1990) 1526-1528.
[177] J.G. Quinn, S. O'Neill, A. Doyle, C. McAtamney, D. Diamond, B.D. MacCraith, R. O'Kennedy, Development and application of surface plasmon resonance-based biosensors for the detection of cell-ligand interactions, Analytical Biochemistry, 281 (2000) 135-143.
[178] O. Tabasi, C. Falamaki, M. Mahmoudi, A Detailed Study on the Fabrication of Surface Plasmon Sensor Chips: Optimization of Dextran Molecular Weight, Plasmonics, 14 (2019) 1145-1159.
[179] C.V. Topor, M. Puiu, C. Bala, Strategies for Surface Design in Surface Plasmon Resonance (SPR) Sensing, Biosensors (Basel), 13 (2023) 465.
[180] Z. Chen, Z. Lv, Y. Sun, Z. Chi, G. Qing, Recent advancements in polyethyleneimine-based materials and their biomedical, biotechnology, and biomaterial applications, Journal of Materials Chemistry B, 8 (2020) 2951-2973.
[181] Z. Saffari, M. Sepahi, R. A. Cohan,M. Khoobi, M. H. Fard, A. Ghavidel, M.R. Aghasadeghi, D. Norouzian, A quartz crystal microbalance biosensor based on polyethylenimine-modified gold electrode to detect hepatitis B biomarker, Analytical Biochemistry, 661 (2023) 114981.
[182] J.J. Virgen-Ortiz, J.C.S. Dos Santos, A. Berenguer-Murcia, O. Barbosa, R.C. Rodrigues, R. Fernandez-Lafuente, Polyethylenimine: a very useful ionic polymer in the design of immobilized enzyme biocatalysts, Journal of Materials Chemistry B, 5 (2017) 7461-7490.
[183] A.H. S. Kurunczia, K. Juhasza, D. Patkoa, N. Orgovana, N. Turckb,J.C. Sanchezb, R. Horvath, Polyethylene imine-based receptor immobilization for label free bioassays, Sensors and Actuators B: Chemical, 181 (2013) 71-76.
[184] J.H. Ryu, P.B. Messersmith, H. Lee, Polydopamine Surface Chemistry: A Decade of Discovery, ACS Applied Materials & Interfaces, 10 (2018) 7523-7540.
[185] D. Hauser, D. Septiadi, J. Turner, A. Petri-Fink, B. Rothen-Rutishauser, From Bioinspired Glue to Medicine: Polydopamine as a Biomedical Material, Materials (Basel), 13 (2020) 1730.
[186] Y. Cong, T. Xia, M. Zou, Z. Li, B. Peng, D. Guo, Z. Deng, Mussel-inspired polydopamine coating as a versatile platform for synthesizing polystyrene/Ag nanocomposite particles with enhanced antibacterial activities, Journal of Materials Chemistry B, 2 (2014) 3450-3461.

[187] M. Toma, K. Tawa, Polydopamine Thin Films as Protein Linker Layer for Sensitive Detection of Interleukin-6 by Surface Plasmon Enhanced Fluorescence Spectroscopy, ACS Applied Materials & Interfaces, 8 (2016) 22032-22038.
[188] H. Li, D. Yin, W. Li, Q. Tang, L. Zou, Q. Peng, Polydopamine-based nanomaterials and their potentials in advanced drug delivery and therapy, Colloids and Surfaces B: Biointerfaces, 199 (2021) 111502.
[189] R. Luo, L. Tang, J. Wang, Y. Zhao, Q. Tu, Y. Weng, R. Shen, N. Huang, Improved immobilization of biomolecules to quinone-rich polydopamine for efficient surface functionalization, Colloids and Surfaces B: Biointerfaces, 106 (2013) 66-73.
[190] L.P. Zhu, J.H. Jiang, B.K. Zhu, Y.Y. Xu, Immobilization of bovine serum albumin onto porous polyethylene membranes using strongly attached polydopamine as a spacer, Colloids and Surfaces B: Biointerfaces, 86 (2011) 111-118.
[191] H.O. Ham, Z. Liu, K.H. Lau, H. Lee, P.B. Messersmith, Facile DNA immobilization on surfaces through a catecholamine polymer, Angew Chem Int Ed Engl, 50 (2011) 732-736.
[192] S. Hong, Y.S. Na, S. Choi, I.T. Song, W.Y. Kim, H. Lee, Non-Covalent Self-Assembly and Covalent Polymerization Co-Contribute to Polydopamine Formation, Advanced Functional Materials, 22 (2012) 4711-4717.
[193] Q. Liu, N. Wang, J. Caro, A. Huang, Bio-inspired polydopamine: a versatile and powerful platform for covalent synthesis of molecular sieve membranes, Journal of American Chemical Society, 135 (2013) 17679-17682.
[194] O. Pop-Georgievski, D. Verreault, M.O. Diesner, V. Proks, S. Heissler, F. Rypacek, P. Koelsch, Nonfouling poly(ethylene oxide) layers end-tethered to polydopamine, Langmuir, 28 (2012) 14273-14283.
[195] M.M. P. Salazar, J.L. González-Mora, Polydopamine-modified surfaces in biosensor applications, Formatex Research Center SL (Spain), (2016) 385-396.
[196] S. Gundagatti, S. Srivastava, An optimization of blocking agents for designing reliable electrochemical biosensors for ovarian cancer, Materials Today: Proceedings, (2023).
[197] R.V. Vogt, D.L. Phillips, L. Omar Henderson, W. Whitfield, F.W. Spierto, Quantitative differences among various proteins as blocking agents for ELISA microtiter plates, Journal of Immunological Methods, 102 (1987) 43-50.
[198] G. Figueroa-Miranda, C. Wu, Y. Zhang, L. Norbel, Y. Lo, J.A. Tanner, L. Elling, A. Offenhausser, D. Mayer, Polyethylene glycol-mediated blocking and monolayer morphology of an electrochemical aptasensor for malaria biomarker detection in human serum, Bioelectrochemistry, 136 (2020) 107589.
[199] H. Lísalová, E. Brynda, M. Houska, I. Víšová, K. Mrkvová, X.C. Song, E. Gedeonová, F. Surman, T. Riedel, O. Pop-Georgievski, J. Homola, Ultralow-Fouling Behavior of Biorecognition Coatings Based on Carboxy-Functional Brushes of Zwitterionic Homo and Copolymers in Blood Plasma: Functionalization Matters, Analytical Chemistry, 89 (2017) 3524-3531.
[200] G.J. Triggs, G.J.O. Evans, T.F. Krauss, Degradation of silicon photonic biosensors in cell culture media: analysis and prevention, Biomedical Optics Express, 8 (2017) 2924-2931.
[201] D. Bogdan, I.-G. Grosu, C. Filip, How thick, uniform and smooth are the polydopamine coating layers obtained under different oxidation conditions? An in-depth AFM study, Applied Surface Science, 597 (2022) 153680.
[202] M.C. Dixon, Quartz Crystal Microbalance with Dissipation Monitoring: Enabling Real-Time Characterization of Biological Materials and Their Interactions, Journal of Biomolecular Techniques, 19 (2008) 151-158.
[203] J. Juan-Colas, I.S. Hitchcock, M. Coles, S. Johnson, T.F. Krauss, Quantifying single-cell secretion in real time using resonant hyperspectral imaging, PNAS, 115 (2018) 13204-13209.
[204] B.T. Wang, Q. Wang, An interferometric optical fiber biosensor with high sensitivity for IgG/anti-IgG immunosensing, Optics Communications, 426 (2018) 388-394.
[205] J.P. Mendes, L.C.C. Coelho, P.A.S. Jorge, C.M. Pereira, Differential Refractometric Biosensor for Reliable Human IgG Detection: Proof of Concept, Biosensors (Basel), 12 (2022) 515.
[206] J. Dong, M. Sang, S. Wang, T. Xu, X. Yu, T. Liu, Ultrasensitive Label-Free Biosensor Based on the Graphene-Oxide-Coated-U-Bent Long-Period Fiber Grating Inscribed in a Two-Mode Fiber, Journal of Lightwave Technology, 39 (2021) 4013-4019.

[207] Y. Zheng, T. Lang, T. Shen, C. Shen, Simple immunoglobulin G sensor based on thin core single-mode fiber, Optical Fiber Technology, 41 (2018) 104-108.
[208] M. Falcone, B. De Angelis, F. Pea, A. Scalise, S. Stefani, R. Tasinato, O. Zanetti, L. Dalla Paola, Challenges in the management of chronic wound infections, Journal of Global Antimicrobial Resistance, 26 (2021) 140-147.
[209] R.G. Frykberg, J. Banks, Challenges in the Treatment of Chronic Wounds, Advances in Wound Care, 4 (2015) 560-582.
[210] T.C. v. Alphen, F. T. Brugge, E. V. Haren, M.M. Hoogbergen, H. Rakhorst, SCI-QOL and WOUND-Q Have the Best Patient-reported Outcome Measure Design: A Systematic Literature Review of PROMs Used in Chronic Wounds, Plast Reconstr Surg Glob Open, 11 (2023) e4723.
[211] C.K. Sen, G.M. Gordillo, S. Roy, R. Kirsner, L. Lambert, T.K. Hunt, F. Gottrup, G.C. Gurtner, M.T. Longaker, Human skin wounds: a major and snowballing threat to public health and the economy, Wound Repair and Regeneration, 17 (2009) 763-771.
[212] J.F. Guest, N. Ayoub, T. McIlwraith, I. Uchegbu, A. Gerrish, D. Weidlich, K. Vowden, P. Vowden, Health economic burden that different wound types impose on the UK's National Health Service, International Wound Journal, 14 (2017) 322-330.
[213] K. Jarbrink, G. Ni, H. Sonnergren, A. Schmidtchen, C. Pang, R. Bajpai, J. Car, Prevalence and incidence of chronic wounds and related complications: a protocol for a systematic review, Systematic Reviews, 5 (2016) 152.
[214] T.R. Dargaville, B.L. Farrugia, J.A. Broadbent, S. Pace, Z. Upton, N.H. Voelcker, Sensors and imaging for wound healing: a review, Biosensors and Bioelectronics, 41 (2013) 30-42.
[215] E.R. Utz, E.A. Elster, D.K. Tadaki, F. Gage, P.W. Perdue, J.A. Forsberg, A. Stojadinovic, J.S. Hawksworth, T.S. Brown, Metalloproteinase expression is associated with traumatic wound failure, Journal of Surgical Research, 159 (2010) 633-639.
[216] N.J. Trengove, H. Bielefeldt-Ohmann, M.C. Stacey, Mitogenic activity and cytokine levels in non-healing and healing chronic leg ulcers, Wound Repair And Regeneration, 8 (2000) 13-25.
[217] S. Dangwal, B. Stratmann, C. Bang, J.M. Lorenzen, R. Kumarswamy, J. Fiedler, C.S. Falk, C.J. Scholz, T. Thum, D. Tschoepe, Impairment of Wound Healing in Patients With Type 2 Diabetes Mellitus Influences Circulating MicroRNA Patterns via Inflammatory Cytokines, Arteriosclerosis Thrombosis and Vascular Biology, 35 (2015) 1480-1488.
[218] L.E. Lindley, O. Stojadinovic, I. Pastar, M. Tomic-Canic, Biology and Biomarkers for Wound Healing, Plast Reconstr Surg, 138 (2016) 18S-28S.
[219] N. Tang, Y. Zheng, X. Jiang, C. Zhou, H. Jin, K. Jin, W. Wu, H. Haick, Wearable Sensors and Systems for Wound Healing-Related pH and Temperature Detection, Micromachines (Basel), 12 (2021) 430.
[220] X. Sun, Y. Zhang, C. Ma, Q. Yuan, X. Wang, H. Wan, P. Wang, A Review of Recent Advances in Flexible Wearable Sensors for Wound Detection Based on Optical and Electrical Sensing, Biosensors (Basel), 12 (2021) 10.
[221] E.M. Jones, C.A. Cochrane, S.L. Percival, The Effect of pH on the Extracellular Matrix and Biofilms, Advances in Wound Care, 4 (2015) 431-439.
[222] S.H. Lu, M. Samandari, C. Li, H. Li, D. Song, Y. Zhang, A. Tamayol, X. Wang, Multimodal sensing and therapeutic systems for wound healing and management: A review, Sensors and Actuators Reports, 4 (2022) 100075.
[223] B.Y. Kim, H.B. Lee, N.E. Lee, A durable, stretchable, and disposable electrochemical biosensor on three-dimensional micro-patterned stretchable substrate, Sensors and Actuators B: Chemical, 283 (2019) 312-320.
[224] G. Rajeev, E. Xifre-Perez, B. Prieto Simon, A.J. Cowin, L.F. Marsal, N.H. Voelcker, A label-free optical biosensor based on nanoporous anodic alumina for tumour necrosis factor-alpha detection in chronic wounds, Sensors and Actuators B: Chemical, 257 (2018) 116-123.
[225] Y. Gao, D.T. Nguyen, T. Yeo, S.B. Lim, W.X. Tan, L.E. Madden, L. Jin, J.Y.K. Long, F.A.B. Aloweni, Y.J.A. Liew, M.L.L. Tan, S.Y. Ang, S.D. Maniya, I. Abdelwahab, K.P. Loh, C.H. Chen, D.L. Becker, D. Leavesley, J.S. Ho, C.T. Lim, A flexible multiplexed immunosensor for point-of-care in situ wound monitoring, Science Advances, 7 (2021) eabg9614.
[226] M. Ganter, A. Zollinger, Continuous intravascular blood gas monitoring: development, current techniques, and clinical use of a commercial device, British Journal of Anaesthesia, 91 (2003) 397-407.

[227] S. Tavakoli, A.S. Klar, Advanced Hydrogels as Wound Dressings, Biomolecules, 10 (2020) 1169.
[228] V.R. Guiza-Arguello, V.A. Solarte-David, A.V. Pinzon-Mora, J.E. Avila-Quiroga, S.M. Becerra-Bayona, Current Advances in the Development of Hydrogel-Based Wound Dressings for Diabetic Foot Ulcer Treatment, Polymers (Basel), 14 (2022) 2764.
[229] S. Nasra, M. Patel, H. Shukla, M. Bhatt, A. Kumar, Functional hydrogel-based wound dressings: A review on biocompatibility and therapeutic efficacy, Life Sciences, 334 (2023) 122232.
[230] I. Firlar, M. Altunbek, C. McCarthy, M. Ramalingam, G. Camci-Unal, Functional Hydrogels for Treatment of Chronic Wounds, Gels, 8 (2022) 127.
[231] M. Ho, A. Au, R. Flick, T.V. Vuong, A.A. Sklavounos, I. Swyer, C.M. Yip, A.R. Wheeler, Antifouling Properties of Pluronic and Tetronic Surfactants in Digital Microfluidics, ACS Applied Materials & Interfaces, 15 (2023) 6326-6337.
[232] B. Yu, C. Wang, Y.M. Ju, L. West, J. Harmon, Y. Moussy, F. Moussy, Use of hydrogel coating to improve the performance of implanted glucose sensors, Biosensors and Bioelectronics, 23 (2008) 1278-1284.
[233] D. Su, X. Bai, X. He, Research progress on hydrogel materials and their antifouling properties, European Polymer Journal, 181 (2022) 111665.
[234] P.K. Robinson, Enzymes: principles and biotechnological applications, Essays in Biochemistry, 59 (2015) 1-41.
[235] S. Bhatia, Introduction to enzymes and their applications, Introduction to pharmaceutical biotechnology, (2018) 1-29.
[236] W.G. Scott, Ribozymes, Current Opinion in Structural Biology, 17 (2007) 280-286.
[237] F. Shao, P.W. Lee, H. Li, K. Hsieh, T.H. Wang, Emerging platforms for high-throughput enzymatic bioassays, Trends in Biotechnology, 41 (2023) 120-133.
[238] C. Lopez-Otin, J.S. Bond, Proteases: multifunctional enzymes in life and disease, Journal of Biological Chemistry, 283 (2008) 30433-30437.
[239] V. Shumeiko, Y. Paltiel, G. Bisker, Z. Hayouka, O. Shoseyov, A Paper-Based Near-Infrared Optical Biosensor for Quantitative Detection of Protease Activity Using Peptide-Encapsulated SWCNTs, Sensors (Basel), 20 (2020) 5247.
[240] R. Oliveira-Silva, M. Sousa-Jeronimo, D. Botequim, N.J.O. Silva, P.M.R. Paulo, D.M.F. Prazeres, Monitoring Proteolytic Activity in Real Time: A New World of Opportunities for Biosensors, Trends in Biochemical Sciences, 45 (2020) 604-618.
[241] M. Drag, G.S. Salvesen, Emerging principles in protease-based drug discovery, Nature Reviews Drug Discovery, 9 (2010) 690-701.
[242] S. Raveendran, B. Parameswaran, S.B. Ummalyma, A. Abraham, A.K. Mathew, A. Madhavan, S. Rebello, A. Pandey, Applications of Microbial Enzymes in Food Industry, Food Technology & Biotechnol, 56 (2018) 16-30.
[243] V. Aruna, V. Chandrakala, G. Angajala, E.R. Nagarajan, Proteases: An overview on its recent industrial developments and current scenario in the revolution of biocatalysis, Materials Today: Proceedings, 92 (2023) 565-573.
[244] J. Kaur, P.K. Singh, Trypsin Detection Strategies: A Review, Critical Reviews in Analytical Chemistry, 52 (2022) 949-967.
[245] V.G. Vertiprakhov, N.V. Ovchinnikova, The activity of trypsin in the pancreatic juice and blood of poultry increases simultaneously in the postprandial period, Frontiers in Physiology, 13 (2022) 874664.
[246] T. Dau, G. Bartolomucci, J. Rappsilber, Proteomics Using Protease Alternatives to Trypsin Benefits from Sequential Digestion with Trypsin, Analytical Chemistry, 92 (2020) 9523-9527.
[247] O.G. Famutimi, V.G. Adebiyi, B.G. Akinmolu, O.V. Dada, I.O. Adewale, Trypsin, chymotrypsin and elastase in health and disease, Future Journal of Pharmaceutical Sciences, 10 (2024) 126.
[248] J. Ko, J. Cho, M.S. Petrov, Low serum amylase, lipase, and trypsin as biomarkers of metabolic disorders: A systematic review and meta-analysis, Diabetes Research and Clinical Practice, 159 (2020) 107974.
[249] A.F. Heeley, S.K. Bangert, The neonatal detection of cystic fibrosis by measurement of immunoreactive trypsin in blood, Annals of Clinical Biochemistry, 29 (1992) 361-376.

[250] J. Huang, V. Lok, C.H. Ngai, L. Zhang, J. Yuan, X.Q. Lao, K. Ng, C. Chong, Z.J. Zheng, M.C.S. Wong, Worldwide Burden of, Risk Factors for, and Trends in Pancreatic Cancer, Gastroenterology, 160 (2021) 744-754.
[251] G.P.C. Collaborators, The global, regional, and national burden of pancreatic cancer and its attributable risk factors in 195 countries and territories, 1990-2017: a systematic analysis for the Global Burden of Disease Study 2017, Lancet Gastroenterology Hepatology, 4 (2019) 934-947.
[252] T.C. Hall, G. Garcea, M.A. Webb, D. Al-Leswas, M.S. Metcalfe, A.R. Dennison, The socio-economic impact of chronic pancreatitis: a systematic review, Journal of Evaluation in Clinical Practice, 20 (2014) 203-207.
[253] G. Ouyang, G. Pan, Q. Liu, Y. Wu, Z. Liu, W. Lu, S. Li, Z. Zhou, Y. Wen, The global, regional, and national burden of pancreatitis in 195 countries and territories, 1990-2017: a systematic analysis for the Global Burden of Disease Study 2017, BMC Medicine, 18 (2020) 388.
[254] J. Yin, T. Cui, Y. Yang, T.-L. Ren, Sensing of Digestive Enzymes-Diagnosis and Monitoring of Pancreatitis, Chemosensors, 11 (2023) 469.
[255] M.A. Seia, P.W. Stege, S.V. Pereira, I.E. De Vito, J. Raba, G.A. Messina, Silica nanoparticle-based microfluidic immunosensor with laser-induced fluorescence detection for the quantification of immunoreactive trypsin, Analytical Biochemistry, 463 (2014) 31-37.
[256] P.A. Everley, C.A. Gartner, W. Haas, A. Saghatelian, J.E. Elias, B.F. Cravatt, B.R. Zetter, S.P. Gygi, Assessing enzyme activities using stable isotope labeling and mass spectrometry, Molecular and Cellular Proteomics, 6 (2007) 1771-1777.
[257] R.B. Lefkowitz, G.W. Schmid-Schonbein, M.J. Heller, Whole blood assay for trypsin activity using polyanionic focusing gel electrophoresis, Electrophoresis, 31 (2010) 2442-2451.
[258] S. Xu, F. Zhang, L. Xu, X. Liu, P. Ma, Y. Sun, X. Wang, D. Song, A fluorescence resonance energy transfer biosensor based on carbon dots and gold nanoparticles for the detection of trypsin, Sensors and Actuators B: Chemical, 273 (2018) 1015-1021.
[259] M. Wang, D. Su, G. Wang, X. Su, A fluorometric sensing method for sensitive detection of trypsin and its inhibitor based on gold nanoclusters and gold nanoparticles, Analytical and Bioanalytical Chemistry, 410 (2018) 6891-6900.
[260] M. Nemati, A. Santos, T. Kumeria, D. Losic, Label-Free real-time quantification of enzyme levels by interferometric spectroscopy combined with gelatin-modified nanoporous anodic alumina photonic films, Analytical Chemistry, 87 (2015) 9016-9024.
[261] M. A. Tabrizi, J. F.Borrull, L.F. Marsal, Remote biosensor for the determination of trypsin by using nanoporous anodic alumina as a three-dimensional nanostructured material, Scientific Reports, 10 (2020) 2356.
[262] J. Xu, E. Prost, K. Haupt, B. Tse Sum Bui, Direct and sensitive determination of trypsin in human urine using a water-soluble signaling fluorescent molecularly imprinted polymer nanoprobe, Sensors and Actuators B: Chemical, 258 (2018) 10-17.
[263] W.A.See, J. L. Smith, Urinary levels of activated trypsin in whole-organ pancreas transplant patients with duodenocystostomies, Transplantation, 52 (1991) 630-633.
[264] C. Duan, M.A. Alibakhshi, D.K. Kim, C.M. Brown, C.S. Craik, A. Majumdar, Label-Free Electrical Detection of Enzymatic Reactions in Nanochannels, ACS Nano, 10 (2016) 7476-7484.
[265] Z.M. Dong, L. Cheng, P. Zhang, G.C. Zhao, Label-free analytical performances of a peptide-based QCM biosensor for trypsin, Analyst, 145 (2020) 3329-3338.